

University of Nebraska - Lincoln

DigitalCommons@University of Nebraska - Lincoln

---

Construction Systems -- Dissertations & Theses

Construction Systems

---

Spring 4-23-2013

## Precast Concrete Insulated Wall Panel Corbels without Thermal Bridging

Mohamed Elkady

University of Nebraska, mohelkady@yahoo.com

Follow this and additional works at: <https://digitalcommons.unl.edu/constructiondiss>



Part of the [Architectural Engineering Commons](#), [Civil Engineering Commons](#), [Construction Engineering Commons](#), [Construction Engineering and Management Commons](#), and the [Structural Engineering Commons](#)

---

Elkady, Mohamed, "Precast Concrete Insulated Wall Panel Corbels without Thermal Bridging" (2013). *Construction Systems -- Dissertations & Theses*. 14. <https://digitalcommons.unl.edu/constructiondiss/14>

This Article is brought to you for free and open access by the Construction Systems at DigitalCommons@University of Nebraska - Lincoln. It has been accepted for inclusion in Construction Systems -- Dissertations & Theses by an authorized administrator of DigitalCommons@University of Nebraska - Lincoln.

**PRECAST CONCRETE INSULATED WALL PANEL CORBELS WITH-  
OUT THERMAL BRIDGING**

By

Mohamed Elkady

A THESIS

Presented to the Faculty of  
The Graduate College at the University of Nebraska  
In Partial Fulfillment of Requirements  
For the Degree of Master of Science

Major: Construction

Under the Supervision of Professor George Morcous and Professor Maher K. Tadros

Lincoln, Nebraska

May, 2013

# **PRECAST CONCRETE INSULATED WALL PANEL CORBELS WITH- OUT THERMAL BRIDGING**

Mohamed Elkady, M.S.

University of Nebraska, 2013

Advisers: George Morcous and Maher K. Tadros

Energy performance of precast concrete sandwich wall panels is greatly affected by thermal bridging at the corbel locations. The common practice for wall-corbel connection is to connect the two wythes with a solid concrete at corbel locations. This connection significantly reduces the energy efficiency of the panel. According to the PCI latest design handbook, the reduction in thermal resistance caused by a solid part with an area equal to 9% of the total panel surface area will be as-high-as 42%. This paper presents two wall-corbel connections that eliminate the thermal bridging. The structural capacity of the two connections was experimentally evaluated by testing seven full-scale specimens. Minor changes have been made during the testing program to optimize the constructability, structural capacity, and thermal efficiency of the proposed connections. This paper presents the design, detailing, and testing results of the proposed connections. The outcome of this research is a thermally efficient and easy to fabricate wall-corbel connection that achieves the target load-carrying capacity for most applications.

## ACKNOWLEDGEMENTS

I want to thank my advisors Professor George Morcous and Professor Maher K. Tadros, and the examining committee member Dr. Christopher Tuan.

Technical and financial contribution of Concrete Industries and Hughes brothers is highly appreciated.

I would like to thank e.construct, my employer and the sponsor for my graduate studies. Thanks to Mr. Sameh Al Ashri, Mr. Nader Jaber, Mr. Hany Nasr and Mr. Arun Tiwari.

Thanks to my parents, my wife and my daughter.

Alhamdulillah!



# Table of Contents

TABLE OF CONTENTS .....	III
LIST OF FIGURES.....	V
LIST OF TABLES.....	VIII
1. INTRODUCTION.....	1
1.1. Background .....	1
1.2. Problem statement .....	3
1.3. Research objectives .....	6
1.4. Report organization .....	7
2. LITERATURE REVIEW.....	9
2.1. Background .....	9
2.2. Current connections approaches and practice .....	11
2.3. Major researches on corbels behavior.....	14
2.3.1. Kriz, L. B. and Raths, C. H. ....	14
2.3.2. Mattock et al.....	18
2.4. Recommended provision by various standards .....	21
2.4.1. ACI318-11 .....	21
2.4.2. PCI design handbook .....	23
2.5. Strut and Tie method .....	25
3. PROPOSED CONNECTIONS .....	29
3.1. Design .....	29
3.2. Analysis .....	46
3.3. Materials and Fabrication .....	55
3.3.1. Materials.....	55
3.3.2. Fabrication.....	57
4. EXPERIMENTAL STUDY .....	61
4.1. Test specimens .....	61

4.2.	Testing setup and procedure .....	65
4.3.	Specimens behavior .....	69
4.3.1.	Specimen A1 .....	69
4.3.2.	Specimen B1 .....	72
4.3.3.	Specimen A2 .....	76
4.3.4.	Specimen B2 .....	78
4.3.5.	Specimens A3, A4 and A5.....	79
4.4.	Summary and discussion of results .....	82
5.	CONCLUSIONS AND RECOMMENDATIONS .....	94
5.1.	Conclusions .....	94
5.2.	Recommendations.....	94
5.3.	Future work.....	96
A.	DESIGN CALCULATION .....	97
B.	TESTING SPECIMEN DETAILS .....	102
C.	NOTATIONS AND DEFINITIONS .....	113
D.	BIBLIOGRAPHY .....	116

# List of Figures

Figure 1-1: Infrared image for thermal bridging in spandrel beams.....	5
Figure 1-2: Thermal bridges caused by solid zone in precast walls .....	6
Figure 2-1: Different composite concepts PSWP PCI Report (2011) .....	12
Figure 2-2: Current practice for corbel connections .....	13
Figure 2-3: Premature failure by too shallow corbel depth at tip .....	16
Figure 2-4: Secondary failure due to poor detailing.....	17
Figure 2-5: Corbel free-body diagram Mattock et al. (1976).....	20
Figure 2-6: D-Regions and B-Regions in corbel connection.....	26
Figure 3-1: Geometric terms used in this study.....	32
Figure 3-2: Various components of NU-Ties system for Specimen A2 .....	35
Figure 3-3: Assembled NU-Ties system for Specimen A2 .....	35
Figure 3-4: Free body diagram – Specimen A2.....	36
Figure 3-5: Free body diagram – Specimen A1.....	37
Figure 3-6: Components of Modified NU-Ties system, Specimens A3, A4 and A5 .....	39
Figure 3-7: Assembled Modified NU-Ties system, Specimens A3, A4 and A5.....	39
Figure 3-8: Free body diagram – Specimens A3, A4 and A5 .....	40
Figure 3-9: Assembled GFRP bars system, Specimen B2.....	41
Figure 3-10: Different components of GFRP bars system, Specimen B2.....	41
Figure 3-11: Free body diagram – Specimen B2.....	44
Figure 3-12: Free body diagram – Specimen B1.....	45
Figure 3-13: FEM Models geometry, Left: A2, Right: B2.....	48
Figure 3-14: FEM Models geometry - 3D View .....	50
Figure 3-15: Deformed shape A2, 3D and side view .....	51
Figure 3-16: Deformed shape B2, 3D and side view .....	52
Figure 3-17: Strut and tie results for specimen B2 at 60 kip applied load.....	53
Figure 3-18: Calculated capacity for specimen B2 equals to 74.02 kip .....	54

Figure 3-19: SCC Slump-Flow .....	55
Figure 3-20: #3 NU-TIE (photo by ASLAN FRP) .....	57
Figure 3-21: FRP tube placed into cut piece of insulation .....	58
Figure 3-22: GFRP Pin 2" diameter x 4½" long .....	60
Figure 4-1: Reinforcing details of specimens A1 and A2.....	64
Figure 4-2: Reinforcing details of specimens B1 and B2.....	64
Figure 4-3: Reinforcing details of specimens A3, A4 and A5 .....	65
Figure 4-4: Testing setup, side View .....	67
Figure 4-5: Testing setup, front view .....	68
Figure 4-6: Forming of leveling grout pad used for specimens A1, A2 and B1.....	69
Figure 4-7: Marked plastic shrinkage cracks in specimen A1 prior to loading .....	70
Figure 4-8: Specimen A1 crack pattern at failure .....	71
Figure 4-9: Cause of failure for specimen A1, concrete breakout .....	72
Figure 4-10: Marked plastic shrinkage cracks in specimen B1, prior to loading.....	74
Figure 4-11: Failure of specimen B1 .....	74
Figure 4-12: Ruptured GFRP Bars in specimen B1.....	75
Figure 4-13: Marked cracks at failure specimen A2 .....	77
Figure 4-14: Ruptured NU-Ties in specimen A2.....	77
Figure 4-15: Marked Cracks at failure and failure mode of specimen B2.....	79
Figure 4-16: Corbel block on ground after cutting the GFRP bars - specimen B2.....	79
Figure 4-17: Break-out zone at failure in specimen A3.....	81
Figure 4-18: Bent stirrups followed by concrete breakout in specimen A5.....	81
Figure 4-19: Cracks diagram in specimen A1 .....	83
Figure 4-20: Cracks diagram in specimen A2 .....	83
Figure 4-21: Loading and results of specimen A1 .....	84
Figure 4-22: Cracks diagram in specimen B1 .....	86
Figure 4-23: Cracks diagram in specimen B2 .....	86
Figure 4-24: Loading and results of specimen A2 .....	87
Figure 4-25: Loading and results of specimen B1 .....	88
Figure 4-26: Loading and results of specimen B2 .....	89

Figure 4-27: Cracks diagram in specimen A3, A4 and A5.....	90
Figure 4-28: Loading and results of specimen A3.....	91
Figure 4-29: Loading and results of specimen A4.....	92
Figure 4-30: Loading and results of specimen A5.....	92
Figure 5-1: Design forces for specimen A2.....	99
Figure 5-2: Forces in NU-Tie.....	100
Figure 5-3: Specimen A1- Details sheet 1.....	103
Figure 5-4: Specimen A1- Details sheet 2.....	104
Figure 5-5: Specimen A2- Details sheet 1.....	105
Figure 5-6: Specimen A2- Details sheet 2.....	106
Figure 5-7: Specimen B1- Details sheet 1.....	107
Figure 5-8: Specimen B1- Details sheet 2.....	108
Figure 5-9: Specimen B2- Details sheet 1.....	109
Figure 5-10: Specimen B2- Details sheet 2.....	110
Figure 5-11: Specimen A3, A4 and A5- Details sheet 1, Unreinforced Wall.....	111
Figure 5-12: Specimen A3, A4 and A5- Details sheet 2.....	112

# List of Tables

Table 1: Key Characteristics of corbels versus ledges .....	10
Table 2: Recommended shear friction coefficient by PCI Handbook (2010): .....	24
Table 3: FEM Models - Support details .....	47
Table 4: FEM Models - Material details .....	47
Table 5: Testing program .....	62
Table 6: Testing results .....	82

# CHAPTER 1

## 1. Introduction

### 1.1. Background

Precast concrete insulated wall panel is a major product in the precast concrete industry. Similar to many precast products, the insulated wall panels offer great characteristics. These desirable characteristics attract designers, contractors and owners to use insulated wall panels in their projects. Precast insulated wall panels have been used for decades with unprecedented success due to its architectural versatility, durability, thermal insulation, ease of production and erection, fire resistance, and structural capacity and performance.

It is not determined exactly when first use of precast concrete insulated wall panels is. However, the insulated wall panels were produced in North America as early as the 1960's. The early versions of insulated wall panels used a thick internal wythe, generally a double-tee or Hollow core, and a layer of rigid insulation and finally an external non-structural layer. Current practice in North America typically uses solid wythes for both the internal and external layers. The structural behavior of insulated wall panels is highly dependent on the connectors used to connect the wythes.

There are three types of design approaches for the insulated panels; Non-composite panels where each wythe behaves separately when subjected to bending moments; Composite panels where the

wythes behave as parts of a single beam and exhibit a similar stress distribution to a beam of total depth equal to the wall thickness including the insulation; the last design approach is a combination of the first two approaches where the wythes behave compositely up to a certain load limit then behaves non-compositely as the load increase. This limit is typically the connector's capacity.

Precast insulated wall panels are typically used to form the external periphery of the building. The wall panels are typically supported vertically by the footings and laterally by the floor system. Load bearing panels is a term used for panels that support the floor system and eventually transfers that load to the footings. The buildings periphery elevations are subject to unique loading conditions. These loads include the thermal gradient between indoor and outdoor temperatures, vertical reactions from the floor system (if load bearing), in plane shear forces (seismic and wind) and lateral wind pressure (suction and pressure). Thermal gradient and wind loads result in bending moments along the longitudinal direction of the wall which typically governs the design of the wall cross section. In plane shear are seldom to govern the wall design.

Insulated wall panels are typically prestressed along the longitudinal direction to a minimum effective pre-compression of 225 psi, the function of the prestressing is to satisfy the strength requirements and maintain the wall within acceptable cracking condition during handling and erection. Along the transverse direction, minimal non-prestressed reinforcement is frequently used to eliminate the plastic shrinkage cracks. Plastic shrinkage reinforcement recommendation for precast elements is lower than cast-in-place elements, since the precast manufacturing process allows more room for the elements to freely shrink without restrains.



The insulation layer is a main component of the insulated wall panels system. Different materials (Polystyrene, Polyurethane, Polyisocyanurate, and Phenolic) are available in the market to be used as thermal insulation. The extruded polystyrene (XPS) and expanded polystyrene (EPS) are the common insulation materials used in the precast walls. Required total thermal resistance of the wall typically governs the thickness of the insulation. The insulation thickness ranges from 2 to 4 inches in typical construction applications. Thermal conductivity is a physical property of the insulation material which measures the time rate of heat flow by conduction only through a unit thickness per unit area per unit temperature gradient. Thermal conductivity is measured by units of  $\left[\frac{\text{Btu}\cdot\text{inch}}{\text{hr}\cdot\text{ft}^2\cdot^\circ\text{F}}\right]$ . Other terms used in the thermal resistance calculations of walls are the U-Value and R-Value, which measure how the heat transfers through an assembly of materials of a specified thickness (U-value in units of  $\left[\frac{\text{hr}\cdot\text{ft}^2\cdot^\circ\text{F}}{\text{Btu}}\right]$ ). R-Value is the reciprocal of U-Value ( $R = 1/U$ ).

## 1.2. Problem statement

The pursuit for better energy utilization practices are driven by two forces; the ever rising energy cost and environmental awareness. Owners continue to invest in building operations after construction completion throughout the lifetime of the building (30 to 50 years). In the last decade, the use of holistic cost estimation methods such as Life-Cycle Cost Analysis became more dominant. The operation energy costs represent a significant portion of the operation costs in addition to maintenance and employee salaries. Investments in the capital cost (initial cost) will eventually payback throughout the extended period after completion. In addition to that, environmentally

aware buildings provide a better end-product for tenants. Building owners and designers include the operation costs as part of the project cost.

Thermal efficiency of the building envelope (insulated wall panels) is a significant aspect of the building total thermal performance. The Thermal performance of the insulation layer can be enhanced by providing a thicker layer of insulation; however this solution will not be always feasible due to the added cost of the materials and reduced utilized area of the building. Another issue which affects the performance of the insulation layer is thermal bridges. Thermal bridges are local areas where the thermal performance of the building envelope is reduced significantly. Many design practices reduce the thermal performance of the insulation layer by imposing thermal bridges. If these thermal bridges are eliminated totally from the design, the thermal efficiency of the building envelope will increase with no cost increase.

Thermal bridges are usually proposed to serve a structural function. A transverse solid zone across the panel width (no insulation) forms a thermal bridge by replacing the thermally non-conductive material (insulation) with a conductive material (concrete). This solid zone could be localized in critical areas. Thermal bridges could result from other thermally conductive materials such as steel rebar and stainless steel inserts. There are different methods to calculate the thermal bridging.

Figure 1-1 and Figure 1-2 show images taken by infrared imaging device for the building envelope. The Light color contours areas represent warm areas on the exterior of the building. These high-temperature areas can be considered as direct loss of heating energy and consequently cost.

Thermal bridges could be used to connect the two wythes together for the purpose of transferring the self-weight of the external layer to the internal layer in non-load bearing panels. A common use of the solid zones is as a shear connector between the two wythes, shear connectors transfer internal shear force between the compression and tension fibers within the cross section. This shear flow is originally caused by applied bending moments to the wall panel cross section. Areas where thermally conductive connectors are used to connect wythes are also considered a thermal bridge.

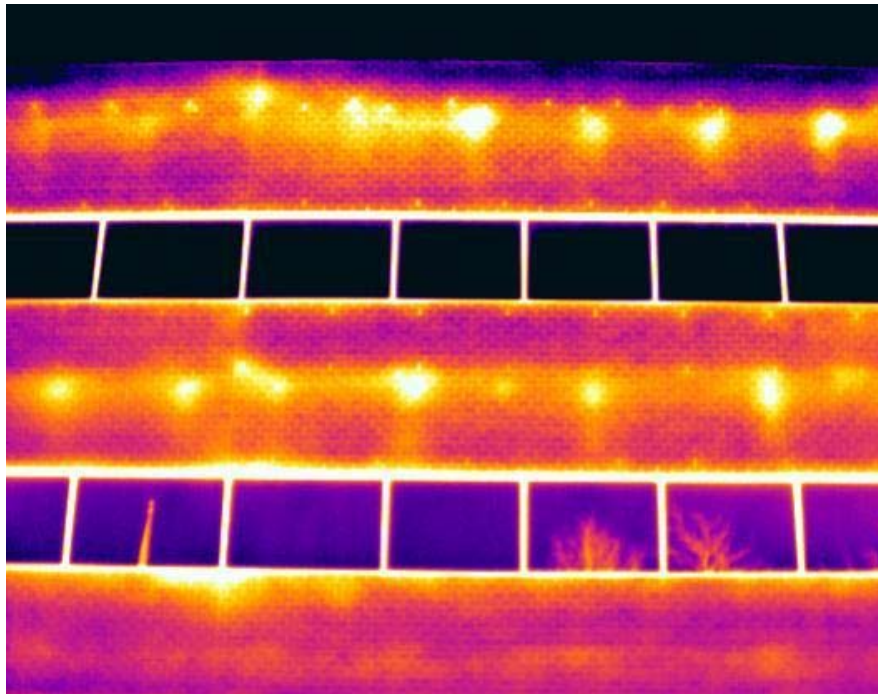


Figure 1-1: Infrared image for thermal bridging in spandrel beams  
Photo by (infraredimagingservices.com)

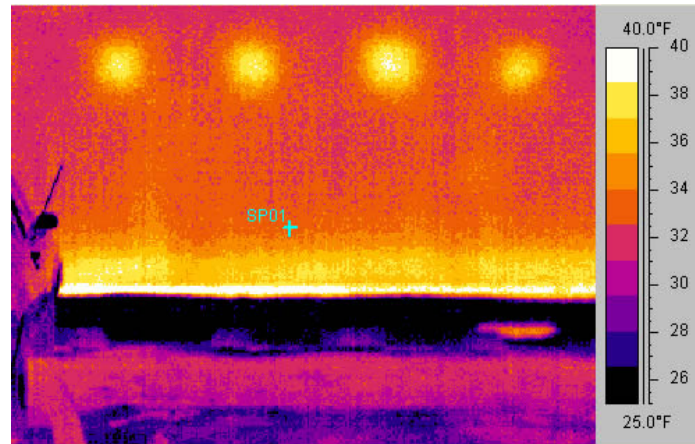


Figure 1-2: Thermal bridges caused by solid zone in precast walls

Photo by (solarcrete.com)

Corbel connections in insulated panels are usually common locations for solid zones (thermal bridges). Designers use details which stop the insulation around the corbel. The solid zone is typically in range of 2 to 3 feet in both transverse and longitudinal direction. These large solid zones drastically reduce the overall thermal efficiency of the insulated wall panel.

### 1.3. Research objectives

The objective of this research is to develop a corbel design that maintains the thermally insulation of the precast insulated walls. The proposed corbel design should satisfy various objectives to facilitate the use of the proposed design in typical precast construction.

The predefined design criterion is listed below:

- Adequate, the proposed corbel design should have the enough capacity to support the target loads. The target loads are thought to cover the majority of buildings applications
- Thermally efficient, the proposed design should maintain the thermal break
- Serviceable, the proposed corbel should exhibit no or very minor cracks and deformations under service loads

- Durable, minimum requirements by building codes should be applied in the proposed design
- Predictable capacity, the behavior of the proposed corbel should be in line with the industry design approaches
- Ease of fabrication, proposed design should easily fit into the production process of the precast walls
- Use of commonly available materials, the introduced materials (if any) used in the design should be readily available to the fabricators
- Architecturally acceptable, dimensions of the proposed design should be within the range of typical design.

This research is initiated in an effort to enhance the thermal efficiency of the precast insulated walls by eliminating the typically used solid zones at corbels. Therefore this study will address the possibilities providing a robust corbel connection while preserving the full thermal break.

Table 1: Key Characteristics of corbels versus ledges .....	10
Table 2: Recommended shear friction coefficient by PCI Handbook (2010): .....	24
Table 3: FEM Models - Support details .....	47
Table 4: FEM Models - Material details .....	47
Table 5: Testing program .....	62
Table 6: Testing results .....	82

#### **1.4. Report organization**

The work done towards achieving the research objective will be presented in this thesis in the following categories:

- Literature and current design approaches review
- Design of the proposed connections
- Experimental study
- Conclusions and design recommendations

The research will commence with collection of the previous works carried out on the corbel strength. Research about insulated wall panels corbels will be more relevant to this study. Different codes recommendations for corbel design will be reviewed. Design guides and recommendations of precast/pre-stressed wall panels will be review in order to use the current design practice.

The design of the proposed connections will be carried out in order to provide a sufficient capacity for typical precast construction application. Finite element method is proposed to be used for the early stages of the design process in order to highlight the critical areas. The design will be an iterative process based on the results of each testing cycle.

The experimental study stage will include selection of the appropriate testing setup in order to utilize the available testing facilities. Design of the testing specimens and selection of materials will be done at this stage. During testing the specimen behavior, observations and results will be recorded for further analysis.

Finally, the conclusion stage will highlight the design recommendation and lesson learnt out of the previous stages.

# CHAPTER 2

## 2. Literature review

### 2.1. Background

Corbels are short cantilevers which project from columns (or walls) face to support and transfer different reactions to the column (or wall). Typically, the corbels are designed to have a larger total depth at the column face than the tip. The corbels are basic connection in the precast construction. The concept of precast construction involves the casting of separate components (e.g. beams, trusses, slabs and columns), then providing a way of connection among these components. In the case of beam-column connection, the connection should be able to transfer the beam reaction to the column. This reaction eventually transfers from the columns to the footings. This is applicable to walls as supporting components as well.

Design methods for corbels changed over the years from using simple “good practice” rules in the early of the 20<sup>th</sup> century to more detailed methods of design. Till more research was done in the 1960’s, it was widely accepted to design corbels the same way cantilevers are designed. This design approaches used the flexural and shear strength of beams. The beam design provisions were developed and verified against results of beam with relatively higher span/depth ratio. In the case of corbels, the span/depth ratio is typically around the unity and may get as large as 2. Hence, using the beam design provision to design corbels will result in uncertainty of the design safety factors.

Table 1: Key Characteristics of corbels versus ledges

		Corbel	Ledge
Geometry	Width	Limited, usually to column width. Walls have limited width corbel too	Continuous over most of the beam or wall length
	Depth	Typically, variable depth. Shallow at the tip and deeper at the supporting components (column or wall) face, for aesthetic reasons.	Uniform depth, might have a fraction of inch draft for production reasons.
Loading		Single point load, in vertical and horizontal directions.	Uniform load or a series of point load spaced almost equally, in vertical and horizontal directions.
Design considerations		Shear strength, Cantilever bending of corbel, Bearing strength.	Shear strength, Transverse (cantilever) bending of ledge, Longitudinal bending of ledge , Attachment of ledge to beam web, Out-of-plane bending near beam end, Bearing strength.

Wight, J. and Macgregor, G. (2009) mentioned that designs using the beam provisions will result in questionable design if the reinforcement ratio exceeds 1%. The beam design provisions use vertical stirrups to capture the expected diagonal shear cracks occurs at 45 deg. On the other hand, shear cracks in corbel occur at a much steeper angle with the horizontal direction, in many cases cracks occur at vertical orientation of 90 deg. Since the cracks are in the same direction of the stirrups, simply the vertical stirrups will not be able to capture these vertical cracks and failure will occur. Researcher have shown that corbels are subject to horizontal reactions in combination with the vertical forces, earlier design approaches always neglected the horizontal forces adverse effects on the corbel capacity.



In Europe the design was based on the recommendation of Rausch, E. (1931) in the early 1940's, work done by Niedenhoff, H. (1961) was the first to address the corbel as a simple truss system.

This truss consists of a horizontal tie and inclined compression strut.

It is worth mentioning that corbels and ledges may have a common function, however the design of the two connections are quite different in many aspects. The Table 1 summarizes the main differences between the corbels and ledges

## **2.2. Current connections approaches and practice**

Designers have different concerns about the corbel connection in insulated wall panels; therefore the current practice for insulated wall panels corbels usually sacrifices the thermal insulation at the connection location. The most typical design concern is about the ability of a relatively thin wythe to resist the applied reaction (strength wise). In other words the strength of the wall cross section at the corbel location to resist the applied bending moment. Commonly, insulated wall panels are prestressed with minimal prestressing to satisfy the ACI 318 (2011). The prestressing strands ( $\frac{3}{8}$  inch diameter) are located at 2 inch from the wythe face. In non-composite walls the thin wythe and location of strands, the wythe capacity is not expected to be much. As for the composite wall cross sections, the strength concern is not very dominant. In composite wall cross sections where both wythes are connected with shear connectors, the wall cross section supplies a significant amount of structural strength. This capacity is much larger than the single wythe capacity due to the increased effective depth between the tension and compression force couple. Figure 2-1 shows the different composite concepts in insulated walls. Thermal performance and rotation of the corbel connection are also concerns for the designer.

Figure 2-2 illustrates the current practice in corbels design for insulated walls;

- In case of large floor reactions the designer may choose to use of thicker load bearing internal wythe and non-load bearing external wythe
- Use of solid part at the connection
- Use of local thickening at of the internal wythe at the connection

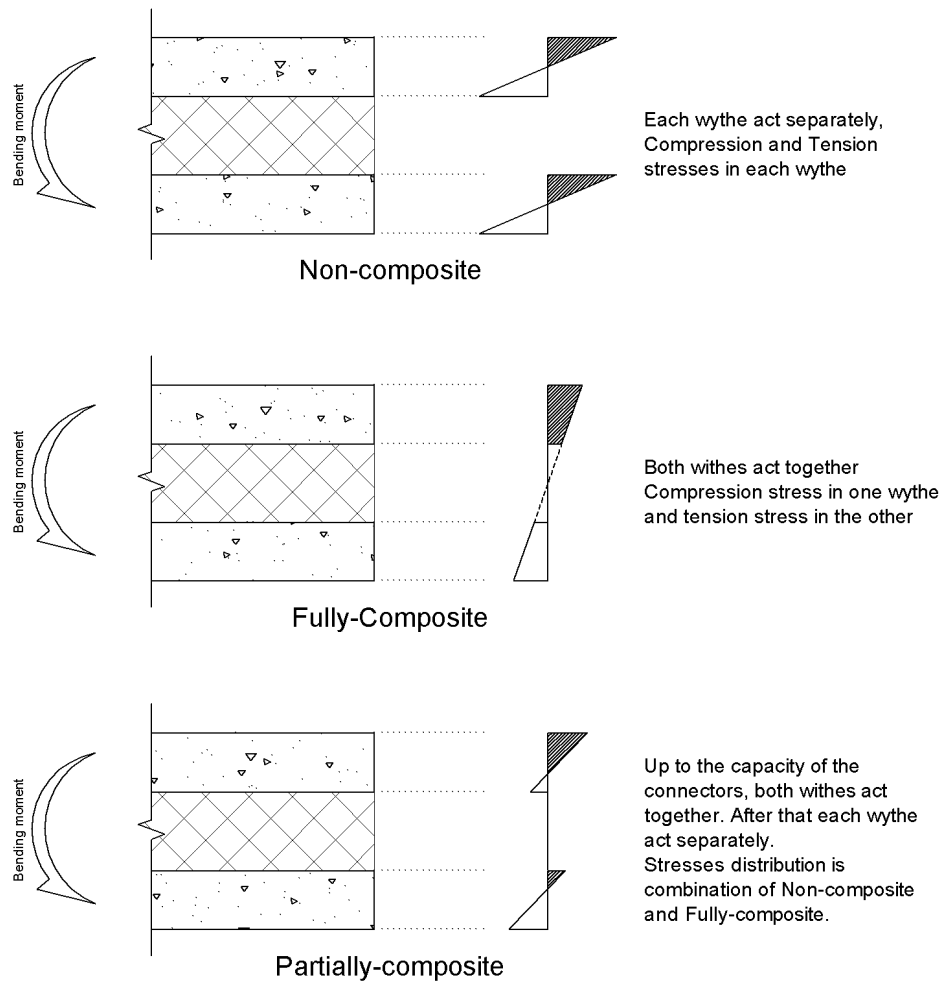


Figure 2-1: Different composite concepts PSWP PCI Report (2011)

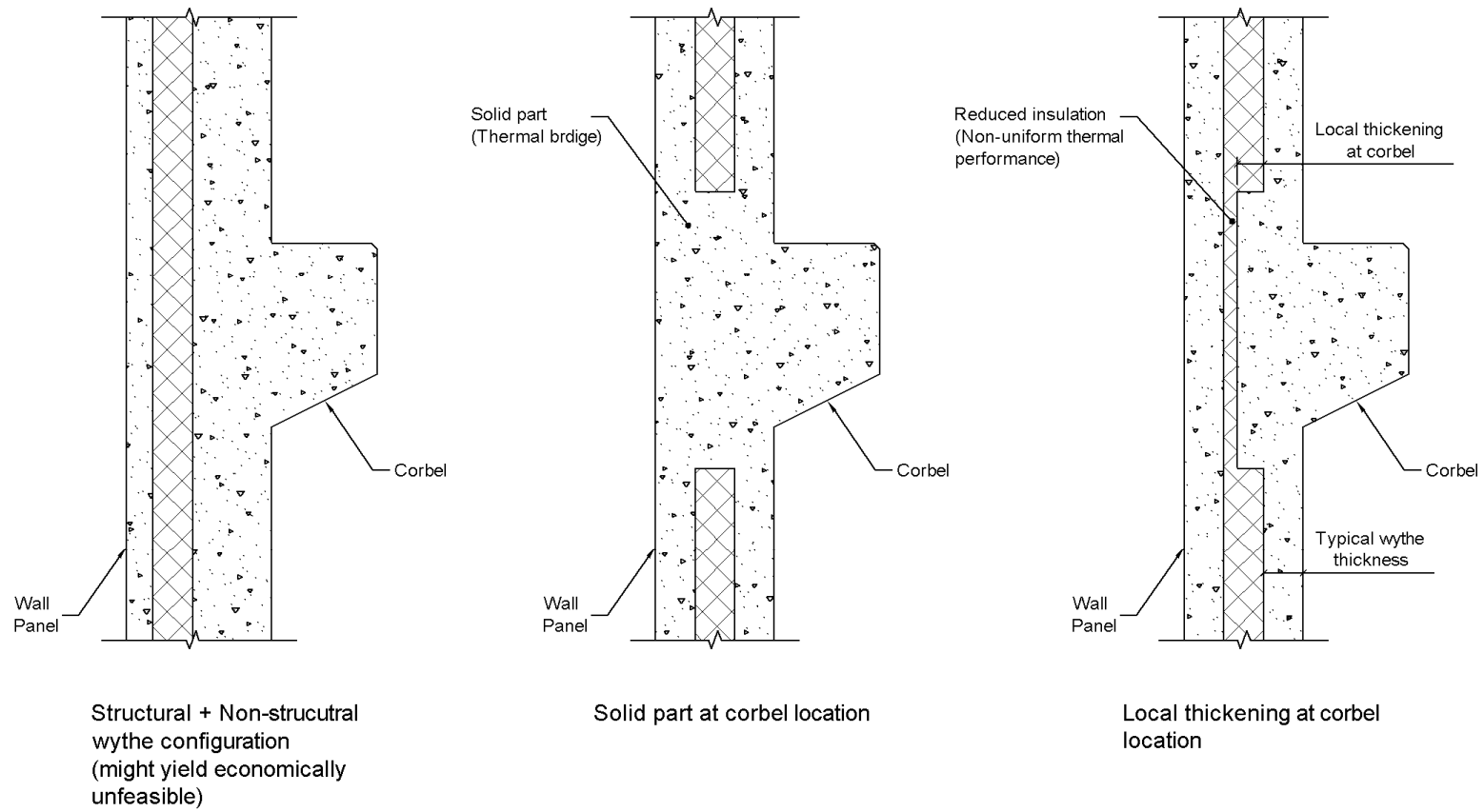


Figure 2-2: Current practice for corbel connections

## 2.3. Major researches on corbels behavior

### 2.3.1. Kriz, L. B. and Raths, C. H.

Kriz, L. B. and Raths, C. H.(1965) carried a large study on concrete corbels; their study included the testing of 124 corbel subjected to vertical loads only in addition to 71 corbels subjected to combined vertical and horizontal loads. The purpose of Kriz, L. B. and Raths, C. H. study was to develop rational design criteria for corbels. Total 195 corbels were tested with at the PCA structural laboratory. The specimens were designed to have shear span to effective depth ratio less than unity. Kriz included several variables in experimental program; Size and shape of corbel, amount and detail of tension reinforcement, concrete strength, amount of stirrups, ratio of shear span to effective depth, and ratio of horizontal to vertical force.

The outcomes of Kriz's study were the development of 2 empirical equations and a list recommendation to be followed in the design.

$$V_u = \phi \left[ 6.5bd\sqrt{f'_c} \left( 1 - 0.5\frac{d}{a} \right) (1000\rho)^{1/3} \right] \quad \text{Equation (1)}$$

$$\text{where } \rho = \frac{A_s + A_v}{bd}, \rho_{\max} = 0.02, A_s \geq A_v$$

Equation used if corbel is subject to vertical load only

$$V_u = \phi \left[ 6.5bd\sqrt{f'_c} \left( 1 - 0.5^{d/a} \right) \left( \frac{(1000\rho)^{\left(\frac{1}{3} + \frac{0.4H}{V}\right)}}{10^{\frac{0.8H}{V}}} \right) \right] \quad \text{Equation (2)}$$

$$\text{where } \rho = \frac{A_s}{bd}, \rho_{\max} = 0.013$$

Equation used if corbel is subject to vertical and horizontal load.

The recommendations developed by Kriz included proportions of the corbel dimensions, amount and details of reinforcement and bearing stress;

- Factored design loads should be increased by a 33%. Since corbels with 1% reinforcement ratio or less, experience yielding of reinforcement and visible cracks at loads equal to 67% of the failure load. This approach is recommended to ensure the serviceability of the corbel under moderate overloading. In other words, this recommendation could be considered as a substitute for serviceability requirements.
- Shear span to effective depth ( $a/d$ ) ratio less than unity, this design limit was mandated by the scope of the discussed study, and not necessarily that the corbels with  $a/d$  ratio greater than one will behavior differently – Wight, J. and Macgregor, G. (2009).

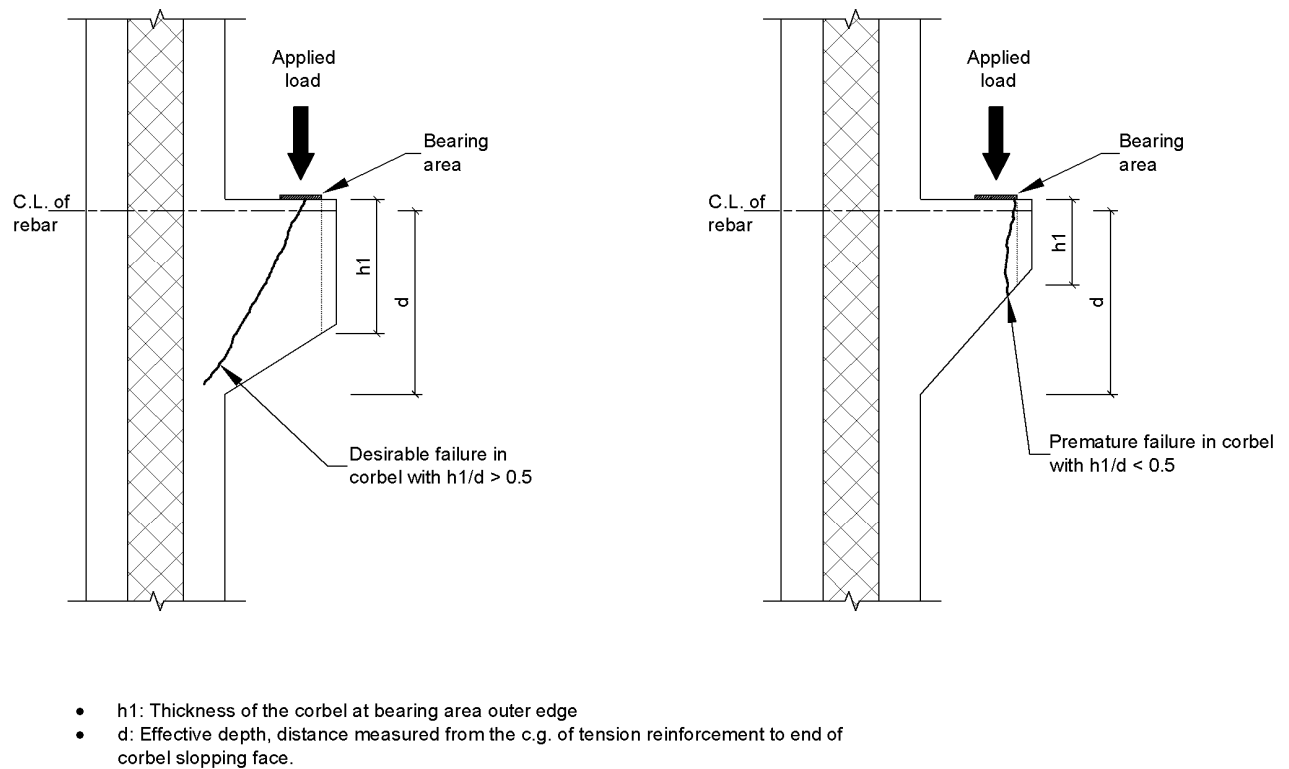


Figure 2-3: Premature failure by too shallow corbel depth at tip

- Depth of corbel at bearing should be at least half the effective depth ( $0.5 d$ ). This recommendation was included to prevent a premature crack surface. This crack could start below the bearing area and propagate to the outer sloping face of the corbel or bracket ACI 318 (2011). Refer to Figure 2-3.
- Amount of tension reinforcement  $A_s$  should not be less than  $0.004 bd$ . The minimum reinforcement ratio recommendation have the same purpose of the increasing the design loads. Once the corbel cracks the reinforcement will maintain the cracks to an acceptable width.

- Closed stirrups  $A_v$  should be provided, At least  $0.5 A_s$  and these stirrups should be distributed within the upper two thirds of the effective depth. This recommendation was based on the observation that horizontal stirrups are very effective

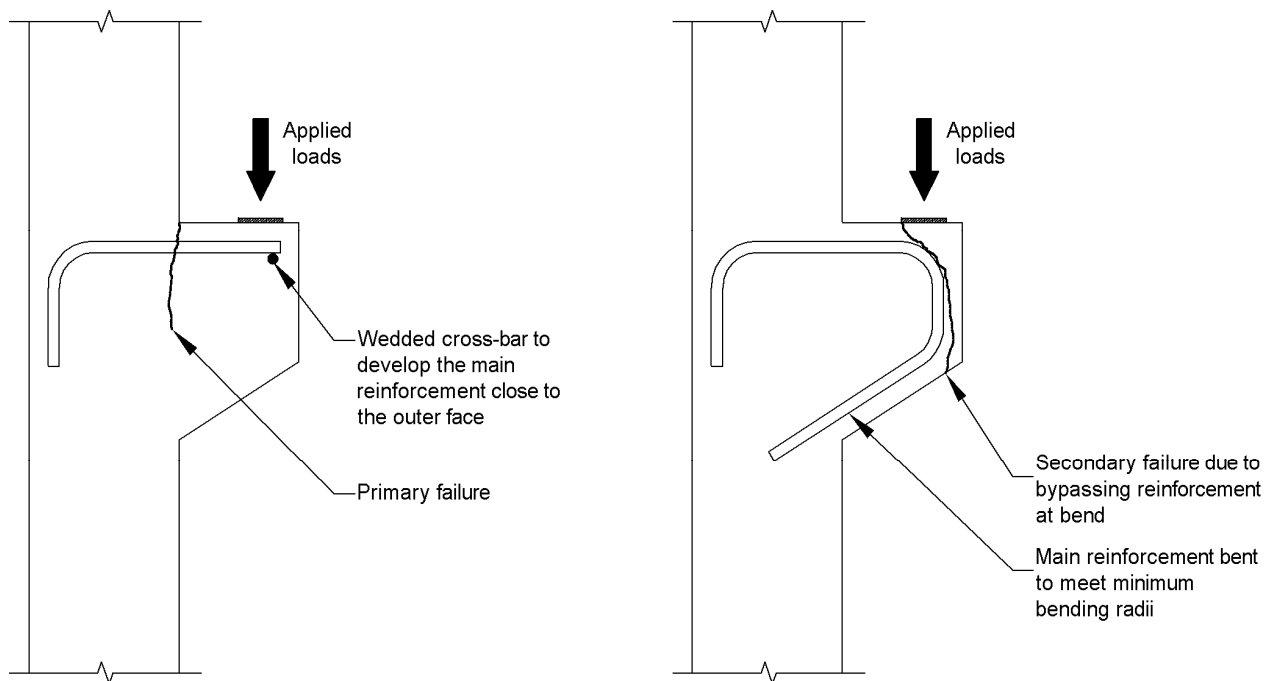


Figure 2-4: Secondary failure due to poor detailing

- Tension reinforcement should be anchored as close as possible to the face of the corbel. Kriz recommended the use of a cross-bar welded to the main reinforcement. This detail ensures the development of the main tensile reinforcement very close to the corbel outer face. Other details of anchorage may cause a secondary failure. Refer to Figure 2-4.
- Bearing plates should be kept at least 2 inch from the face of the corbel. Bearing stress at the load should be less than  $0.5 f'_c$ . These recommendation is in line with the code provisions for the maximum allowable bearing stress. Some specimens experienced a second-

ary failure where the bearing plate was located at a distance closer than 2 inch. It is critical to insure that the expected rotation of the supported elements can be accommodated within the actual distance provided (considering tolerance).

### 2.3.2. Mattock et al.

The work done by Mattock et al. (1976) was a continuation for the research done by Kriz, L. B. and Raths, C. H.(1965) . Mattock et al. (1976) based his work on previous researches about the simultaneous action of bending moment and shear-friction at the same cross section. In Mattock's work new design equations were developed to replace the empirical equations developed by Kriz, L. B. and Raths, C. H.(1965). Figure 2-5 illustrates the forces considered by Mattock et al. (1976). Mattock et al. (1976) carried out experimental study to verify the proposed design equations. The main conclusion of Mattock's study is that the corbel ultimate strength can be taken to be the lesser of the following:

- a) Shear strength of the corbel-column interface, calculated using the shear-friction provisions
- b) Vertical load corresponding to the ultimate flexural strength of the corbel-column interface.

$$\sum f_y = 0 \rightarrow V_u = \mu C \quad \text{Equation (3)}$$

$$\sum f_x = 0 \rightarrow N_u = \phi A_s f_y + \phi A_h f_{vy} - C \quad \text{Equation (4)}$$



$$\sum M_{@C} = 0 \rightarrow V_u \cdot a + N_u \cdot (h - d + jd) = \phi A_s f_y \cdot (jd) + \phi A_h f_{vy} \cdot (j_1 d) \quad \text{Equation (5)}$$

By substituting the value of  $jd$  in Equation 5 and conservatively neglecting the contribution of stirrups reinforcement to the flexural strength:

$$A_s = \frac{V_u + N_u(h - d)}{\phi f_y j' d} + \frac{N_u}{\phi f_y} \quad \text{Equation (6)}$$

$$A_s = A_f + A_t \quad \text{Equation (7)}$$

Eliminating  $C$  between equations 3 and 4 and assuming  $f_y = f_{vy}$ :

$$A_h = \frac{V_u}{\phi \mu f_y} + \frac{N_u}{\phi f_y} - A_s \quad \text{Equation (8)}$$

$$A_h = A_{vf} + A_t - A_s \rightarrow A_h = A_{vf} - A_f \quad \text{Equation (9)}$$

Where:

$A_f$ : area of reinforcement necessary to resist the applied moment  $[V_u \cdot a + N_u \cdot (h - d)]$

$A_t$ : area of reinforcement necessary to resist the horizontal force

$A_{vf}$ : area of reinforcement necessary to resist the applied shear force using shear friction

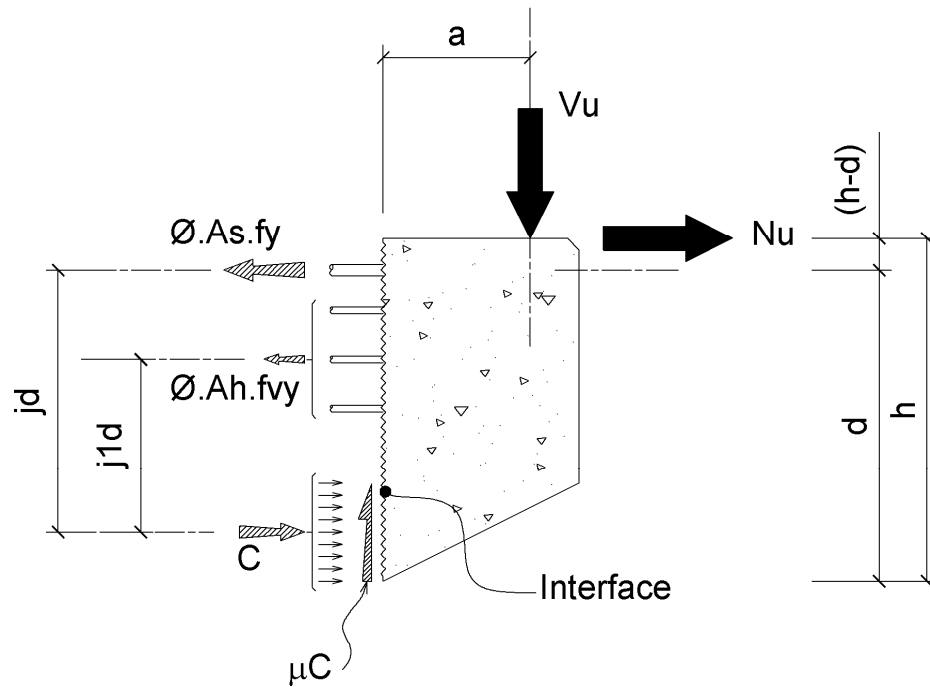


Figure 2-5: Corbel free-body diagram Mattock et al. (1976)

Mattock et al. (1976) based his recommendation for the minimum horizontal reinforcement on previous researches done on the concrete strength of beams without stirrups. These recommendations were verified by the experimental program. Mattock et al. (1976) concluded:

$$\rho_h f_{vy}(\text{min.}) = \frac{V_u}{bd} - 150 \left( f'_c \rho \frac{d}{a} \right)^{1/3} \quad \text{Equation (10)}$$

The experimental program of Mattock's et al. (1976) study consisted of 28 corbel specimens, and included variables of; Ratio of shear span to effective depth, ratio of horizontal to vertical force, amount of tension reinforcement and stirrups and type of concrete aggregate.

## 2.4. Recommended provision by various standards

### 2.4.1. ACI318-11

ACI 318 (2011) recognizes 4 failure modes for the corbel; shearing along the interface, yielding of the tension tie, crushing or splitting of the compression strut and local bearing or shearing close to the bearing plat. Two design methods are included in the ACI 318 (2011); cantilever beam method and strut-tie method. ACI 318 (2011) classifies corbels based on the shear span/depth ratio  $a_v/d$  into 2 categories. The corbels satisfying the condition  $1.0 < a_v/d$  are permitted to be designed using series of design equations based on tests by Kriz, L. B. and Raths, C. H.(1965) and Mattock et al. (1976). Corbel with longer spans  $1.0 < a_v/d < 2.0$ , the strut and tie method are the only permitted method for design. For corbels having relatively large spans  $2.0 < a_v/d$ , the corbel design provisions are cannot be used; therefore the designer is limited to the beam flexural and shear provisions.

The limit set on using the Cantilever-beam method  $1.0 < a_v/d$  was historically adopted for (2) reasons; (a) The Cantilever-beam method was not verified for  $a_v/d$  greater than unity, (b) Horizontal stirrups are insufficient for corbels with larger span since the diagonal tension cracks will be closer to the horizontal axis. Since the Cantilever-beam method was not verified for corbels with  $N_u/V_u$  greater than unity, The ACI 318 (2011) adopted this horizontal to vertical force ratio.

Shear failures are more predominant in corbel, therefore ACI 318 (2011) adopted the use of strength reduction factor equal to  $\phi = 0.75$ .

The maximum shear-friction strength of corbel-column interface could be used as a sizing guidance for the corbel cross section made of normal weight concrete. Equations 11, 12 and 13 list the different limits for various ranges on concrete strengths.

$$V_n \leq 0.2f'_c b d, \text{ governs for } f'_c \leq 4 \text{ ksi} \quad \text{Equation (11)}$$

$$V_n \leq (480 + 0.08f'_c) b d, \text{ governs for } 14 \text{ ksi} > f'_c > 4 \text{ ksi} \quad \text{Equation (12)}$$

$$V_n \leq 1600 b d, \text{ governs for } f'_c \geq 14 \text{ ksi} \quad \text{Equation (13)}$$

The corbel depth at outside edge of the bearing plate cannot be less than  $0.5 d$  where  $d$  is the effective depth at the columns interface. This minimum depth is set by the ACI 318 (2011) to provide a sufficient strength against a possible vertical crack starting close to the outer edge of the bearing area and propagating till it reaches the sloped face of the corbel.

The following reinforcement requirements are required to be calculated by ACI 318 (2011) cantilever-beam method:

$A_{vf}$ : Area of shear-friction reinforcement to resist direct shear  $V_u$

$A_f$ : Area of flexural reinforcement to resist moment  $[V_u \cdot a_v + N_u(h - d)]$

$A_n$ : Area of tensile reinforcement to resist direct tensile force  $N_u$

The placement of reinforcement in corbels is categorized in (2) locations:

$A_{sc}$ : Area of primary tension reinforcement, larger of  $A_f + A_n$  and  $\frac{2}{3} A_{vf} + A_n$

$A_h$ : Area of horizontal reinforcement equal to  $0.5(A_{sc} - A_n)$ , placed within adjacent  $\frac{2}{3} d$  from the primary reinforcement.

ACI 318 (2011) mandates a minimum primary reinforcement for corbel cross section as serviceability requirement. This minimum requirement is used to insure against opening of cracks too widely.

$$A_{sc \min} = 0.04 \frac{f'_c}{f_y} bd \quad \text{Equation (14)}$$

Anchorage of the primary reinforcement is highlighted to be critical by ACI 318 (2011). The anchorage could be achieved by several ways; welding to a cross bar or armor angle and bending the bar horizontally.

#### 2.4.2. PCI design handbook

PCI Handbook (2010) adopts the same methods mentioned in the ACI 318 (2011). However the design hand book simplifies the design equations further.

$$A_f = \left[ \frac{V_u \cdot a_v + N_u(h - d)}{\phi f_y d} \right] \quad \text{Equation (15)}$$

Approximation of ACI 318 (2011) provision by elimination the depth of the compression block compression

PCI Handbook (2010) adopts the same methods mentioned in the ACI 318 (2011). However the design hand book simplifies the design equations further.

While PCI Handbook (2010) adopts the same shear friction concept to calculate  $A_f$ , the design handbook recommended less conservative values for the shear friction coefficient to be used.

Table 2: Recommended shear friction coefficient by PCI Handbook (2010):

Crack interface condition	Maximum $\mu_e$	$V_n$
Concrete to concrete, cast monolithically	3.4	$\leq 0.30f'_c bd$ $\leq 1000 bd$
Concrete to hardened concrete, with roughened surface	2.9	$\leq 0.25f'_c bd$ $\leq 1000 bd$
Concrete placed against hardened concrete not intentionally roughened	Not applicable	$\leq 0.20f'_c bd$ $\leq 800 bd$

A comparison is done between the two methods (Cantilever-beam and strut-tie) recommended in the building code and the design handbook. Typically the Cantilever-beam method requires less primary reinforcement than strut-tie method. However, additional horizontal ties are required along the depth of the corbel which is not required in the strut-tie method. Based on the proposed truss model for the strut-tie method the, additional column ties may be required near the bottom of the corbel.

## 2.5. Strut and Tie method

Strut and tie method is relatively a new design approach. The first introduction of the strut-tie method into building codes was in ACI-318 in (2002) code edition based on the work done Schlaich et al. (1987) and Wight, J. and Macgregor, G. (2009). Before that code version, a similar design method was introduced in the AASHTO code in (1994).

The practice of structural engineer generally involves the design of two distinctive members region. The first member region is the continuous member; this member region can be designed using the beam theory (B-Region). In the B-Region, the classical principles of strain distribution (Euler–Bernoulli beam theory, 1750) can be applied. Euler–Bernoulli's theory state that, Plane sections rotate but remain plane, as long as the deformations are small and shear deformations are negligible compared to bending deformations. There are few situations where the previous theory is not applicable because of the discontinuity. The discontinuity can be; geometric or loading discontinuity. Examples of geometrical discontinuity are regions close to holes of sudden change in cross section. Loading discontinuity exist near the concentrated loads, prestressing force or reactions. Within the (D-Region) the strut-tie method could be applied successfully - Wight, J. and Macgregor, G. (2009).

Till the 1980's the design of the D-Regions was based on either good practice rules or empirical equations. Several researches were carried out by Schlaich et al. (1987) and Wight, J. and Macgregor, G. (2009) in an effort to develop accurate design approach for use with the D-Regions. The extent of the D-Region is approximately defined by (Saint Venant's principle). This principle can be interrupted that the stress concentrations (disturbance) around discontinuity regions

will eventually change to a uniform stress within a small distance. This distance can be considered equal to the member depth on both sides of the D-Region Wight, J. and Macgregor, G. (2009).

Corbels are considered to be D-Regions, both geometrical and loading discontinuity occurs at the corbel regions. This classification of corbels as D-Regions allowed the use of Strut-Tie method in designing corbels. Figure 2-6 defines the D-Regions and B-Regions for corbel connection.

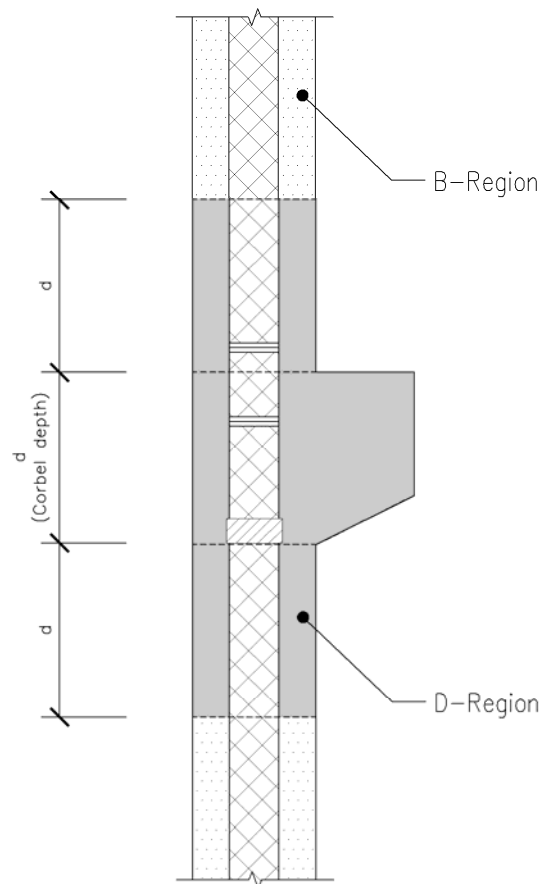


Figure 2-6: D-Regions and B-Regions in corbel connection



D-Regions behave in an elastic manner up to the cracking. After cracking the stress flow changes into a different orientation. These new orientation could be modeled using the strut–tie elements in order to estimate the ultimate capacity of the region.

Strut and tie method modeling uses 3 components; Strut, Ties and Nodes. Struts are the basically concrete members responsible for carrying the compressive stresses. Struts could be prismatic, tapered or bottle-shaped, obviously prismatic struts have uniform width over it length. Bottle-shaped have wider width within the middle region of the strut length. Bottle shaped struts usually used when more stringent requirements are applied to the ends of the struts. Due to that wider dispersion of stresses at the middle region of the bottle shaped struts, transverse tensile stresses occur and usually reinforcement ties are provided to account for these tensile stresses. Compressive strength of the strut is affected by several reasons; shape of the strut, use of transverse reinforcement within the strut and the presence of the strut within a tensile zone. Therefore the design provision in different building codes permits the use of a fraction of  $f'_c$ , in ACI 318 (2011) the usable compressive strength of struts is defined as follows:

$$F_{ns} = 0.85 \beta_s f'_c \quad \text{Equation (16)}$$

Where  $\beta_s$  ranges from 0.4 to 1.0

Tie elements are responsible for transferring the tensile forces among the joints of the chosen truss and the supports points. Detailing and anchorage of ties are crucial for its effectiveness; ties may fail due to lack of anchorage and the nodal zones. Prestressing reinforcement (if present)

could be utilized as part of the ties strength. A concrete prism is required by ACI 318 (2011) to surround the tie reinforcement; the function of this prism is to define the width of the nodal zones and to increase the axial stiffness of the tie Wight, J. and Macgregor, G. (2009).

$$F_{nt} = A_s f_y + A_{ps} (f_{se} + \Delta f_p) \quad \text{Equation (17)}$$

The last component of the strut-tie model is the Node or Nodal zones. Nodal zones are the limited regions where the different truss forces meet. Nodal zones can be classified to CCC, CCT and CTT based on the types of forces meet at the node (Compression or Tension). Hydrostatic nodal zones are a term for the nodes where 3 forces at a node and the node side length are proportioned to the magnitude of the force. In these nodes the stress is equal in all directions. The strength of nodal zones according to ACI 318 (2011) is dependent on the type of forces meeting at the node.

$$F_{nn} = 0.85 \beta_n f'_c \quad \text{Equation (18)}$$

Where  $\beta_n = 0.65$  for CTT,  $0.80$  for CCT and  $1.0$  for CCC

There are several possible layouts for the strut-tie truss, the layout should as close as possible to the expected post-crack behavior. The more realistic the elements layout is considered, the less reinforcement content required and the less crack width. ACI 318 (2010) recommends struts angle ranges from  $25^\circ$  to  $65^\circ$ .

# CHAPTER 3

## 3. Proposed connections

### 3.1. Design

In order for this study to propose a sound, adequate and practical connection, the design criteria for connections included the following aspects:

- Preservation of the thermal break
- Flexural capacity
- Durability and fire endurance
- Expected rotation of corbel (rotation of support)

Several corbel connection proposals that satisfy the above criteria were studied and evaluated. In general the tension element of the connection was the main variable. The selection preferences was based on; availability of the basic components, expected strength and practicality of fabrication. Out of the studied possibilities for the tension element were:

- Threaded GFRP rod with nut, at the corbel side and/or both sides
- Bell shaped GFRP bars
- Several bend configurations for the GFRP bars
- FRP Hollow structural section (HSS)

Corbel connections are subject to horizontal loads transferred to connections from the supported elements. Various sources can result in that horizontal force, volume changes of the supported element is one of the major sources for the horizontal force. The ACI 318 (2011) mandates a minimum horizontal force equal to 20% of the vertical design force to be including in the corbel design. Kriz, L. B. and Raths, C. H.(1965) and Mattock et al. (1976) developed a rational procedure to include horizontal force in the design. In this study the horizontal force were not included in the analysis or the testing. However, however based on the work of Kriz, L. B. and Raths, C. H.(1965) and Mattock et al. (1976) the effect can be included in the calculations.

In real life precast construction, corbels are used basically to support the floor system components (beams and slabs). A large part of the projects were precast construction is used have modular configuration. Parking structures, schools, data centers and industrial buildings are projects where precast construction is commonly used in the US practice. The proposed connection was designed with these typical building in mind, with regards to the imposed ranges, components used and range of spans. The typical floor systems used in the building types mentioned earlier are; Double-Tee and steel joist. As far as the connection design, Double tee is more critical. The reason is the greater self weight reaction of Double-Tee if compared to the steel joist.

Figure 3-1 illustrates the reference components used in this study to describe the corbel connection.

The proposed connection must satisfy two limit states to be considered acceptable; Ultimate limit state and service limit state. Similar to the typical corbel connection design, flexural strength, shear strength and bearing strength is applicable to the proposed connection. The service limit

strength are considered be minimizing any excessive cracking or rotation at the support. Refer to Appendix A for the adopted loading criteria.

In addition to the mentioned limit states, since the proposed connection uses mostly GFRP bars as a basic load carrying components. The creep rupture is included as one of the limit states.

GFRP reinforcing bars will be subjected to a constant load over time, during this constant loading can GFRP suddenly fail after a time period called the endurance time. This phenomenon is known as creep rupture. Creep rupture is insignificant with steel bars in reinforced concrete except in extremely high temperatures. As the ratio of the sustained tensile stress to the short-term strength of the GFRP bar increases, endurance time decreases. As will be concluded later in this study, the creep rupture will be the governing limit state in many cases. Refer to ACI 440 (2006).

The loading and system criteria mentioned earlier are thought to be adequate for large part of the precast construction in the US market. Based on that criteria the following loads is set to be “target loads”, and the connections is considered adequate if meets or exceeds these loads:

- Factored load = 42 kip
- Service load = 28 kip
- Sustained load = 20 kip

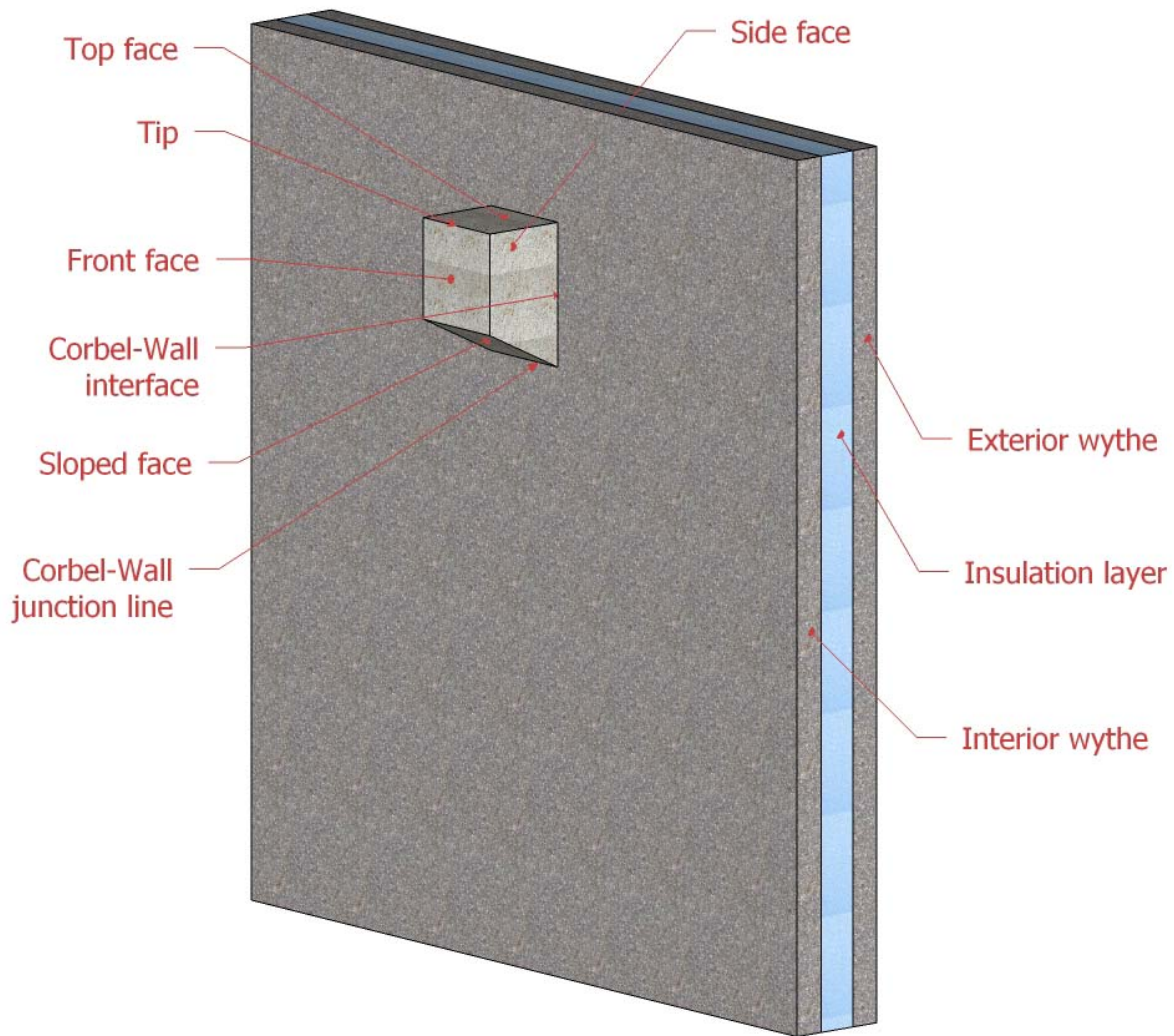


Figure 3-1: Geometric terms used in this study

Each of the proposed connection adopted a certain system to transfer the applied to the external support points. Generally the connection purpose is to transfer the applied load and the corresponding moment from the corbel to the wall wythes. In precast insulated walls, the wythe thickness is relatively small (3 to 5 inch) if compared to the solid walls (8 to 12 inch). The transfer of the corbel reaction to the supporting wall becomes a challenge to the designer. Typically, the corbel rebar can be bent into the solid walls; rebar detail transfers the tension force within the bar

to the wall through bond, mechanical interlocking between the rebar ribs and wall concrete and by bearing at bent portion. Meanwhile, these forces usually available in the solid walls have limited capacity in the insulated walls. This limited capacity is due to the thinner concrete cross sections. The next step after transferring the load successfully to the insulated wall is to assure that the wall will be capable to transfer these forces back to the supports. A single wythe is seldom capable to do that. The typical single wythe thickness of 3 in. to 5 in. will mostly crack severely or experience an excessive rotation. Therefore, a superior corbel connection design will engage the both wall wythes to minimize the cracking and provide a limit the rotation of the corbel. The engagement of both wythes is more effective is provided at the corbel location. However, the composite connectors used at many locations over the wall panel offer another way to ensure the wythes work compositely.

Specimens A1, A2, A3, A4 and A5 use similar structural system to resist the externally applied eccentric force resulting in bending moment and shear force. The bending moment is the critical components in corbel connections. Figure 3-2 and Figure 3-3 show a 3D view for specimen A2 components. Figure 3-4 and Figure 3-5 illustrate the load path for specimens A2 and A1 respectively:

1. The vertical applied force to the corbel is transferred to the corbel by bearing to the top surface of the corbel
2. After the cracking stage, the bending moment is resisted by tension force in the top horizontal stirrups and compression stress block (Whitney's stress block) near the corbel-wall junction. The force in the stirrups decrease linearly as the tie distance from plastic

neutral axis decrease. Therefore, the lowest horizontal stirrup is ignored in the calculations

3. Tension force in the stirrups then transferred to the anchorage bar by direct bearing (rebar-rebar) and/or bearing through concrete (rebar-concrete-rebar). The stirrups are oriented that the continuous side encloses the anchorage rebar. The stirrups overlapping legs are thought to be a less strong side; therefore this side is embedded in the corbel where enough embedment could be assured
4. Shear force (equal to the applied force) is transferred to the interior wythe through friction at the corbel-wall interface. However, this interface will be cracked at loads close to failure loads; the force can still be transferred by shear friction concept in addition to contact shear at the un-cracked part (compression stress block)
5. Specimen A1 anchorage bar works as a beam, loaded with 2 point loads from the stirrups and. This beam is supported by at 1 point with the NU-Ties and with bearing stress between the anchorage bar and the concrete. In specimen A2, the bearing supports of the concrete was replaced by another NU-Tie. In specimen A1, the level of the NU-tie support was lower than the applied load. This location of load caused the anchorage bar to work in a similar way to a beam with overhang. The difference in behavior is clear in failure diagrams in chapter 4. In case of specimen A2, the applied point loads to the anchorage bar are not equally spaced from the support points (NU-Ties), this eccentricity of the loading imposes higher reaction on the lower NU-Tie.



6. Compression stress block near the corbel-wall junction results in bearing stress applied to the interior wythe. Large transverse rebar are used to reinforce this zone to distribute this force to a wider area of the wythe in order to avoid possible failure in bearing.

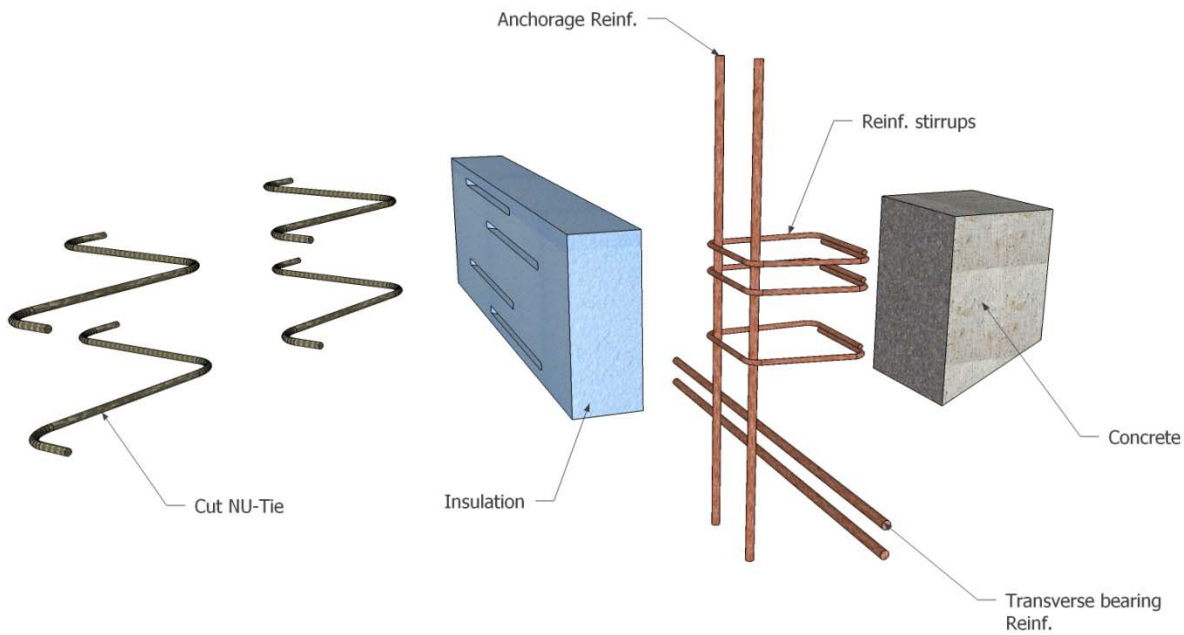


Figure 3-2: Various components of NU-Ties system for Specimen A2

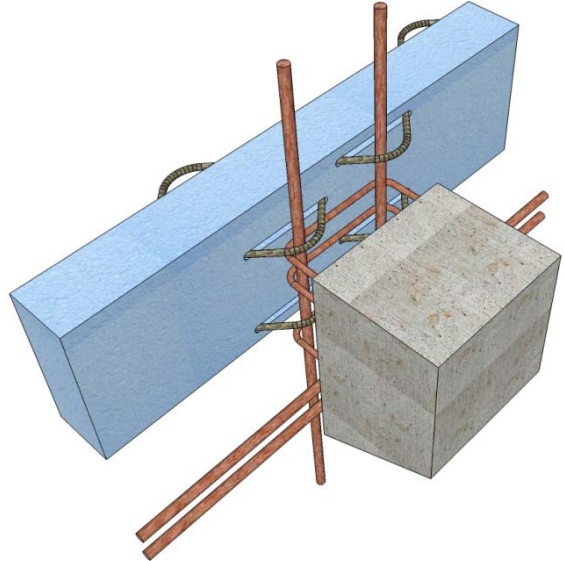
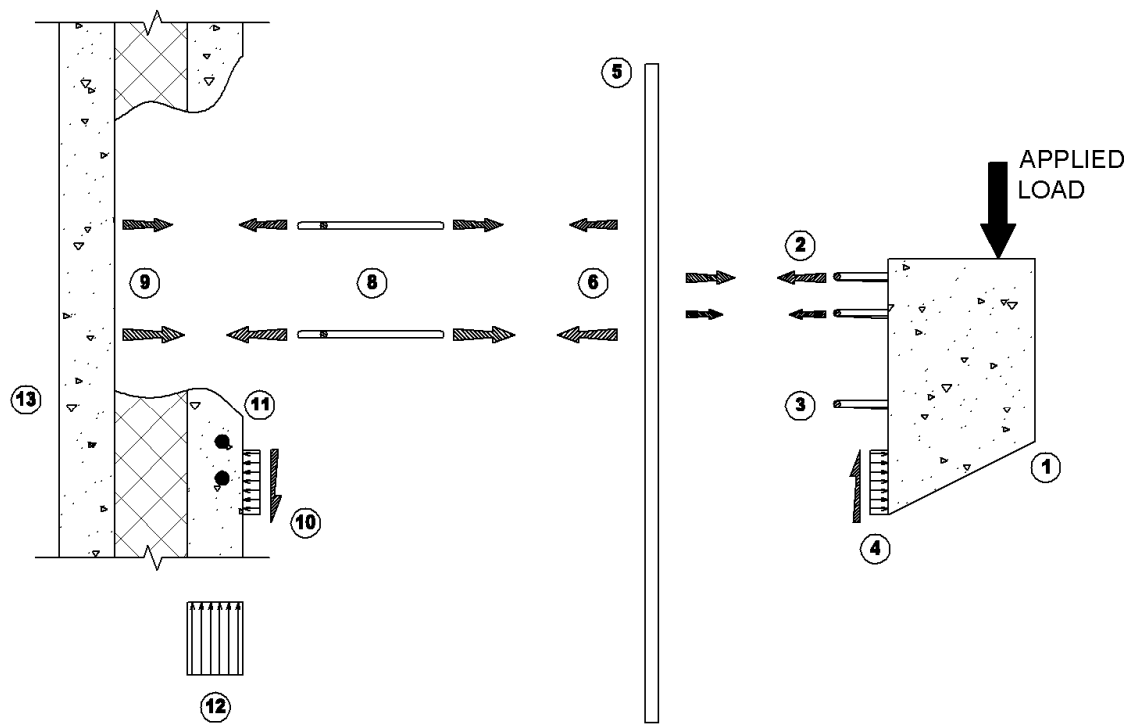
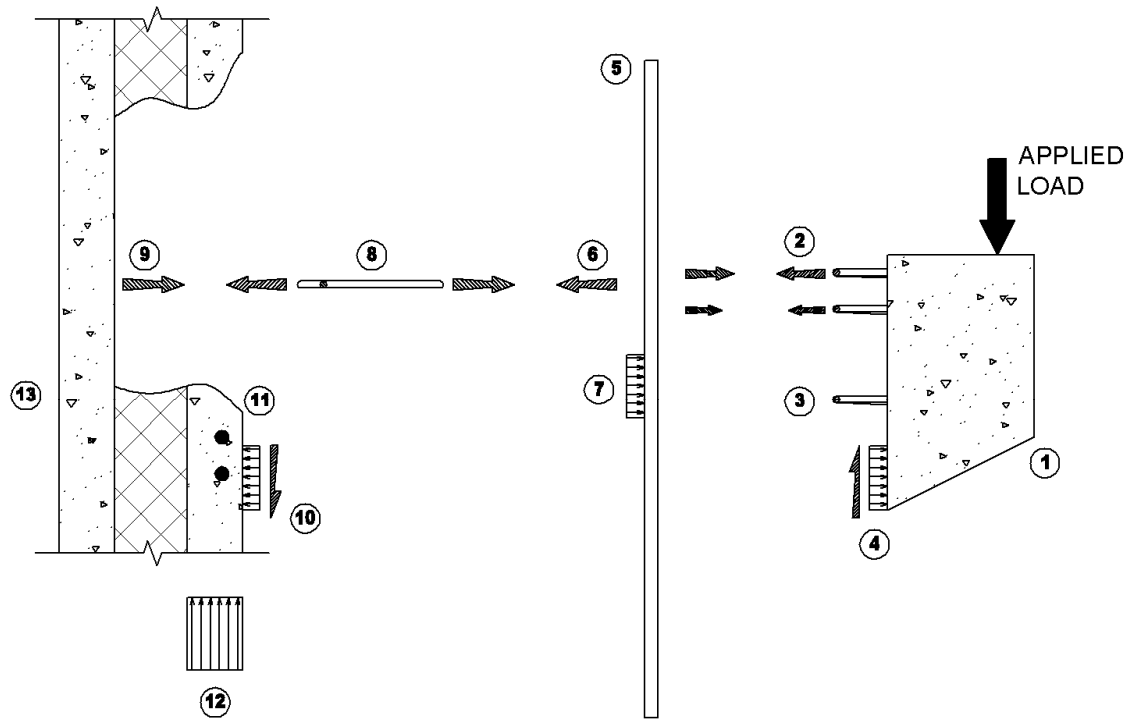


Figure 3-3: Assembled NU-Ties system for Specimen A2



- 1: Prefabricated corbel block
- 2: Tension forces in top steel stirrups
- 3: Bottom steel stirrups, conservatively ignored
- 4: Compression force/stress and corresponding friction between corbel and the interior wythe
- 5: Anchorage rebar
- 6: Reaction tension force in NU-Ties due to ②
- 7: Not used
- 8: NU-Tie
- 9: Tension force transferred to exterior wythe by anchorage of NU-Tie
- 10: Compression force/stress and corresponding friction between corbel and the interior wythe
- 11: Transverse rebar to distribute compression force
- 12: Vertical force/stress equal to the applied load in interior wythe
- 13: Exterior wythe

Figure 3-4: Free body diagram – Specimen A2



- 1: Prefabricated corbel block
- 2: Tension forces in top steel stirrups
- 3: Bottom steel stirrups, conservatively ignored
- 4: Compression force/stress and corresponding friction between corbel and the interior wythe
- 5: Anchorage rebar
- 6: Tension force in NU-Ties due to bending moment by ②
- 7: Bearing force/stress due to eccentric loading on the anchorage bar due to bending moment by ②
- 8: NU-Tie
- 9: Tension force transferred to exterior wythe by anchorage of NU-Tie
- 10: Compression force/stress and corresponding friction between corbel and the interior wythe
- 11: Transverse rebar to distribute compression force
- 12: Vertical force/stress equal to the applied load in interior wythe
- 13: Exterior wythe

Figure 3-5: Free body diagram – Specimen A1

7. In specimens A3, A4 and A5, additional non-conductive compression element (GFRP pin) were used. The purpose of this element is to enhance the compression stress sharing between the interior and exterior wythes and reduce the deformation

8. The NU-Ties are capable of transferring the tension force to the exterior wythe. The NU-Ties system uses the anchorage and bearing forces between the NU-Tie and the concrete. Large number of tests has been carried out on the NU-Ties embedment requirements. The tension force transferred from the NU-ties to the walls will cause the exterior wythe to bend towards the insulation (the wythe thickness as depth). This bending of the wythe will share part of the tension force with the interior wythe. Both wythes will finally transfer this force as a beam to the horizontal supports
9. Shear force transferred from the corbel to the interior wythe is resisted by the wall interior wythe. This vertical force results in bearing stress in the interior wythe. Since both wythes are designed to work compositely by providing composite connectors, this bearing stress eventually will be shared between both wythes. At the wall panel bottom support, this shear force will be transferred to the support
10. In typical precast construction the mentioned vertical supports and horizontal supports are foundation and floor diaphragm respectively.

Figure 3-6 and Figure 3-7 show a 3D view for specimen A3, A4 and A5 components, and Figure 3-8 load path for same specimens (A3, A4 and A5).

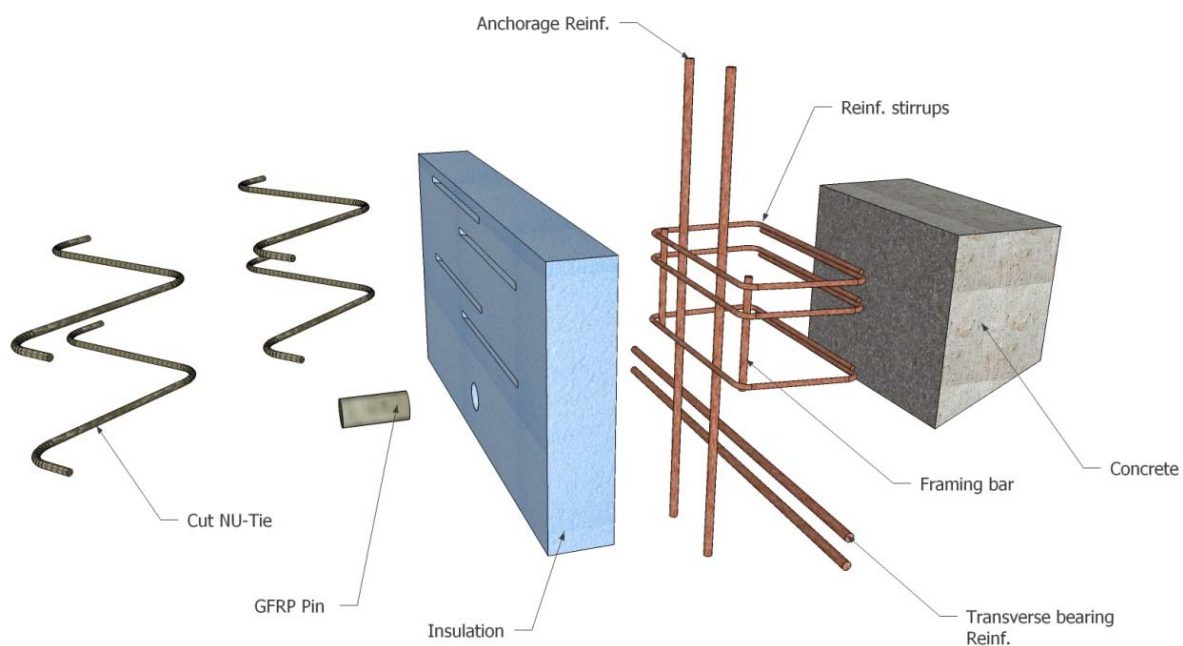


Figure 3-6: Components of Modified NU-Ties system, Specimens A3, A4 and A5

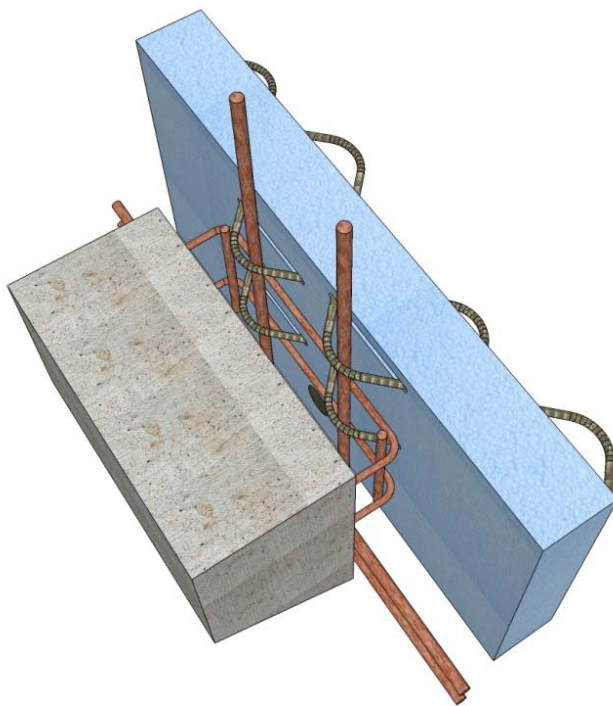
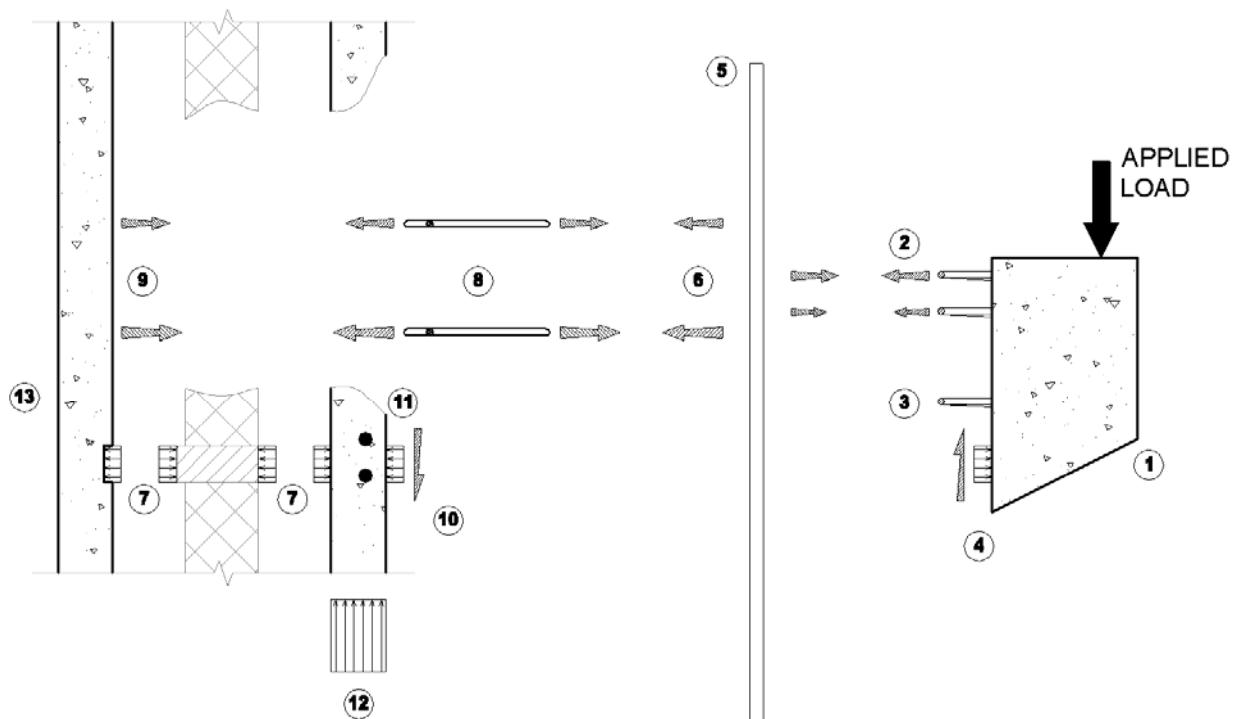


Figure 3-7: Assembled Modified NU-Ties system, Specimens A3, A4 and A5



- 1: Prefabricated corbel block
- 2: Tension forces in top steel stirrups
- 3: Bottom steel stirrups, conservatively ignored
- 4: Compression force/stress and corresponding friction between corbel and the interior wythe
- 5: Anchorage rebar
- 6: Reaction tension force in NU-Ties due to 2
- 7: Compression force/stress transferred through the FRP from interior wythe to exterior wythe
- 8: NU-Tie
- 9: Tension force transferred to exterior wythe by anchorage of NU-Tie
- 10: Compression force/stress and corresponding friction between corbel and the interior wythe
- 11: Transverse rebar to distribute compression force
- 12: Vertical force/stress equal to the applied load in interior wythe
- 13: Exterior wythe

Figure 3-8: Free body diagram – Specimens A3, A4 and A5

Specimen B1 and B2 use a similar structural system to resist the externally applied eccentric force. Figure 3-9 and Figure 3-10 show a 3D view for specimen B2 components. Figure 3-11 and Figure 3-12 illustrate the load path for specimens B2 and B1 respectively:

Figure 3-5 illustrates the path of the applied force from application till it partially transferred to the external supports as listed next:

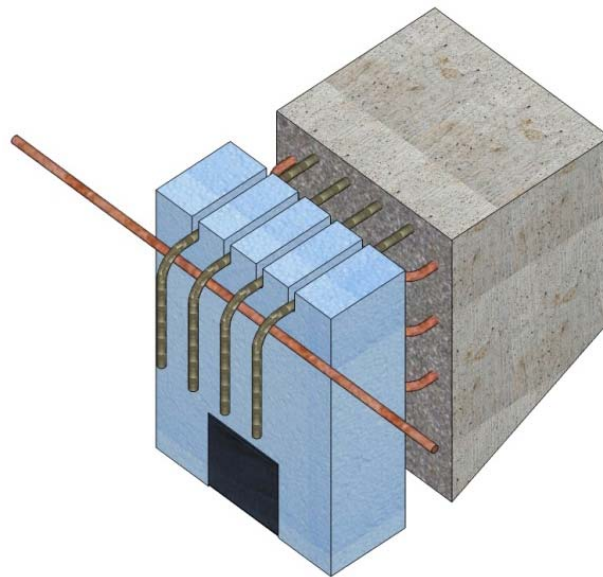


Figure 3-9: Assembled GFRP bars system, Specimen B2

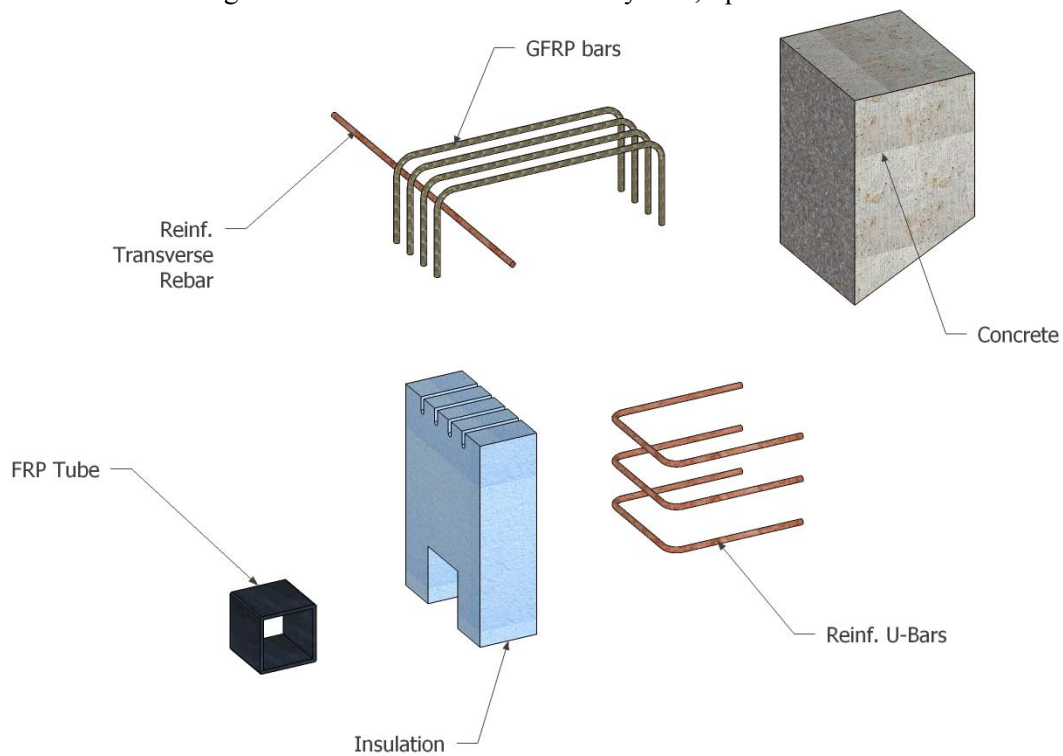
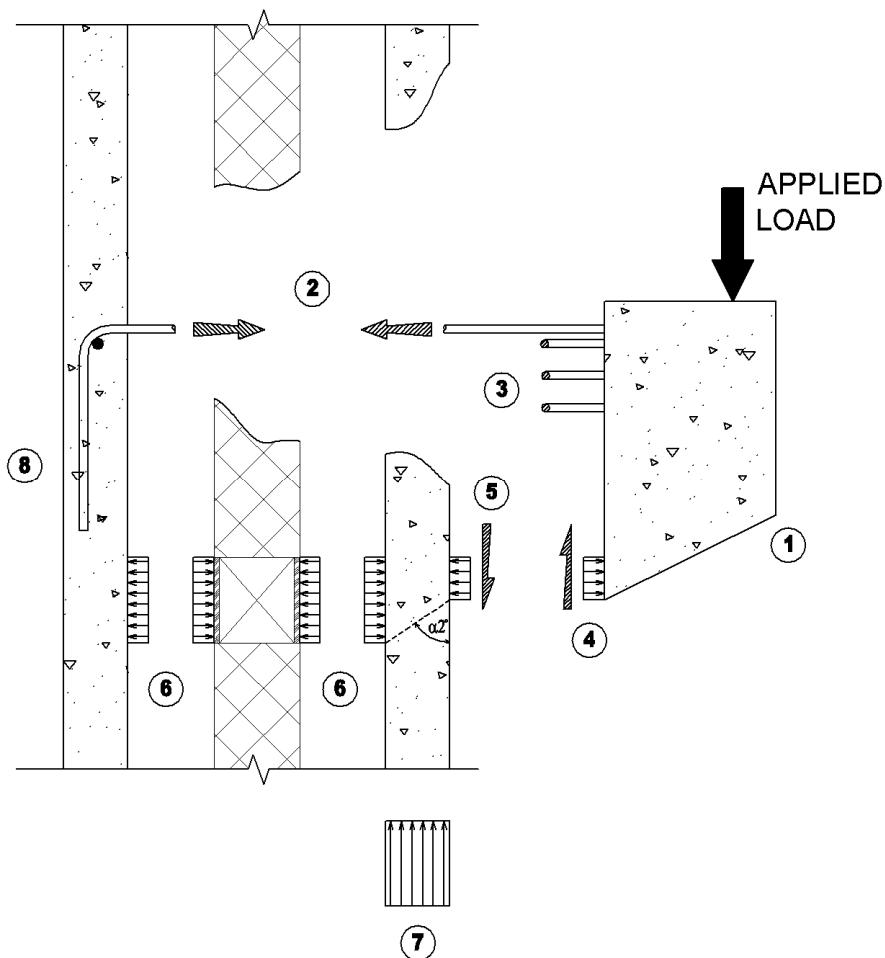


Figure 3-10: Different components of GFRP bars system, Specimen B2

1. The vertical applied force to the corbel is transferred to the corbel by bearing to the top surface of the corbel
2. After the cracking stage, the bending moment is resisted by tension force in the GFRP bars. The horizontal U-Bars of specimen B2 are not included in the flexural capacity, the U-Bars are provided to attach the corbel to the wall after rupture of GFRP bars. A compression stress block is formed near the corbel-wall junction
3. Tension force in the GFRP bars is transferred directly to the exterior wythe by means of bond and bearing - Ehsani et al.(1995).
4. Shear force (equal to the applied force) is transferred to the interior wythe through friction at the corbel-wall interface in specimen B1. As for specimen B2, the horizontal U-Bars provide more shear strength through shear friction concept
5. Compression stress block near the corbel-wall junction results in bearing stress applied to the interior wythe. Part of the compressive stress is transferred transversely by the wythe thickness as beam to the supports. The rest of this stress is transferred through the compression component -plastic lumber boards for specimen B1 and structural plastic tube for specimen B2- to the back wythe. Similar to the interior wythe, the exterior wythe transfers the compressive stress in form of reaction to external supports
6. Transverse rebar are used to reinforce the zone of GFRP bars are anchored in the back wythe. It was expected that the bars will enhance the anchorage of the GFRP bars. However these rebar were eliminated in specimen B2 since the GFRP bars ruptured close to the bend.

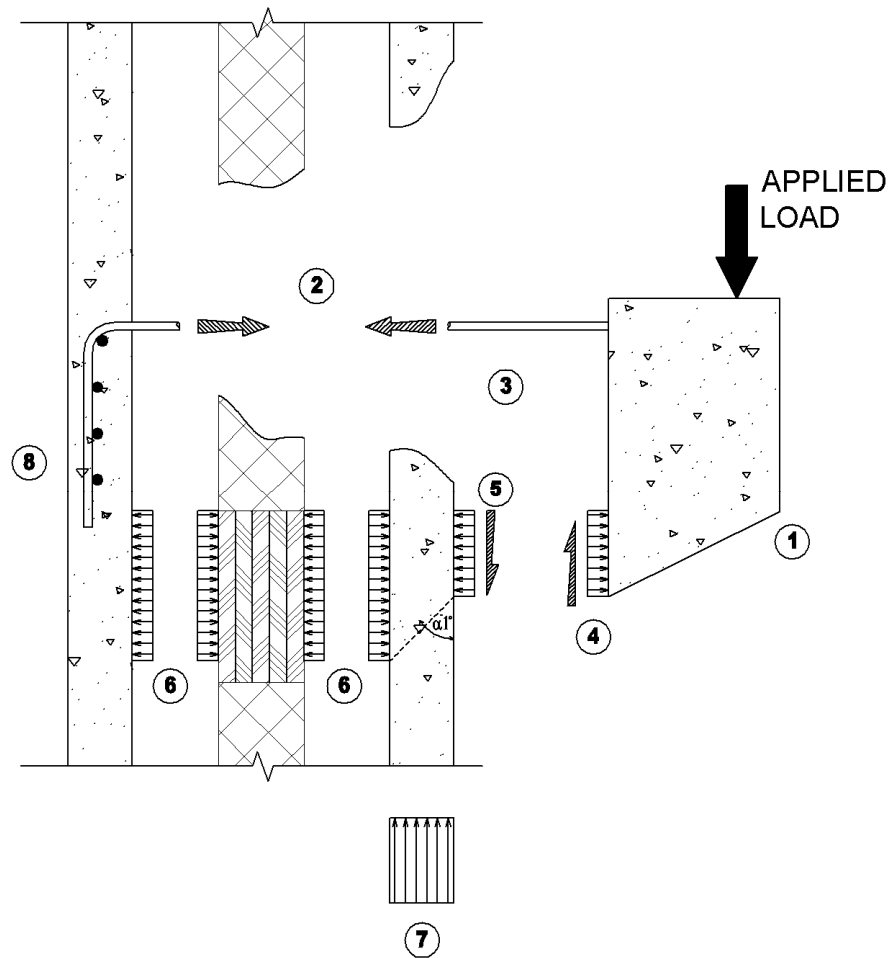


7. Since both wythes are designed to work compositely, the vertical bearing stress caused at the interior wythe will be shared between both wythes. This vertical bearing stress will be transferred to the bottom support
8. The tension force transferred from the GFRP bars to the exterior wythe will cause the it to bend towards the insulation (the wythe thickness as depth). This bending of the wythe will share part of the tension force with the interior wythe. Both wythes will finally transfer this force as a beam to the horizontal supports.



- 1: Prefabricated corbel block
- 2: Tension forces in GFRP bars
- 3: Steel stirrups, conservatively ignored
- 4: Compression force/stress and corresponding friction between corbel and the interior wythe
- 5: Compression force/stress and corresponding friction between corbel and the interior wythe
- 6: Compression force/stress transferred through the FRP from interior wythe to exterior wythe
- 7: Vertical force/stress equal to the applied load in interior wythe
- 8: Exterior wythe

Figure 3-11: Free body diagram – Specimen B2



- 1: Prefabricated corbel block
- 2: Tension forces in GFRP bars
- 3: Steel stirrups, conservatively ignored
- 4: Compression force/stress and corresponding friction between corbel and the interior wythe
- 5: Compression force/stress and corresponding friction between corbel and the interior wythe
- 6: Compression force/stress transferred through the FRP from interior wythe to exterior wythe
- 7: Vertical force/stress equal to the applied load in interior wythe
- 8: Exterior wythe

Figure 3-12: Free body diagram – Specimen B1

This paragraph will describe some of the design consideration for the proposed connections:

1. Appendix A shows the calculations procedure for specimens A2, It can be concluded from the calculations that the govern limit state was the Creep-rupture of the GFRP NU-Ties.
2. The width of the corbel was chosen to be accepted architecturally. Set 3, corbel width was changed to allow more tolerances for the anchorage bars
3. In order to fit the GFRP bars of specimens B1 and B2 in the exterior wythe, a tighter bend radius was used. This tight bend radius was different from the recommendations of the manufacture. However, the expected reduced capacity of the rebar due to the e tight bend was compensated was more rebars than needed. This is thought to be adequate since the GFRP bars are not expected to reach high levels of stresses similar to steel rebar.

### **3.2. Analysis**

The analysis is carried out using MIDAS-Gen software package. The purpose of the FEM modeling is to evaluate the behavior of the specimen within the elastic range of behavior. Since the strength was determined using the code prescribed equations and assumptions, the behavior of the connection beyond the elastic range was not included. The governing criteria of the connections design is a creep-rupture which occurs within the elastic range.

FEM models for specimens A2 and B2 only were constructed to simulate the behavior of the different connections. The results of the modeling included the expected deformation up to the elastic range. Other results similar to the support reactions were extracted.

Linear elastic materials were used to model the concrete, NU-Ties, GFRP bars and structural plastic tube. As mentioned earlier the use of elastic linear materials is suitable for the intended purpose of the FEM models. The concrete withies were modeled as three-dimensional 8 points solid elements. The solid elements were constructed on a 1x1x1 inch grid. NU-Ties, GFRP bars and tube were modeled using two-dimensional truss elements. Rotational degree of freedom was omitted at these elements ends.

Insulation layer (Expanded polystyrene) was omitted from the FEM models. The insulation material offers a compressive strength of 25 psi at relatively low elasticity modules. This non-structural layer can enhance the behavior of the specimen, however it was chosen not to rely on this layer due to various reasons; degradation of the properties along time and insufficient information about the elasticity. Figure 3-13 and Figure 3-14 show the geometry of the FEM models used.

Table 3: FEM Models - Support details

	Type	Stiffness kip/in
Vertical support	Compression Only	12000
Horizontal support Bottom	Compression Only	1000
Horizontal support Top	Tension Only	950

Table 4: FEM Models - Material details

	Material	Elastic Modules ksi	Poison ratio
Concrete	Grade C5000	4070	0.2
NU-Ties, GFRP Bars and FRP structural tube	GFRP	5890	0.2

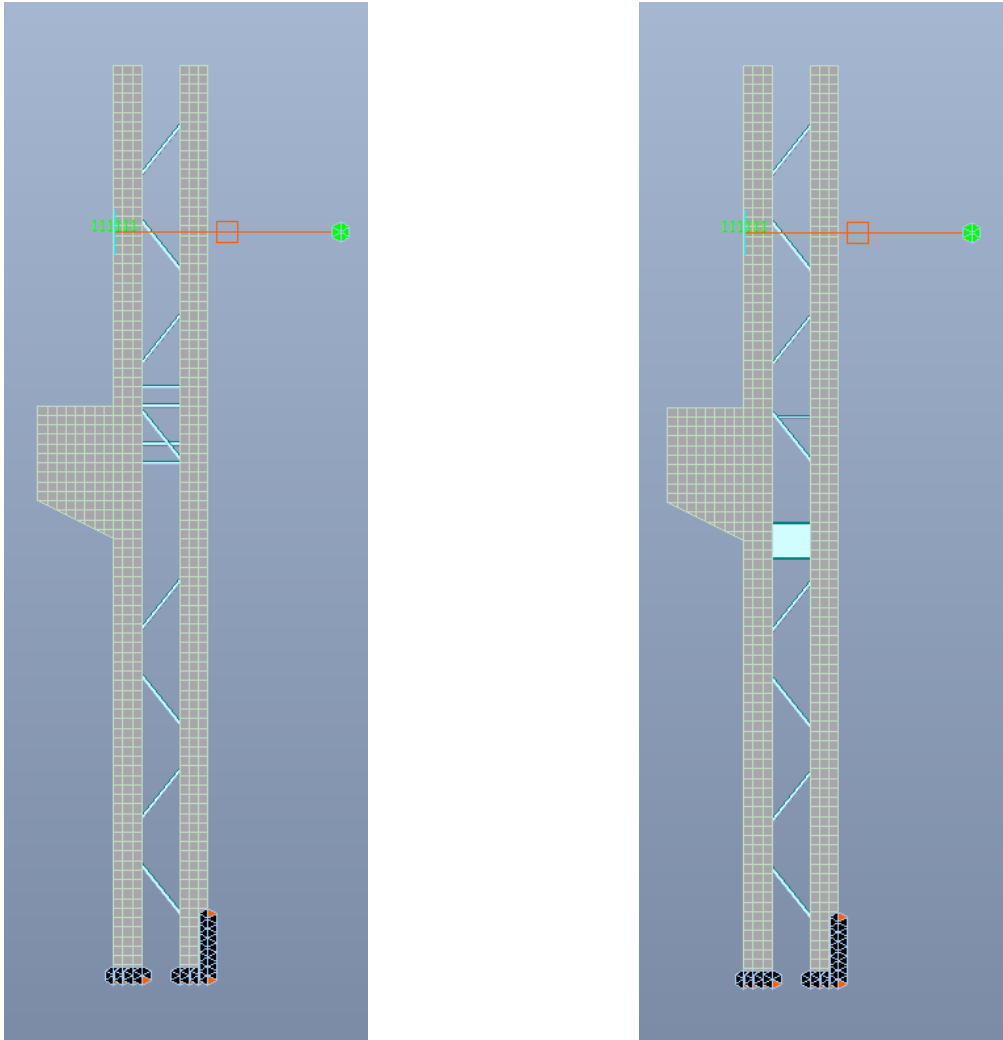


Figure 3-13: FEM Models geometry, Left: A2, Right: B2

The boundary conditions of the FEM model were equal to the actual to the testing conditions. Vertically, the full bottom edge of the wythes was used as supporting points spaced at 1x1 inch grid. These vertical supports were assigned a springs. The spring constant is equal to the values listed in Table 3. As explained in chapter 3, the lower 6 inch of the overlapping area between the

wall panel and the reactions wall were used as horizontal compression-only spring support. To form a resisting force-couple to the applied eccentric force, a top tension-only spring support was used at the location of the reaction frame. A simplified geometry was adopted for the NU-Ties and GFRP bars.

The theoretical cracking load at corbel-wall interface was used for the compression purpose, the concrete modulus of rupture is calculated using:

$$f_r = 7.5 \lambda \sqrt{f'_c} \quad \text{ACI 318 (2011)}$$

Figure 3-15 and Figure 3-16 illustrates the different deformation behavior of the two compared specimens. It is obvious that use of a compression strut at the bottom of the corbel reduces the deformation of the corbel and the rotation support. Reduction percentage of A2 deformation is approximately equal to 9%. Therefore this strut was used in specimens A3, A4 and A5. However the form of the strut is different from specimen B1 and B2.

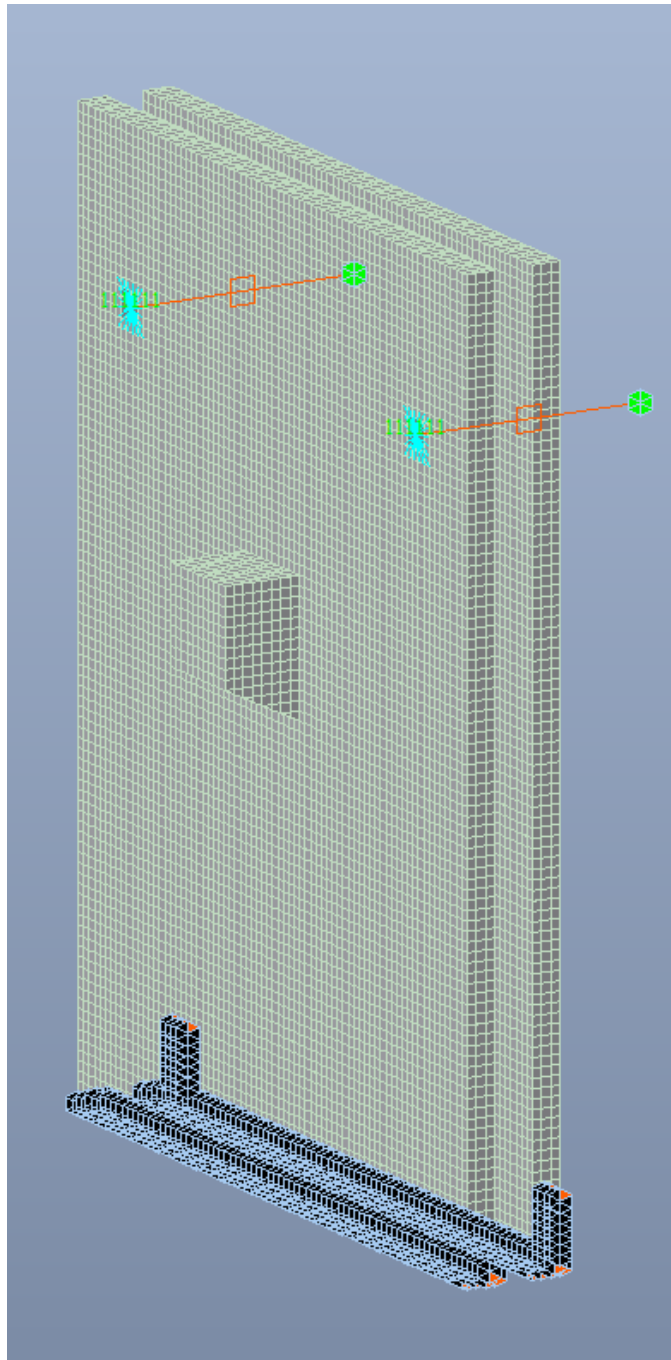


Figure 3-14: FEM Models geometry - 3D View



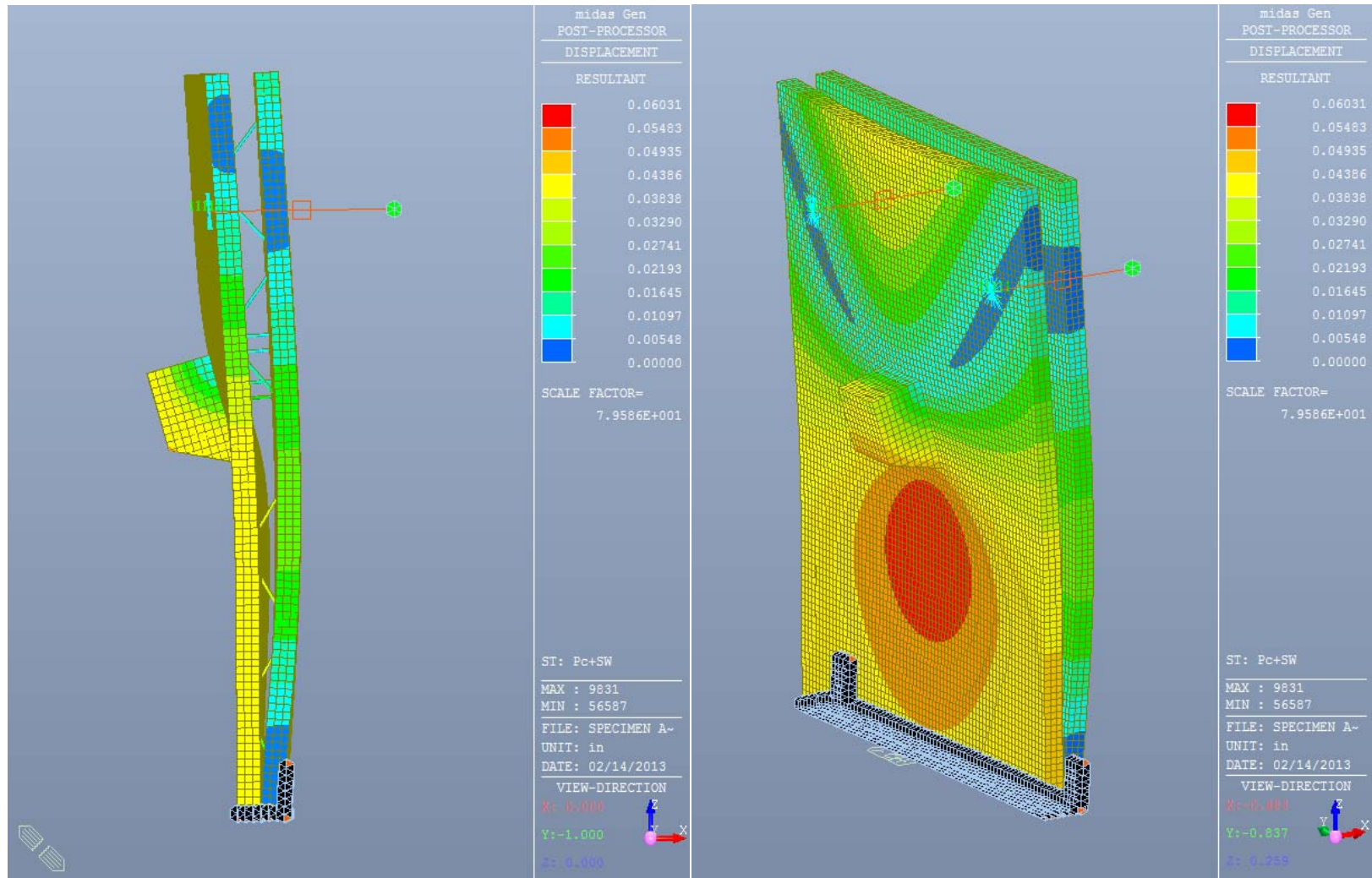


Figure 3-15: Deformed shape A2, 3D and side view

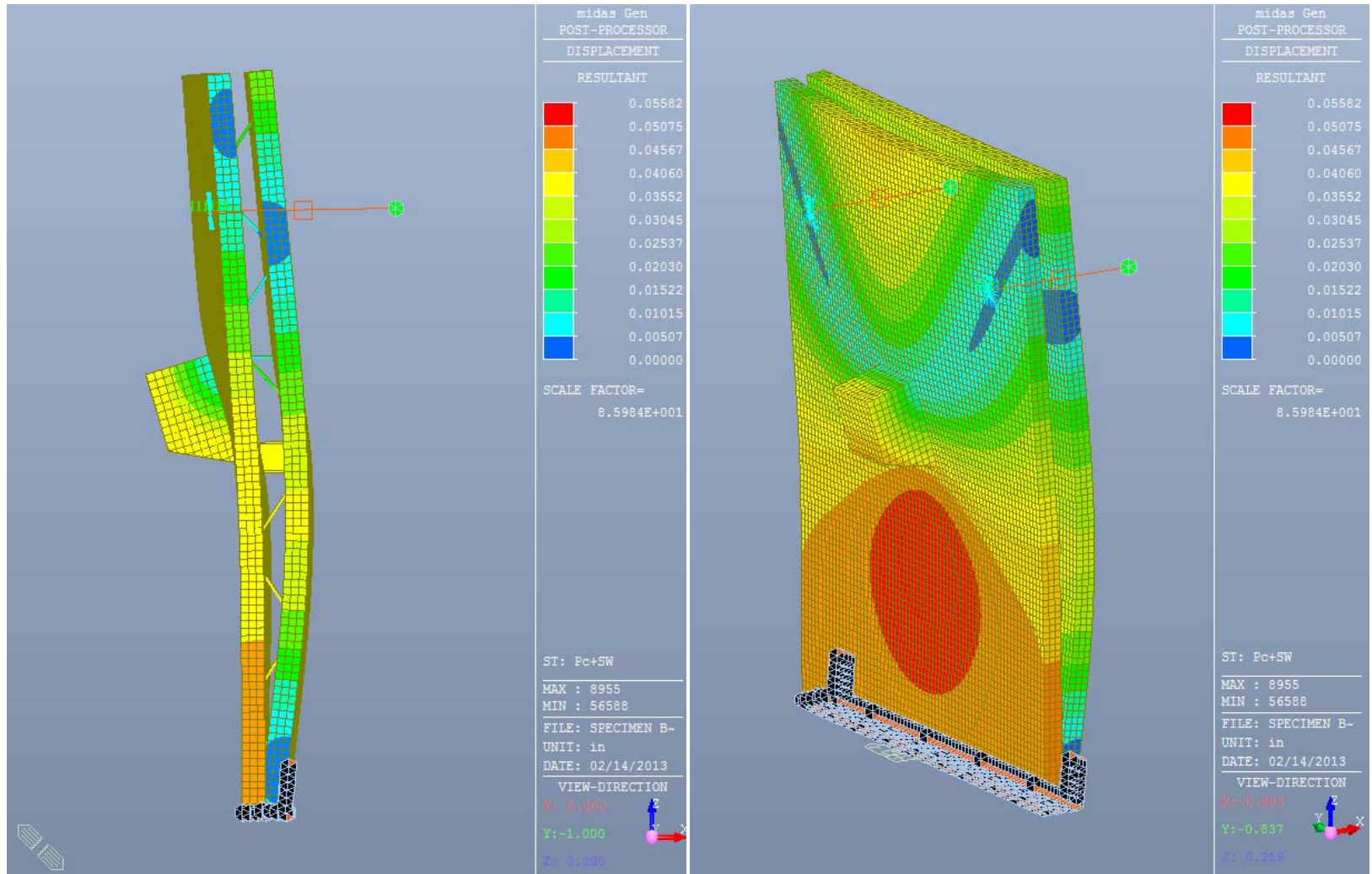


Figure 3-16: Deformed shape B2, 3D and side view

Strut and Tie model was developed for specimen B2 in order to estimate the failure load. Figure 3-17 and Figure 3-18 illustrates the different components of the strut and ties method for connection B2 along with the corresponding forces in each component.

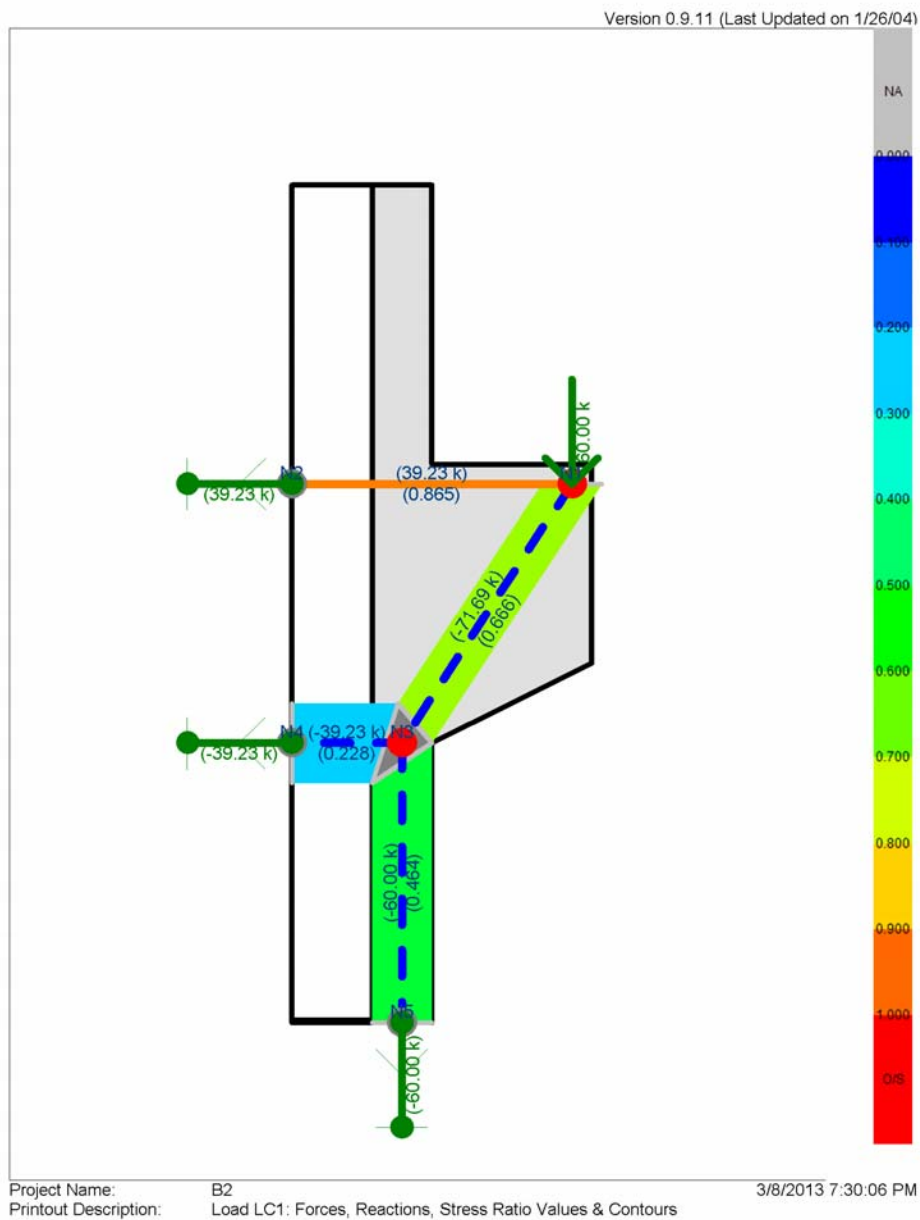


Figure 3-17: Strut and tie results for specimen B2 at 60 kip applied load

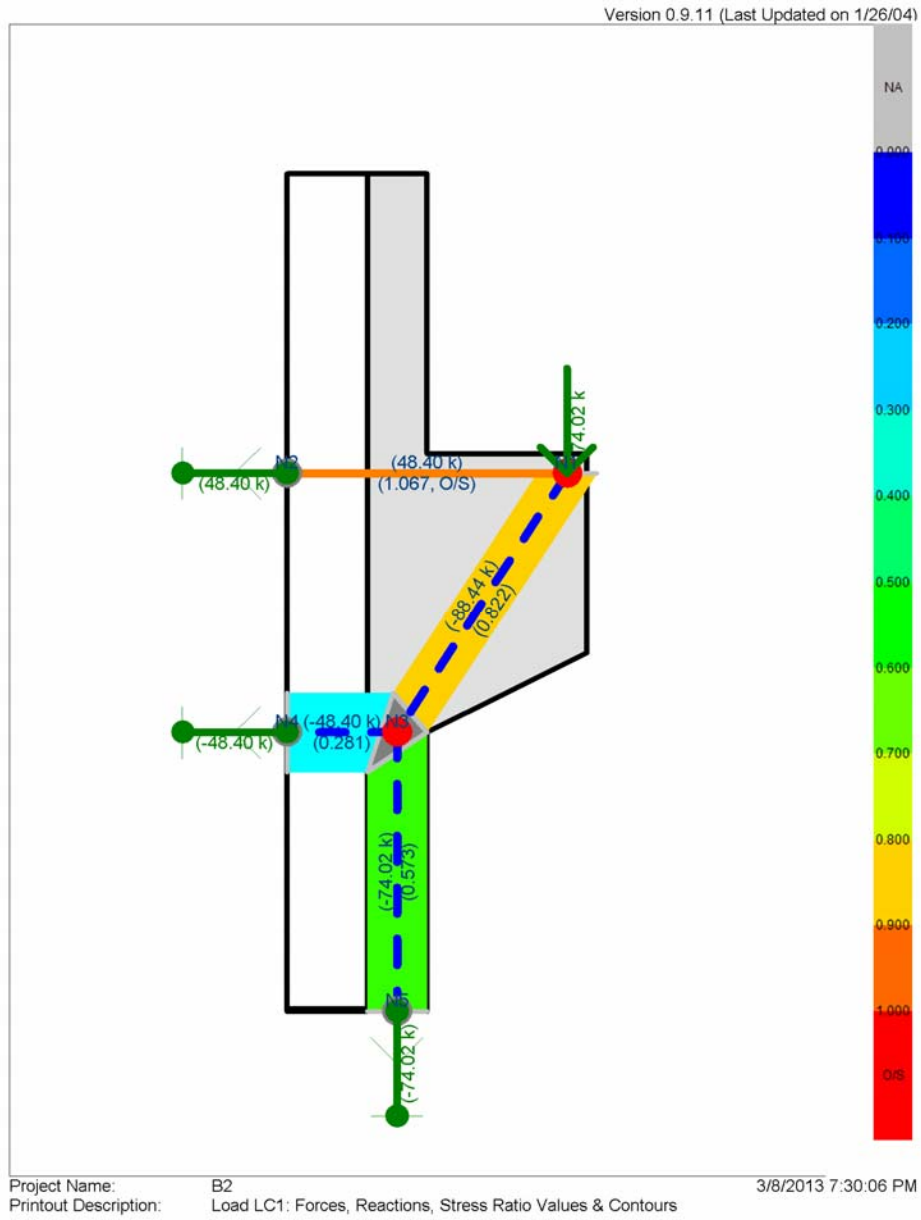


Figure 3-18: Calculated capacity for specimen B2 equals to 74.02 kip

### 3.3. Materials and Fabrication

#### 3.3.1. Materials

Self consolidated concrete (SCC) is commonly used in precast construction. SCC offer excellent workability characteristics. The concrete workability is critical property in the concrete used to cast relatively thin elements similar to the insulated wall wythes. Ready-mix supplied SCC was used to cast the specimens of this study to follow the common practice in the industry. Figure 3-19 show the slump flow for the concrete used in specimens A2 and B2.



Figure 3-19: SCC Slump-Flow

As mentioned earlier in this chapter, the insulated panels are typically loaded with relatively light reactions from the floor system. Concrete strength for precast insulated panels is typically 5000 psi to 8000 psi. The concrete strength used in specimen's sets 1 and 2 was ordered to meet the upper limit of this range. However, the actual concrete strength at time of testing was greater than that. This issue was corrected in specimen set 3. The use of a concrete strength to match the common industry practice will lead to a better utilization of the connection. Several cylinders

4x8 inch, diameter x height were prepared during casting to be tested in order to determine the concrete strength at time of testing. The cylinders were kept in moist room immediately after casting. At the day of testing the cylinders were taken out of the moist room and prepared by surface grinding for testing. The test was done in Compression Test Machine. The loading rate was maintained in range of 450 lb/s = 35 psi according to ASTM C 39.

Typically, the design of insulated wall panels is governed by forces induced after the casting (stripping and handling) and the final wind loads. Both loading conditions result in out-of-plane stresses in the wall panel. Therefore, the common practice in the precast industry is to use longitudinal prestressing in the wall panels. The longitudinal prestressing provides enough strength in the cross section to resist the out-of-plane bending moment and provides a pre-compression force to keep the wall panel un-cracked during operations done after casting. In this study it was chosen to use non-prestressed reinforcement to reinforce the wall panels. Non-prestressed cross section is more vulnerable to cracking. It is a conservative approach to use non-prestressed cross sections since the cracking load is a main design criteria in this study.

Deformed reinforcing bars (rebar) of minimum yield strength 60,000 psi were used in this study. Rebars are usually required to meet ASTM A615 or A996. For specimen set 1 and 2, the bent bars (Stirrups and U-Bars) and straight bars were provided by a local rebar fabricator. For specimen set 3, the precast manufacture provided the bent rebar.

NU-Ties are a proprietary product of Aslan FRP. Refer to Figure 3-20. The NU-Ties are composite connector designed to be stiff in one direction (one-way shear connector). NU-Ties are designed to transfer the shear flow between the wall wythes and provide the required composite action. Nu-Ties are manufactured of glass fiber reinforced polymer (GFRP). NU-Ties inherently

have a low thermal conductivity  $0.2 \left[ \frac{\text{Btu.inch}}{\text{hr.ft}^2.\text{°F}} \right]$  as per the manufacture data, this thermal conductivity is close to the thermal conductivity of the insulation itself 0.2 to 0.3  $\left[ \frac{\text{Btu.inch}}{\text{hr.ft}^2.\text{°F}} \right]$  PSWP PCI Report (2011) . NU-Ties were chosen due its superior performance and being commonly used in the precast industry.

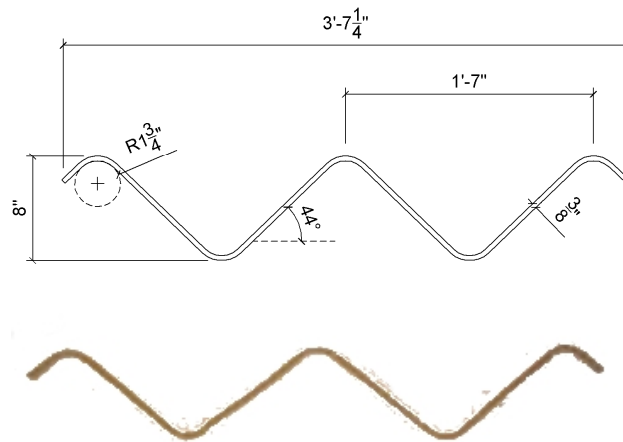


Figure 3-20: #3 NU-TIE (photo by ASLAN FRP)

Insulation boards used in this study were Extruded polystyrene foam (XPS) a product of DOW. The manufacture data show a minimum compressive strength of 25 psi measured at 10 % deformation or at yield, whichever occurs first according to ASTM D1621. The thermal conductivity of the insulation boards is not relevant to this study. However the thermal conductivity for 1 inch thick board is equal to  $0.2 \left[ \frac{\text{Btu.inch}}{\text{hr.ft}^2.\text{°F}} \right]$  as provided by the manufacture.

### 3.3.2. Fabrication

The fabrication of the precast insulated panels was done in steps following the industry practice; placement of reinforcement for bottom wythe, casting bottom wythe, placement of insulation boards, placement of top wythe reinforcement and finally casting of the top wythe. The pre-

fabricated corbel placement fitted the casting of wall panel at different stage. For connections type A, no reinforcement were required in the bottom wythe. However the insulation and NU-Ties configuration was altered to provide the required element. For connection type B, additional reinforcement were required in the bottom wythe. The top wythe was reinforced with additional rebars for connection type A only. More information about the fabrication details are attached in Appendix B. Figure 3-21 shows the FRP tube placement in the insulation.

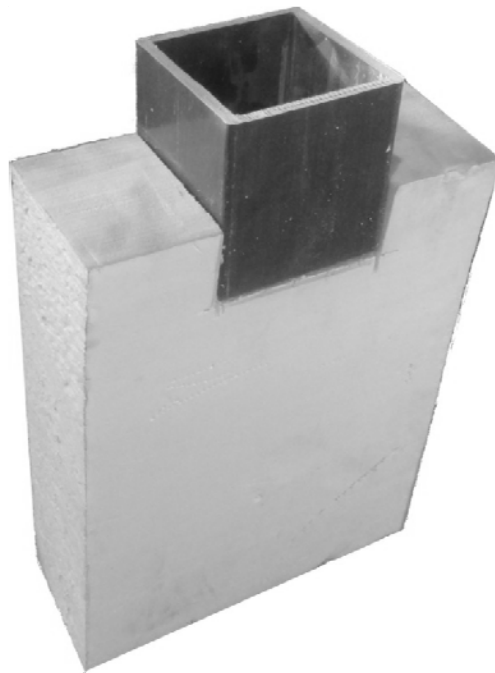


Figure 3-21: FRP tube placed into cut piece of insulation

The following observations were recorded during the fabrications process:

- The placement of the prefabricated corbel in type A connections was difficult due to the method adopted. The prefabricated corbel was placed on top of the insulation boards with no attachments to any fixed body. This approach caused the corbel in specimen A1 and A2 to tilt in the elevation view of the wall. However this tilting mandated the use of lev-



eling grout pad at the corbel top surface. This concern could be overcome in the precast plant by providing sufficient ties between the corbel and the forms or any fixed body.

- By the time the top wythe of specimens B1 was cast, the SCC workability was reduced. This caused the concrete to flow partially below the prefabricated corbel. This concern is applicable to all connections where a prefabricated corbel will be used. This situation could be avoided by maintaining the workability of the concrete specifically at casting the corbel zone.
- The stacked plastic lumber used in specimen B1 showed some irregularity in the level, this is thought to have a significant reduction in the connection strength. In addition to that the placement of the staked plastic boards was impractical, since the boards tend to sink in the concrete under its self weight. These issues were solved by using the structural plastic tube in specimen B2. The Tube fitted easily into the insulation which prevented any movement towards the concrete or sideways.
- The anchorage bars used in connections A1 and A2 had a tight tolerance. The horizontal stirrups and the NU-Ties formed a tight envelope where the anchorage bars are prevented from moving outside it. This tight placement is not required structurally. Therefore, specimen A3, A4 and A5 were designed to allow more space for the anchorage bars to move with no structural effect.
- Prestressing strands pattern must be coordinated with the profile of the cut Nu ties used in connection A. Typically, NU-Ties are placed parallel to the prestressing strands along the longitudinal direction of the wall height. The proposed connection places the cut NU-Ties perpendicular to the strands. Since the NU-Ties are having a wavy profile, the strands could be placed to miss the peak on each wythe. Therefore the strands pattern will not be

identical in the both exterior and interior wythe. This issue is applicable to any reinforcement in the longitudinal direction of the wall; however the rebar design exhibit flexibility to be shifted sideways in the wall if compared to the strands.

- GFRP pins used in Set 3 showed great flexibility in fabrication. The pin was placed in hand sawn hole in the insulation board. Refer to Figure 3-22.



Figure 3-22: GFRP Pin 2" diameter x 4½" long

# CHAPTER 4

## 4. Experimental study

### 4.1. Test specimens

In this chapter the results of testing 7 full scale specimens are addressed. There are 2 basic connections included in the experimental program:

- a) GFRP bars connection, 2specimens,
- b) NU-Ties connection, 5 specimens.

The testing program consisted of 3 sets, the specimen of each set were cast at the same time. Testing of each set was carried out in a limited time window, usually within a week. The first and second sets consisted of 2 specimens, one of each of the types mentioned above. The first set had 1 specimen of GFRP connection and 1 specimen of NU-Ties connection, this specimen configuration applies to the second set as well. The third set consisted of 3 specimens of NU-Ties connection only.

After the testing of each specimen set the results and modes of failure were studied in order to enhance the next set of specimens. In the second and third set of specimens slight changes were carried out in the design or detailing of the connections. The changes were mainly to facilitate the fabrication or enhance the capacity by avoiding the mode of failure of the previous set.

Table 5 lists the configuration of each set and the types of the specimens tested.

Table 5: Testing program

	NU-Ties connection	GFRP bars connection	
Specimens set 1	A1	B1	Cast and tested at University of Nebraska – Omaha structural testing lab
Specimens set 2	A2	B2	
Specimens set 3	A3,A4 andA5	---	Cast at Concrete Industries Precast manufacturing facility and tested at University of Nebraska –Omaha structural testing lab

The specimens' dimensions were selected to represent the most critical wythe configuration in the current practice of precast industry. The 3 inch wythe is the usually the thinnest wythe used in load bearing wall panels. The thinner the wythe gets the more challenging becomes the design and detailing of the connections. One of the possible modes of failure is the pull-out of the GFRB bars or the NU-Ties, as the wythe gets thinner this mode failure is more likely to occur.

The insulation thickness used in all specimens was 4 inch. On the contrary to the wythe, the thicker the insulation gets the more likely the cross-wythe elements (GFRP bars, NU-Ties and compression elements). The expanded insulation was used in this study, since it s the type wildly used in the precast construction.

There are several types of wythe connectors available in the market, the connectors can be classified into composite and non-composite connectors. Some connector's types are made of thermally conductive materials like steel. The thermally conductive materials compromise the thermal performance of the insulated panels. The NU-Ties are one of the commonly used wythe connectors, it is considered to be composite connector since it provides a structural function.

This type of connector was chosen for its superior structural capacity and for its excellent thermal properties.

The precast insulated panels are usually made of 6 to 10 ft wide. This width is usually an architectural requirement. In many projects the spacing of the floor main structural element (steel joist or double tee) is chosen to match the width of the wall panels. The width of the specimen was chosen to include as few as possible of the wythe-wythe connectors. Using the smallest practical width 6 ft of the panels will assure the proposed connection can be generalized to wider panels. The same concept is applied to the height of the specimens. The NU-Ties connectors are fabricated in typical length. The standard NU-Ties are fabricated to fit into a 4 ft insulation board. Therefore the panel was composed of 2 standard insulation boards, to be 8 ft total height.

The wall panel reinforcement was chosen to represent a lightly reinforced cross section. The use of light reinforcement permits the proposed connection to be used in any cross section. The use of prestressing was studied to reinforce the wall panel. However, it is thought to be a beneficial addition to the specimen especially for the cracking load. Therefore, the conventional reinforcement was used.

Ready mix concrete was used in casting the wall panels. The target strength was 8000 psi. Typically, the precast insulated wall panels are cast using Self-consolidating concrete (SCC) due to the shallow thickness of wythes. SCC was used in this study.

Figure 4-1, Figure 4-2, Figure 4-3 show the reinforcement details for all specimens. Fabrication drawings for the specimens are included in Appendix A.

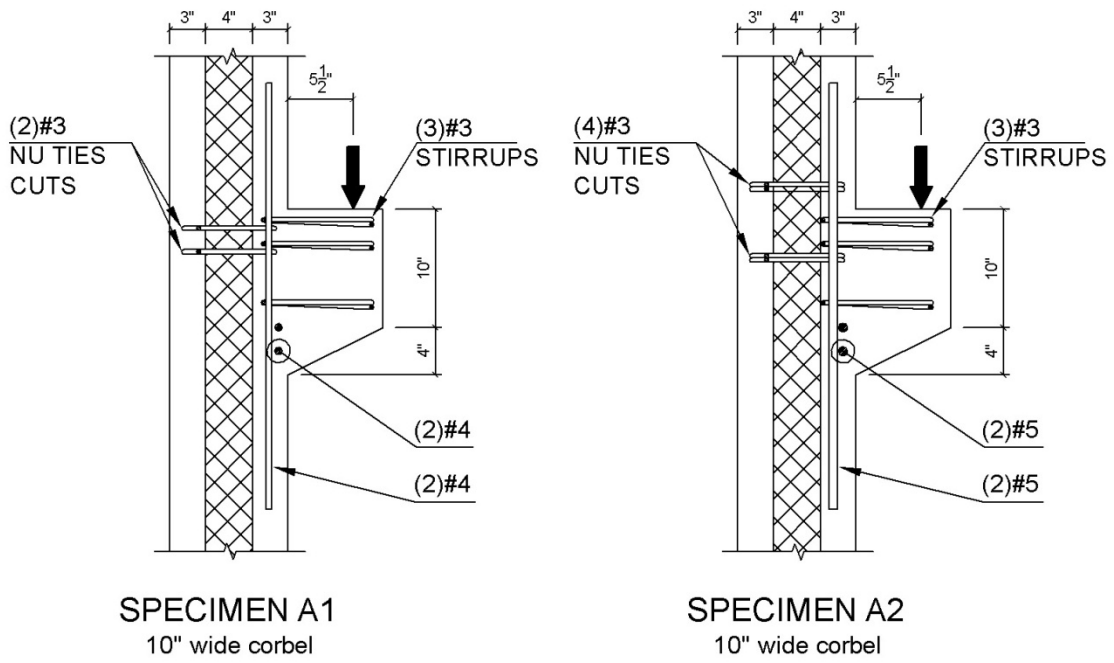


Figure 4-1: Reinforcing details of specimens A1 and A2

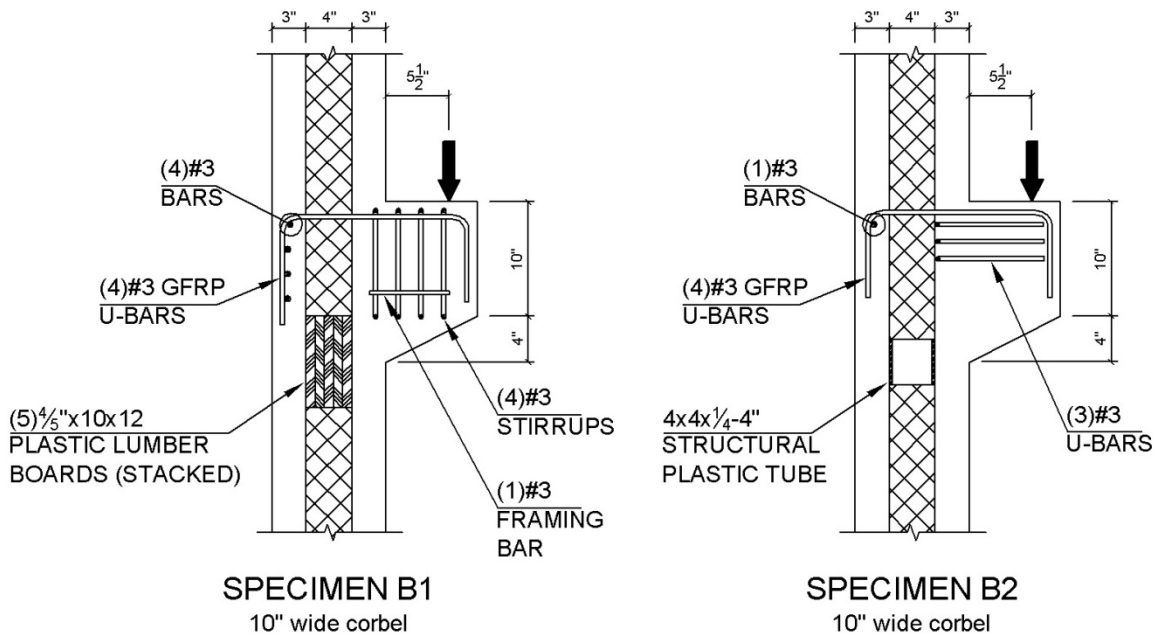


Figure 4-2: Reinforcing details of specimens B1 and B2

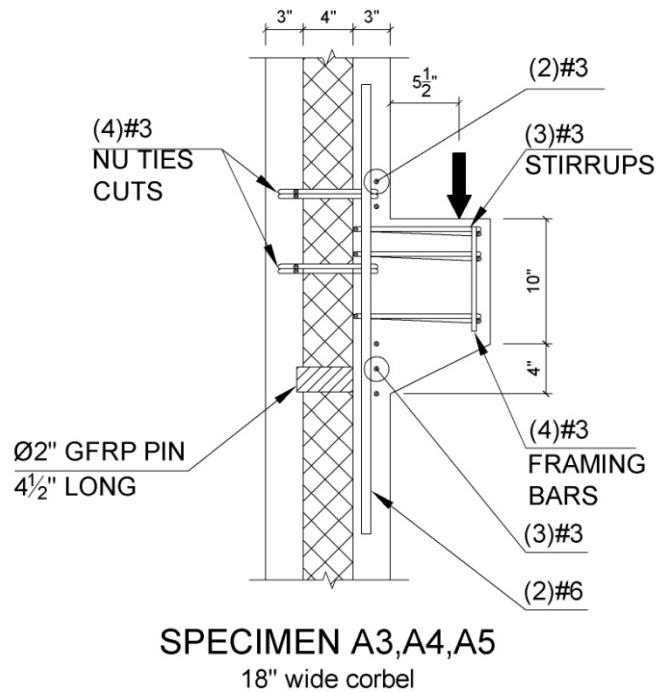


Figure 4-3: Reinforcing details of specimens A3, A4 and A5

## 4.2. Testing setup and procedure

Figure 4-4 and Figure 4-5 show the adopted test setup, this setup provides a clear access to the front and back withies of the wall. A few items were considered critical for correct and safe testing of the corbel. First, load eccentricity with respect to interior face of the wall of panels. Second, providing reaction couple to balance the moment caused by loading the wall at an eccentricity. The test setup components are the following:

- Reaction wall
- Loading frame (beam + vertical threaded rods)
- Hydraulic jack
- Load cell

- Tie back frame (beam + horizontal threaded rods)
- Timber joist (for backing)

As a result of the eccentric loading applied to the corbel, the vertical reaction is accompanied with a horizontal couple. The purpose of the loading frame is to transfer the hydraulic jack reaction to the floor through the beam and the vertical threaded rods. The vertical threaded rods are chosen to be 3 inch diameter; the vertical threaded rods are attached to the lab ground by a threaded floor holes. The location of the floor holes determines the load position. The function of the tie back frame and the timber joist is to provide the horizontal couple of tension and compression, respectively.

The tie back frame will transfer the horizontal tension reaction near the top of panel to the reaction wall, The steel tube of the tie back frame is pulled enough against the reaction wall to tightly pick the tension reaction and transfer is to the reaction wall by bearing. Two Timber joist are provided between the panels and the reaction walls to provide the compression reaction.

The bearing capacity of wall to the ground was not an issue. In 2 specimens the bottom side had more irregularities than accepted, a full width grout bed was cast below the specimen, and then the specimen was lowered in place to bear on the fresh grout. The testing was not carried out until the grout achieved the required strength. Figure 4-6 show the mentioned pad.

The placement of the precast-corbel was a challenge. The corbel of GFRP system was not tied to the form during the casting process; this caused the corbel top surface to be unparallel to bottom side (bearing side on ground) of the wall. This issue was solved by providing a grout pad at the corbel top surface.



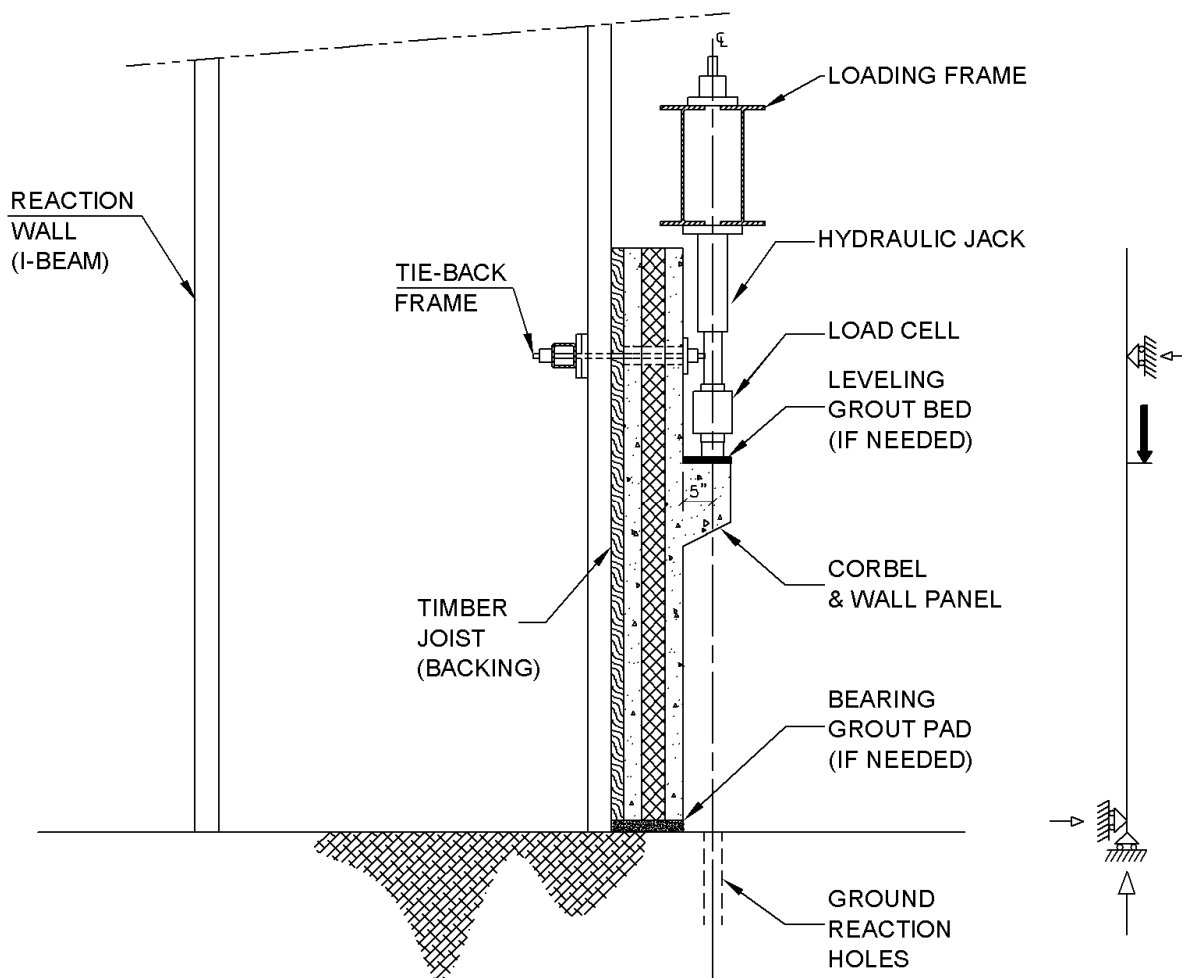


Figure 4-4: Testing setup, side View

The loading procedures were similar for all the specimens, the loading started from the unloaded state and increased with multiple load steps each equal to 5 kip, after each load step the loading was kept constant for minutes. Within this pause period the research team approached the specimens for any sign of failure or visible cracks. Once spotted, the cracks were marked with the current load value.

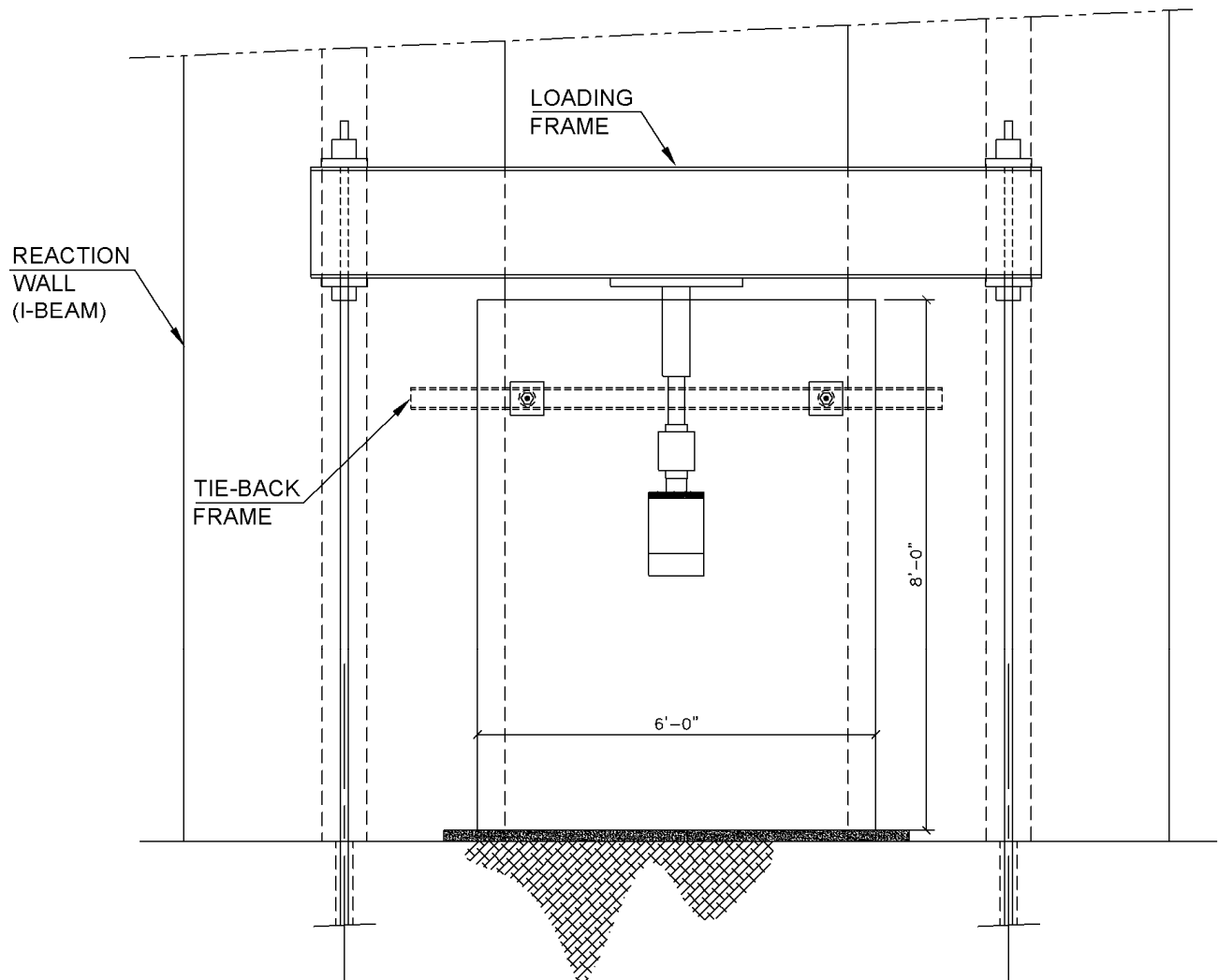


Figure 4-5: Testing setup, front view

The first visible crack was recorded and referred to as “cracking load” in this study. The target factored load capacity of these connections is 35 kip. Once the total load applied to the connection is equal to the target load 35 kip, the load was increased gradually till failure with no further steps or checks. When the connection withstands an applied load of 35 kip, it was considered to be adequate.



Figure 4-6: Forming of leveling grout pad used for specimens A1, A2 and B1

### **4.3. Specimens behavior**

#### **4.3.1. Specimen A1**

Prior to testing, early-age shrinkage cracks were observed in the exposed face of this specimen. Refer to Figure 4-7. These plastic shrinkage cracks originated from the prefabricated corbel location and were directed towards the vertical edges of the wall. These shrinkage cracks were observed only in the top face 2 days after casting. The cracks should be considered as an adverse factor to the capacity of the connection, since these cracks will form a weak plane across the interior wythe.



Figure 4-7: Marked plastic shrinkage cracks in specimen A1 prior to loading

The age of specimen at day of testing was 12 days. Two Concrete cylinders (4x8 inch, diameter x height) were tested under compression loading to evaluate the average concrete strength at testing. The average of the 2 cylinders compressive strength is 9.72 ksi. The bearing grout bed for this specimen achieved a compressive strength of 6.0 ksi. The grout pad used for leveling of the corbel achieved compressive strength of 6.3 ksi.

Specimen A1 didn't exhibit any visible cracks up to an applied load of 20kip; the first visible crack was 45 deg crack at the top of the corbel in interior wythe. Another main crack formed shortly after exceeding the 20 kip, was a vertical crack starting at the top right hand side corner

of the corbel, these two 45 deg and vertical cracks continued to grow in length with the load increase till edges of the wall. Fewer cracks were observed at the compression side of the corbel (bottom). No cracks were observed in the exterior wythe as any stage. The failure occurred with approximately 1 in. deflection of the corbel at the tip. The failure occurred at 55.1 kip.

There was neither explosion nor loudly failure just a regular increase in the deflection of corbel. The cracked part was the top part of the wall just above the corbel, around 10 inches vertically from top of corbel by 16 inch horizontally almost symmetrical about the corbel center line. After the loading was completed, the cracked part was taken-off to observe the cause of failure. The observations were that the 2 ties in corbel were intact and the anchorage bar was bent outwards. One bar only was obviously bent and the other bar was not clear. There was no sign of slippage of any rebars. Refer to Figure 4-8, Figure 4-9 and Figure 4-19.



Figure 4-8: Specimen A1 crack pattern at failure



Figure 4-9: Cause of failure for specimen A1, concrete breakout

### 4.3.2. Specimen B1

The age of specimen at day of testing was 20 days. Although the same concrete mix and test cylinder preparation method used for specimen A1 was used for specimen B1, the concrete cylinder testing results were unrealistically low if compared to specimen A1. The available result of concrete strength was 5.8 ksi. The compressive strength of grout used for both bearing bed and leveling pad for this specimen achieved a compressive strength of 6.0 ksi.

Similar to specimen A1, shrinkage cracks were observed in this specimen B1. Refer to Figure 4-10. These cracks originated from the prefabricated corbel adjacent area and were directed towards the vertical edges of the wall. The bottom face of the prefabricated corbel was intention-

ally roughed, which provided a sort of restraint to prevent the concrete volume close to the corbel from shrinking.

Up to an applied load of 15kip there were no visible cracks, cracks started in form in a similar pattern to specimen A1. The first visible crack was an inclined crack of 45 deg near the top of the corbel, the cracks continued to grow in length with the load increase till in reached the vertical edge of the wall. No vertical cracks were observed in this specimen neither cracks exterior wythe as any stage. The failure occurred with 3/4 in. deflection of the corbel at the tip; the corbel block exhibited a slight separation 1/2 in. away from the wall exterior face. Refer to Figure 4-11. The failure occurred at 62.1 kip. During the test the load fluctuated back as a loud noise of cracking was heard, this fluctuation is noticeable as a drop in the load value applied to the specimen Figure 4-22.

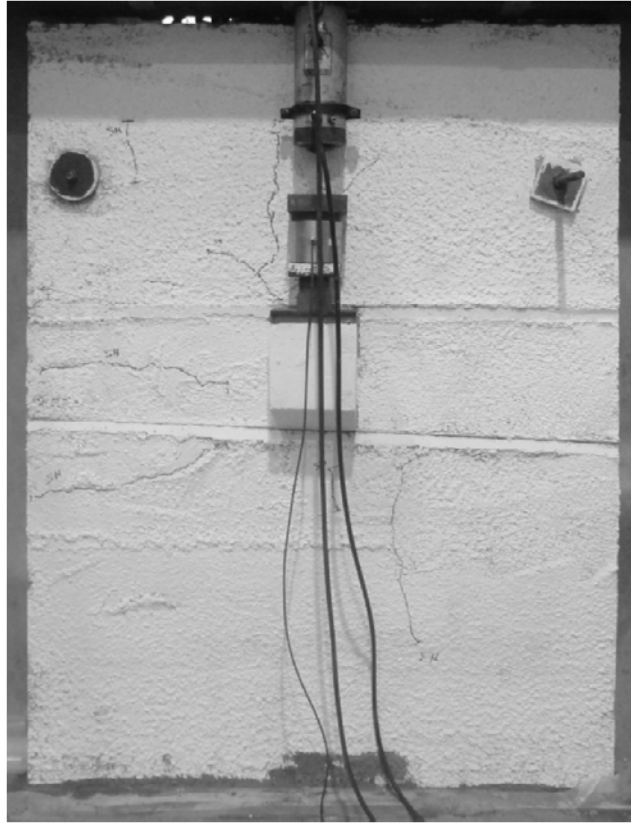


Figure 4-10: Marked plastic shrinkage cracks in specimen B1, prior to loading



Figure 4-11: Failure of specimen B1



The prefabricated corbel could be easily separated from wall panel after loading was stopped after failure. The failure is caused by the rupture of the GFRP bars in the proximity of the bend location; this can be seen obviously in Figure 4-12. After the corbel was disengaged from the wall, it was noticeable that concrete of exterior wythe did not flow freely behind the corbel. The concrete flew behind the corbel approximately 3in. measured from the corbel faces, except that the bottom face where concrete flew 4 inch. The casting of the exterior wythe started from the bottom edge (bearing side) and then continued towards the top edge. This casting direction gave the bottom part of the corbel advantage to allow concrete flow. In the following specimens, special care was taken for the concrete flow behind the prefabricated corbel. Refer to Figure 4-22.



Figure 4-12: Ruptured GFRP Bars in specimen B1

### 4.3.3. Specimen A2

This specimen is part of specimens set 2; Table 5 lists the contents of each set. The age of wall panel concrete at date of casting was 9 days. The average of 2 cylinders (4" diameter by 8" height) crushed under compression loading at the same day of testing was 10.35 ksi.

Unlike specimens set 1 specimen, this set of specimens didn't exhibit any shrinkage cracks. The reason for that is; the specimen was covered by plastic sheets immediately after casting to entrap the moisture within the fresh concrete in addition to starting the curing the next day after casting.

The casting quality of set 2 was sufficient to achieve a leveled bottom edge, therefore the grout bed was not required and the wall panel had an almost full length of bearing surface against the lab floor. However, the corbel had a slightly inclined top surface. Therefore a grout pad was used.

The first crack was observed at an applied load of 30kip. The failure load for this specimen was 74.8kip. Similar to set 1 specimens no cracks were observed on the back wythe. The first crack was a 45 deg crack near the top of the corbel; At applied load close to failure load, new cracks started to appear close the bottom of the corbel at 45 deg. The cracks started to get longer till it reached the edge of the wall in a manner similar to specimen A1 and B1. The failure occurred with 2 in. deflection of the corbel at the tip. Refer to Figure 4-13, Figure 4-14 and Figure 4-20. Since the wall panel bottom side was not grouted for this specimen, more noise was heard during the test. The cause of failure was the rupture of NU-Ties.

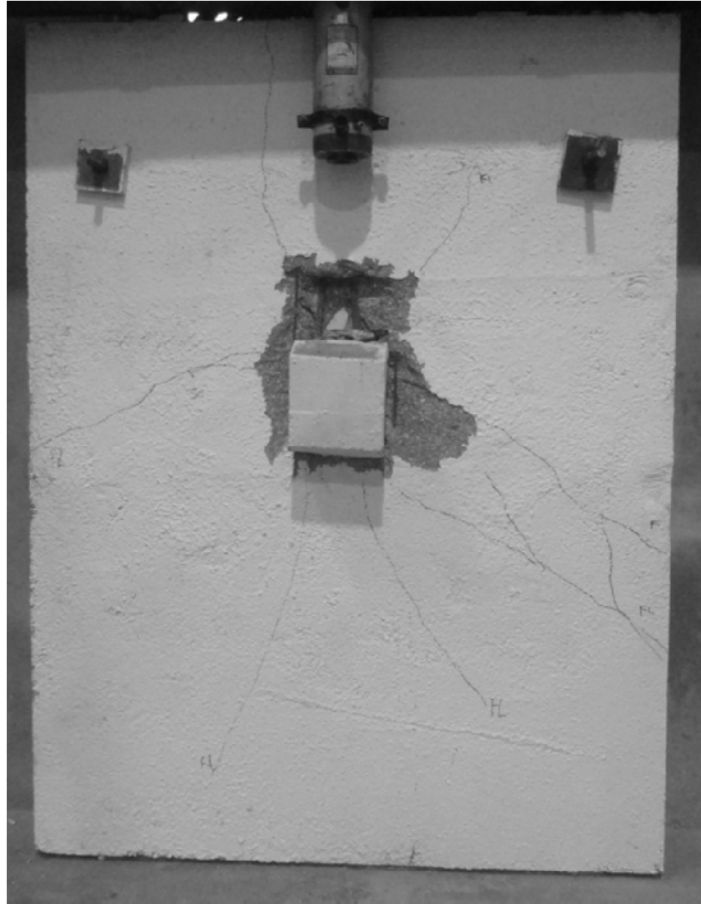


Figure 4-13: Marked cracks at failure specimen A2



Figure 4-14: Ruptured NU-Ties in specimen A2

#### 4.3.4. Specimen B2

Age of specimen at testing was 14 days, at this age the concrete compressive strength was 11.30 ksi. This is average of 2 cylinders tested at the same day of connection testing.

Specimen B2 was cast to an acceptable quality so the bearing level was almost in full contact with the lab floor. Leveling grout pad was not necessary for the corbel top surface, a heavy duty neoprene pad. Similar to specimen A2, no spastic shrinkage cracks were observed in this specimen.

There were no visible cracks up to an applied load of 40kip. The failure occurred at 75.5kip. There was not cracks in the back wythe. The first crack was a horizontal crack near the top of the corbel; at later stage vertical cracks started to form the top corners of the corbel. Closer to failure load, short and closely spaced cracks became obvious at the interface of wall-corbel which seemed to be signs of crushing. The horizontal and vertical cracks started to get longer till it reached the edge of the wall in a manner similar to specimen A1 and B1. The failure occurred with 1/2 in. deflection of the corbel at the tip.

The failure cause was the concrete shear break-out, this can be seen in Figure 4-15, Figure 4-16 and Figure 4-23.



Figure 4-15: Marked Cracks at failure and failure mode of specimen B2



Figure 4-16: Corbel block on ground after cutting the GFRP bars - specimen B2

#### **4.3.5. Specimens A3, A4 and A5**

Prior to testing, cracks were observed in the exposed face of this specimen. These cracks directed from the lifting points to the corbel block. These cracks were similar to the shrinkage cracks ob-

served in specimens A1 and B1. The reason for these cracks could be the plastic shrinkage or induced tension stress during lifting. However, the cracks are thought to be an adverse factor to the capacity of the connection.

The age of specimens at testing was 8, 9 and 10 days. The average concrete strength at testing is 7.73 ksi.

For specimen A3 and A5, the first observed cracking load was close to 30 kips. Specimens A4 didn't exhibit cracks till the next checking cycle at 35 kips, The cracking load could be an intermediate value between 30 and 35 kips since the wall surface were checked at 5 kips interval. Similar to the previous specimens, the first visible crack was 45 deg crack at the top of the corbel (interior wythe). The cracks originated from the prefabricated corbel top corner and were directed towards the vertical edges of the wall. This crack continued to grow in length with the load increase till edges of the wall. Specimen Fewer cracks were observed at the compression side of the corbel (bottom). No cracks were observed neither in compression side of the corbel nor the exterior wythe as any stage. The failure occurred with approximately 1/2 in. deflection of the corbel at the tip. The failure occurred at an average load of 52.0 kip.

There was neither explosion nor loudly failure just a regular increase in the deflection of corbel. The cracked part was the top part of the wall just above the corbel, around 2 inch vertically from top of corbel had sloped crack surface (Break-out failure). After the loading was completed, the cracked part was taken-off to observe the cause of failure. The observations were that the 2 ties in corbel were bent just beyond the #5 anchorage bars. There was no sign of slippage of any rebars. Refer to Figure 4-17, Figure 4-18 and Figure 4-27.

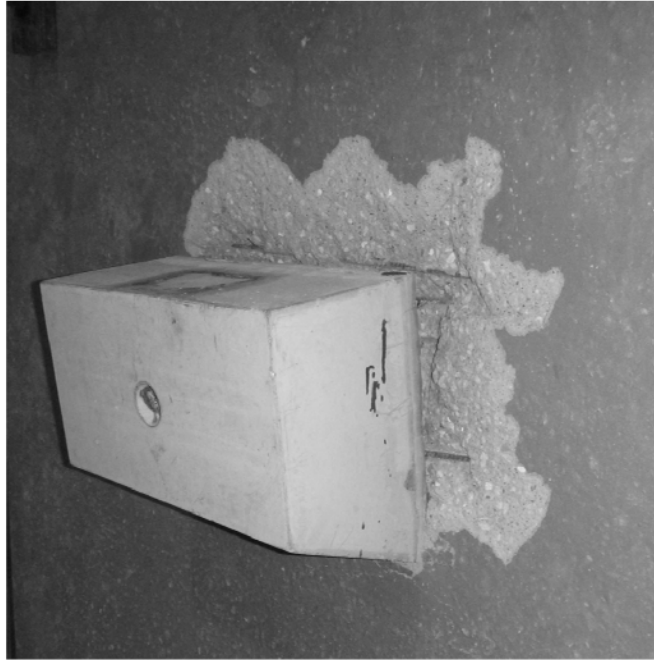


Figure 4-17: Break-out zone at failure in specimen A3



Figure 4-18: Bent stirrups followed by concrete breakout in specimen A5

#### 4.4. Summary and discussion of results

Cause of failures is listed in Table 6. The failures can be related to primary or secondary components of the connection. The primary components are the GFRP and NU-Tie, these components are the main focus of this study and are not feasible to change. The primary components should be utilized to the maximum capacity prior to addressing any increase in their intrinsic capacity (size or strength). A comparison between specimens A1 and A2, show that the number of NU-Ties was doubled; This specific change was an increase in the intrinsic capacity of the primary components. This change was proposed to change the behavior of the connection to a more robust one. Other secondary components could be changed to enhance the connection behavior. The secondary components should not be the weakest link in the connection.

Table 6: Testing results

Specimen	Ultimate capacity [kip]	Observed cracking load [kip]	Wall concrete strength [ksi]	Cause of failure
A1	55.1	20	5.8	Break-out of concrete due to imposed load by the longitudinal #4 bar near top of corbel
B1	62.1	15	9.7	Rupture of GFRP bars
A2	74.9	30	10.3	Rupture of NU-Ties
B2	75.5	40	11.3	Break-out of a part of the wall concrete below the corbel
A3	52.7	30	7.5	Break-out of wall concrete due to bending of #3 corbel stirrups
A4	53.3	35*	7.8	
A5	50.1	30	7.9	

\* The wall was checked for cracks each 5 kips load step, the cracks might occur at a load between the consecutive load steps.



As discussed in section 3.1-Design of this study, the horizontal stirrups are subjected to tension force caused by the externally applied bending moment. This tension force should be transferred to the anchorage bar which is supported by the NU-Ties. The NU-Ties in turn will transfer the force back to the exterior wythe and eventually to the supports. The ideal behavior would be that the NU-Ties will rupture (weakest link).

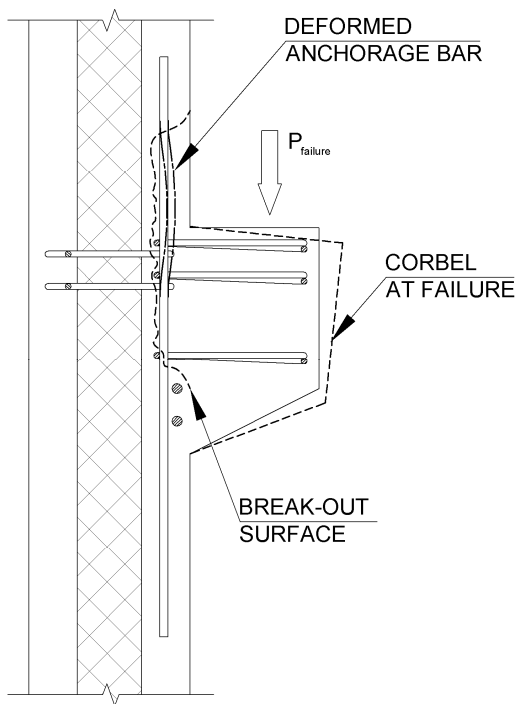


Figure 4-19: Cracks diagram in specimen A1

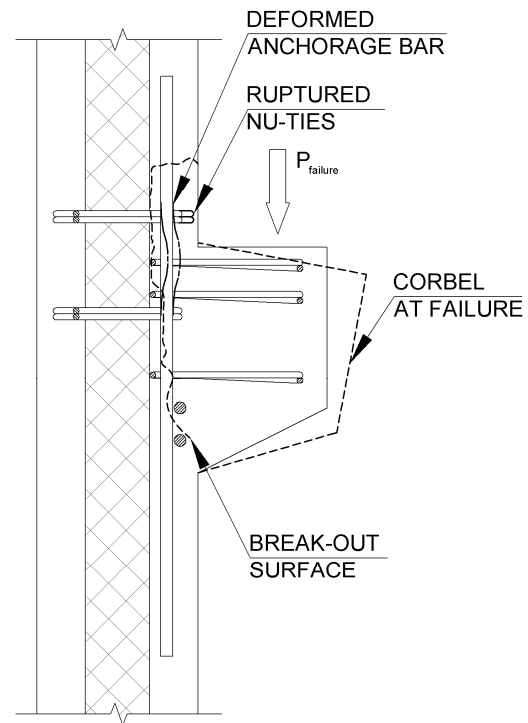


Figure 4-20: Cracks diagram in specimen A2

In specimen A1, the horizontal tension force of the 2 top stirrups was transferred to anchorage bar. The anchorage bar was supported by 2 NU-ties, The way the connection was detailed resulted in applying one of the horizontal stirrup reaction outside the span of the anchorage bar (outside the distance between the NU-Ties). One of the stirrups reaction application point was located between the NU-Ties. If the reactions are applied within the distance between the NU-Ties,

the anchorage bar will act similar to a simply supported beam on the NU-Ties. In specimen A1, the anchorage bar was subject to a fraction of the load between the supports and the rest of the load beyond the supports. The way the reactions were applied to the anchorage bar lead to a formation of additional support by the bar embedment into the concrete above the corbel. Since this embedment length required to form the support are relatively large, the deformation of the rebar was significant. This significant deformation caused the concrete cover of the rebar to break-out. Once the concrete cover was lost the embedment support significantly diminished. The anchorage bar exhibited excessive deformation after the loss of support and eventually was not able to carry any additional load. Refer to Figure 4-21.

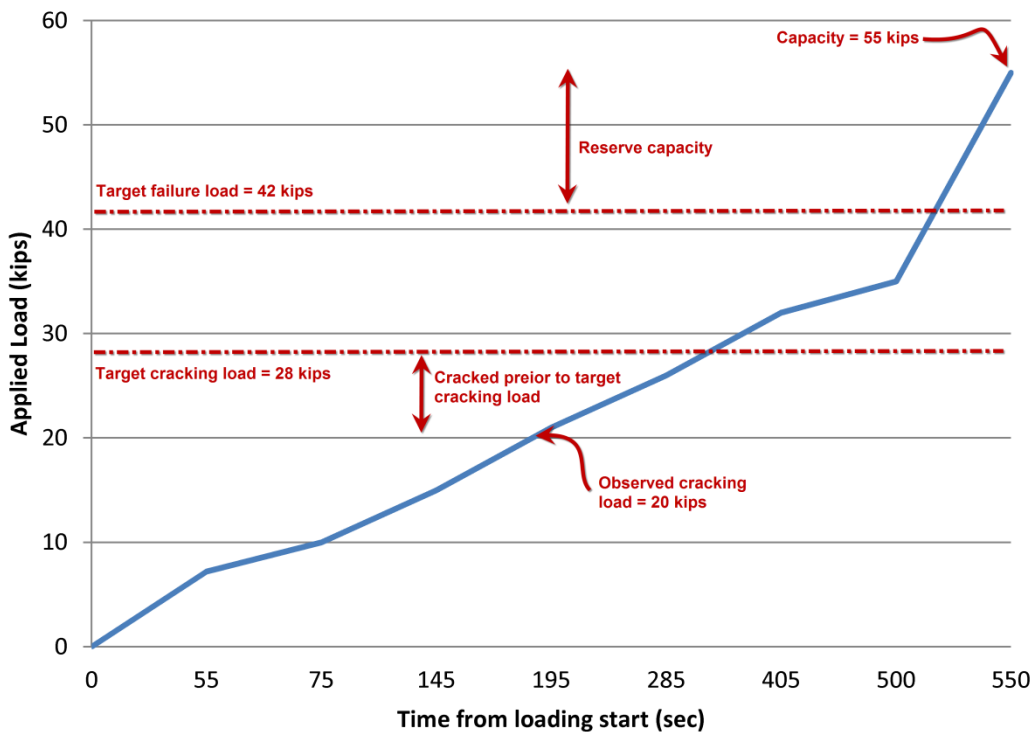


Figure 4-21: Loading and results of specimen A1

Specimen A2 will be discussed in this section, the failure of specimen A2 occurred due to the rupture of the NU-Ties at the bearing point of anchorage bar. The same design concept was used

for A1 and A2 specimen. The extent of the break-out part of the exterior wythe is very limited in A2 if compared to specimen A1. As discussed in specimen A1, the anchorage bar was supported by the NU-Ties close enough to the reaction application point. The anchorage bars used in specimen were large in diameter if compared to specimen A1 (#5 and #4 respectively). The larger bar diameter contributed to limiting the outward bar deformation which eventually caused the break-out. The horizontal stirrups exhibited noticeable deformation at the bearing location against the anchorage bar. The horizontal ties reactions were fully transferred to the anchorage bar within the distance between the NU-Ties (support points for anchorage bar). In addition to the outward deformation of the anchorage bars, a slightly transverse deformation could be noticed. This deformation is thought to be caused by the imperfect placement of the anchorage bar within the NU-Ties bent peak. Refer to Figure 4-24.

In both specimens A1 and A2, there was no sign on the effectiveness of the transverse rebars placed close to the compression face of the corbels.

The design concept of specimens B1 and B2 is mentioned in Item 3.1 of this study. Briefly, external bending moment (eccentric load) is resisted by a force-couple internally in the wall. The GFRP bars used as tension element to transfer the internal force to back wythe. Meanwhile the compression force is taken by a thermally non-conductive material with the insulation layer. The failure in specimen B1 occurred by the rupture of the GFPR bars close to the bent portion. The GFRP bars were thought to be the weakest link in the connection, the testing results confirmed that. Generally the GFRP bars require a large bend radius which represent a challenge for the designer to fit this large radius within the wall wythe. To ensure that the proposed connection will work for any wythe configuration and will not be limited to relatively thick wythes, this

study adopted a relatively thin wythe (3 in.). A tight bend radius was required from the GFRP bars manufacturer. It was expected that the GFRP bars will not develop the full strength of the material because of the tight bend radius. Refer to Figure 4-25 and Figure 4-26.

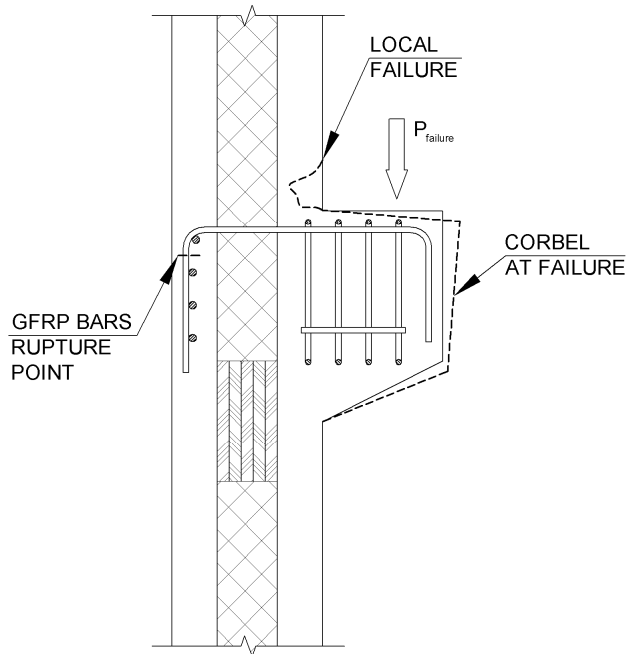


Figure 4-22: Cracks diagram in specimen B1

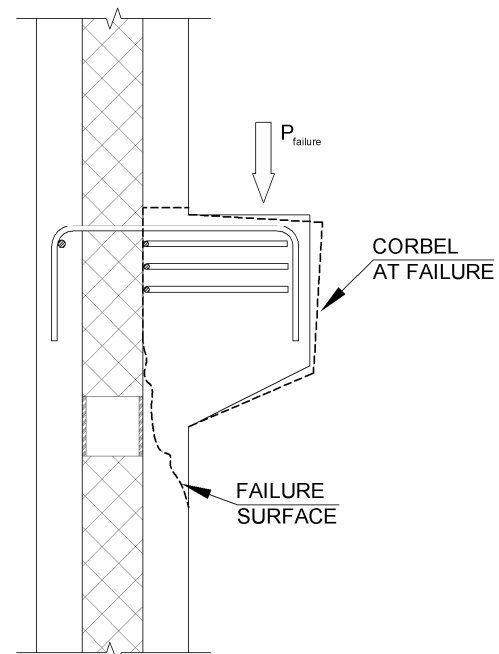


Figure 4-23: Cracks diagram in specimen B2

It was quite easy to separate the corbel from the wall panel after the GFRP bars have ruptured. This issue was successfully addressed in the following panel by using horizontal U-Bar instead of vertical U-Bars. It was clear after the separation of the corbel from the wall that the concrete didn't flow freely between the corbel and the insulation. Since the bottom part of the corbel had nearly 3in of concrete behind it, this part is thought to be enough to provide the compression block formed by the external bending moment. There is no sign on the effectiveness of the Plastic lumber stacked boards.

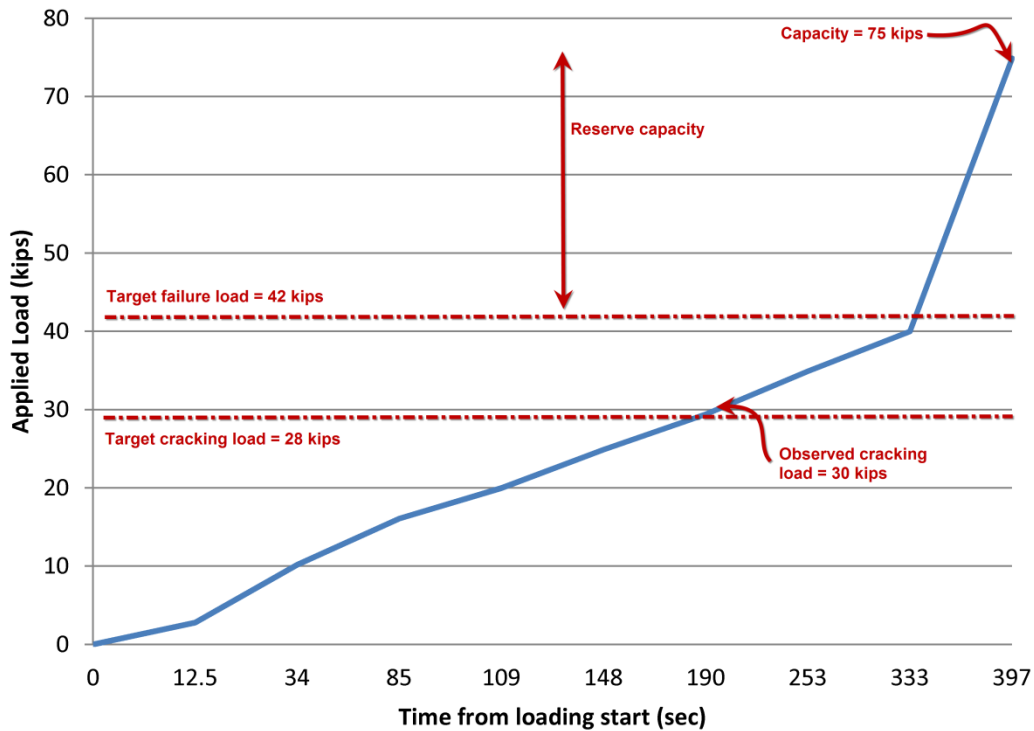


Figure 4-24: Loading and results of specimen A2

In specimen B2 the orientation of the U-Bars was changed from vertical to horizontal. The behavior of U-Bars was similar to the full stirrups used in specimens A1 and A2. The GFRP bars were intact at failure. This behavior is different from specimen B1. The major difference between specimens B1 and B2 are; concrete wall strength and compression element type. There is no evidence on what changed the behavior in this specimen. However, it is expected that the plastic tube would perform better than the stacked boards. Since the stacked boards had a slight wrapping, the final assembly of the boards had gaps in some areas.

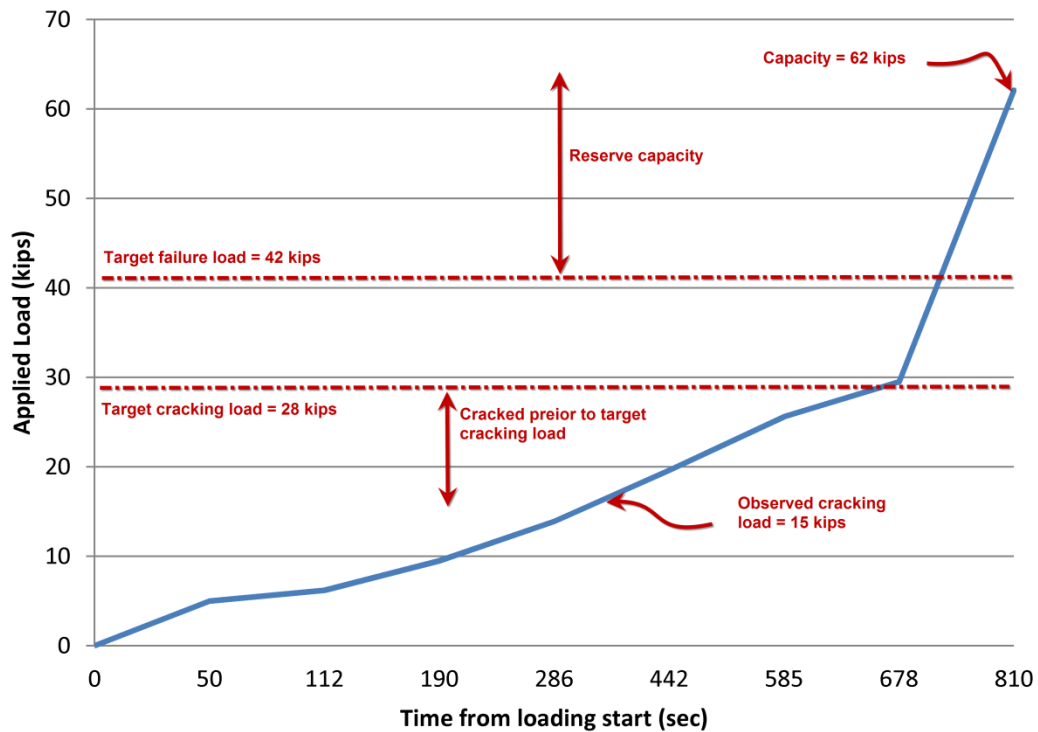


Figure 4-25: Loading and results of specimen B1

The failure of specimen B2 occurred due to break-out of the bottom part just below the corbel-wall junction. This failure could be resembled to a sliding failure of soli wedge. The vertical load is transferred to the wall by 3 components;

1. Bearing of the corbel on wall wythe,
2. Vertical friction force between the corbel and the wall at the compression block,
3. Clamping force across the interface generated in the horizontal stirrups and the GFRP bars.

In order to utilize the clamping force across the interface, it is thought that quite large relative displacement has to occur first between the corbel and the wall interface. This displacement was not observed during the testing. Therefore this force is neglected in this study.

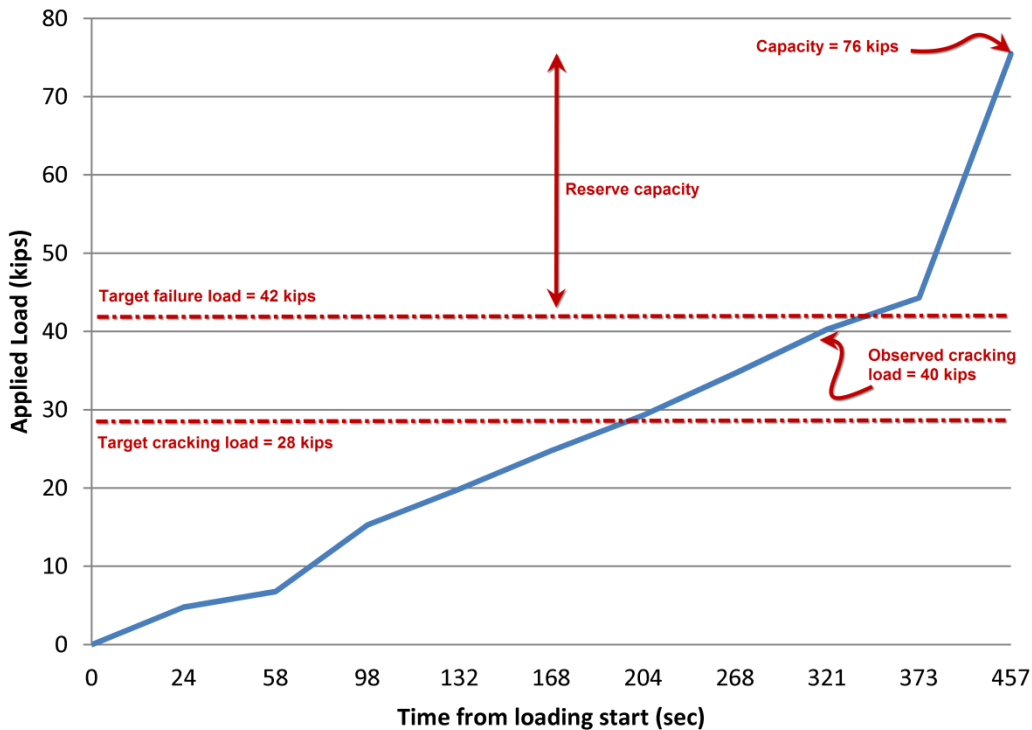


Figure 4-26: Loading and results of specimen B2

Specimens A3, A4 and A5 failed due to a secondary failure. The cause of failure for these 3 specimens was identical. The failure caused by the excessive bending of the corbel stirrups as shown in Figure 4-27. In specimens A1 and A2 the anchorage bar passed through the NU-Tie and the corbel stirrups were located very close to the bend location, this limited space is thought to be unforgiving for any fabrication tolerances. In this specimen set the anchorage bars were repositioned towards the interior of the corbel in order to allow more fabrication tolerances. Eight inches long #3 framing bars were used in order to fix the stirrups in place. The corbel stirrups bent outward just beyond the location of the anchorage bars.

The exclusion of wall transverse and longitudinal reinforcement didn't change nor does the cracking load neither the failure load. Longitudinal reinforcement was provided in specimens A1, A2, B1 and B2 at close to the mid-thickness of the concrete wythe. Therefore it didn't affect

the observed cracking load. In typical precast construction in US, the walls are commonly prestressed longitudinally. The prestressing is expected to increase the magnitude of cracking load, therefore the exclusion of any reinforcement in these specimen set is thought to be the worst case scenario.

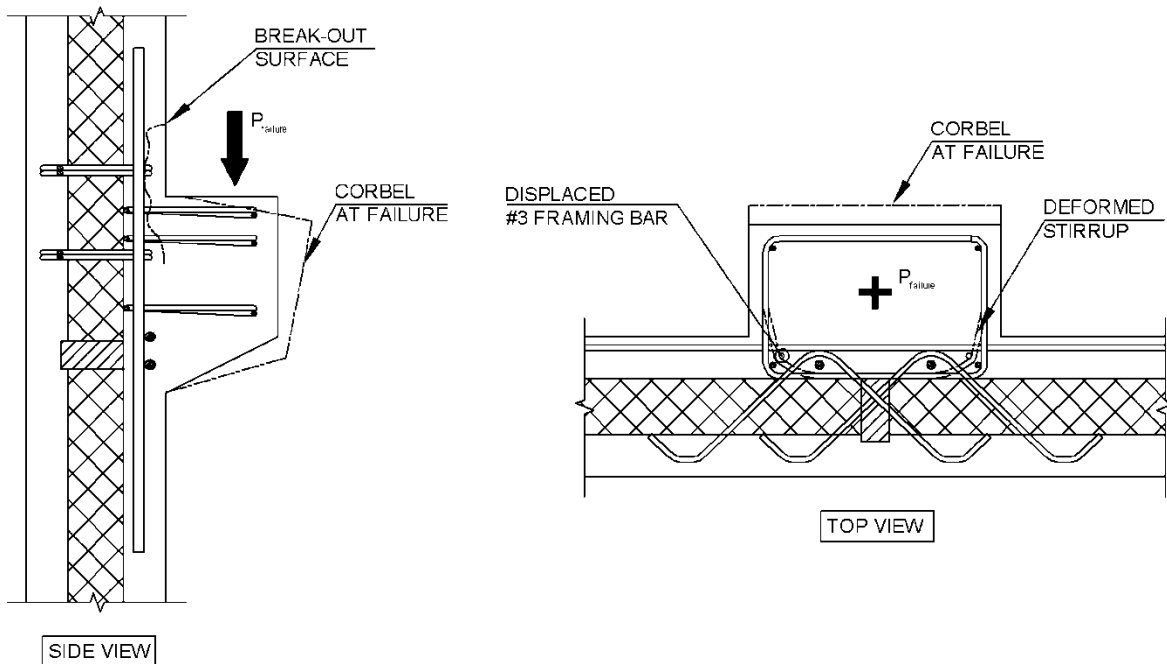


Figure 4-27: Cracks diagram in specimen A3, A4 and A5

The premature failure of the connection due to the stirrups bending didn't allow the test to evaluate the capacity of the main connection elements. Set 3 was expected to exhibit more ultimate capacity if compared to the Set 1 or 2 due to the enhancement in the detailing. However, the testing showed high consistency of the capacity results and cracking load among the identical 3 specimens (A3, A4 and A5). Based on the observed failure, it is recommended that the anchorage bars to be relocated to its original location (close to the bend of the stirrups). The option of extending the framing bars to develop its full strength by embedment into interior wythe concrete



will not be sufficient, the framing bars will be bent-out at large tension for the stirrups. This failure mode will be similar to the failure of the anchorage bars in specimen A1. The loading and results for specimens of A3, A4 and A5 are shown in Figure 4-28, Figure 4-29 and Figure 4-30.

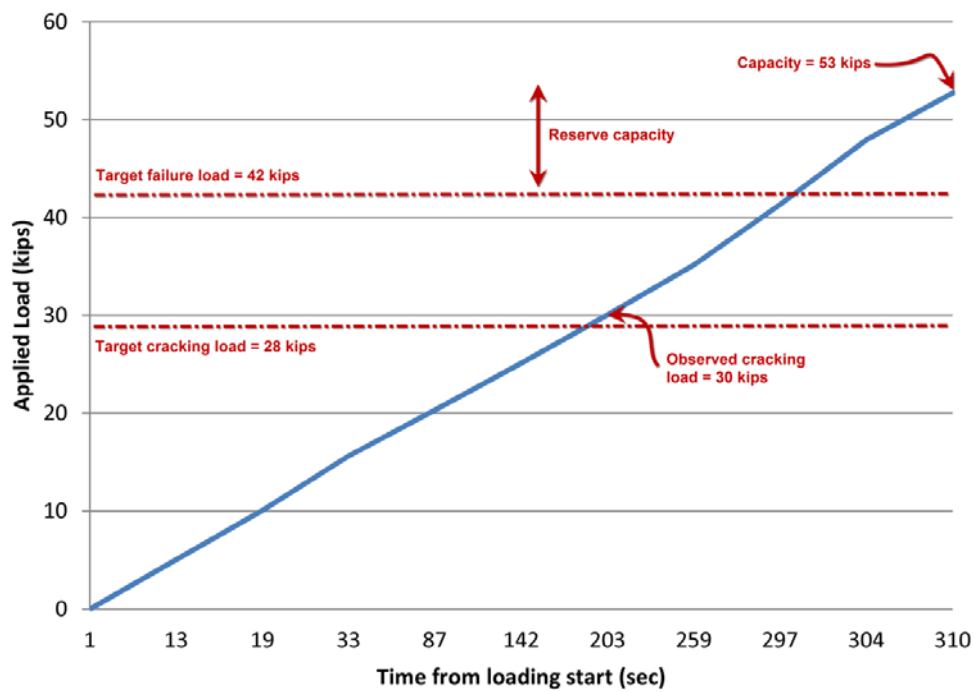


Figure 4-28: Loading and results of specimen A3

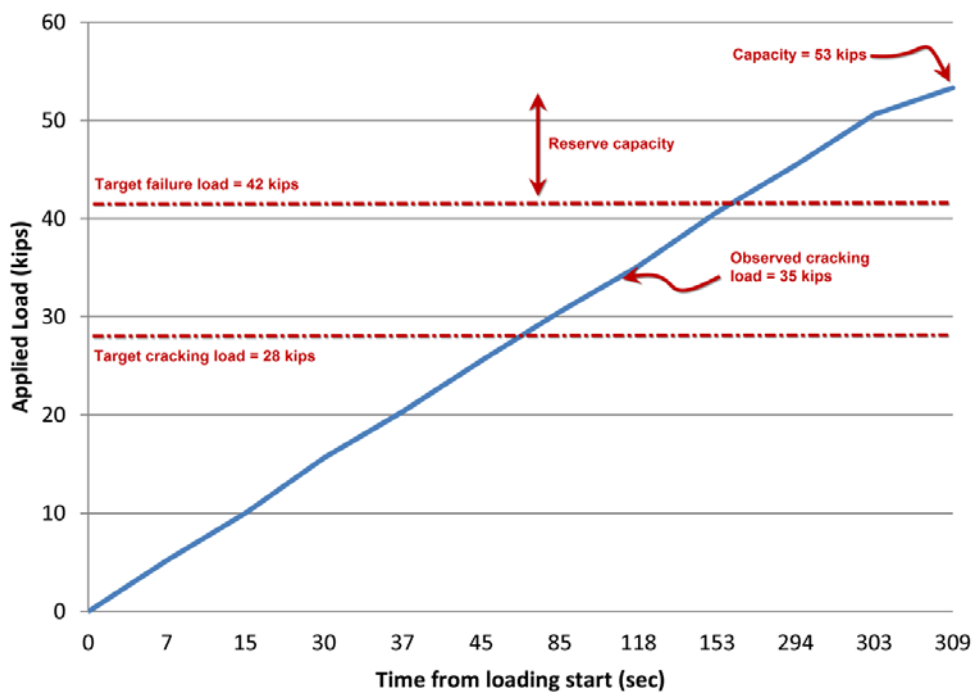


Figure 4-29: Loading and results of specimen A4

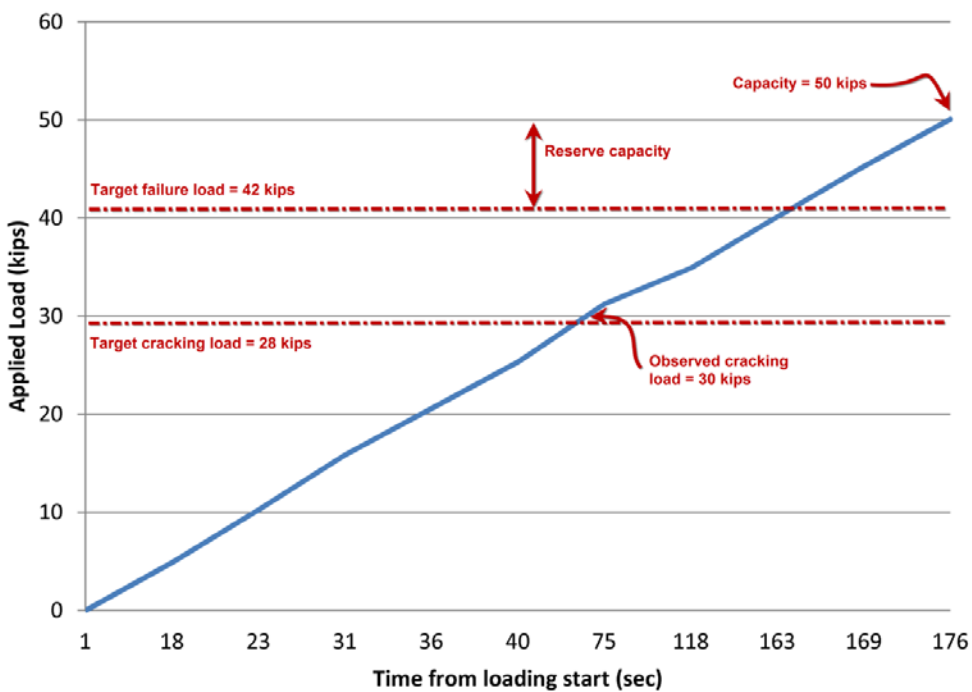


Figure 4-30: Loading and results of specimen A5

For all specimens the observed first crack was located close to the top of the corbel, the test setup allows the wall panel to resist the externally applied bending moment (load x eccentricity) to a force-couple. This force couple will create 2 bending moments with different bending direction. In the length between the applied moment and the top reaction, the internal bending moment will cause an outward bending moment i.e. tension stress at corbel face. The opposite will occur to below the corbel level i.e. tension stress in the wall wythe at back face. This falls in line with the experimental investigation. In specimens B1, A2 and B2, the crack was at 45 deg. This could be related to the effect of the nearby support point.

The failure load is significantly higher than the factored load since the design will be govern by the sustained or service reaction. The change in cracking load among the different specimens is dependent on the transfer of load to the back wythe. Since the wall panel reinforcement was identical in each specimen. The tested specimens didn't show any sign of premature failure in the corbels itself. Although specimen B1 had only vertical stirrups, the expected vertical shear crack didn't occur. The reason for this is the relatively large depth chosen for the corbel compared to the expected failure load. In practical situations, corbels are rarely limited to an upper limit of the depth. Typically, engineers use the same width of the column as a corbel width to facilitate the fabrication and forming. Specimen B2 were subject to slight bearing damage close to the failure load, after that damage the loading continued with no-sign of failure. The ultimate failure of the specimen was not due to the bearing.

# CHAPTER 5

## 5. Conclusions and Recommendations

### 5.1. Conclusions

This study addressed the current practice for corbel connections in precast insulated wall panels in order to find alternative connections that eliminate the thermal bridging problem in the current practice. This included the design and testing of a replacement connections with full perseverance of the thermal break.

- Corbel connection without thermal bridging in precast insulated walls is achievable.
- The proposed connections satisfy the strength and serviceability requirements. The target factored capacity was exceeded with a considerably large margin (120 to 180%)
- Specimens with compression element, stacked plastic boards, FRP hollow section or GFPR pin, showed better performance regarding the failure load and observed deformation.

### 5.2. Recommendations

The tensile stress in GFRP bars corresponding to sustained loads should not exceed recommended values for creep rupture by ACI 440 (2006). The sustained loads are considered to be the full dead load plus a portion of the design live loads (25 to 75% of the load specified). The designer is required to use engineering judgment to decide on the portion most likely to occur according

to the expected building use. Compression elements provide a defined and stiff path for the compression force close to corbel-wall junction line. Compression elements share the compression force between both wythes. It is more practical to use single element to form the compression rather than multiple elements.

Common corbel failures include a steep crack, therefore nearly all researches recommend providing horizontal ties to capture that crack effectively. This falls in line with the observations from this study. These few rebars enhances the redundancy of the corbel connection under loads beyond the design loads. The presence of longitudinal reinforcement within the width of the corbel will change the failure to a ductile failure based on the shear friction concept. It is also noticed that reposition the anchorage bars away from the stirrups bent portion will cause the stirrups to bend out-ward and cause a premature failure by break-out.

None of the corbel connections tested exhibited any cracks within the corbel itself. The first crack was typically where the corbel top face meets the wall interior wythe. The wall is the weakest link as far as cracking concerns. Therefore, these cracks can be eliminated by increasing the cracking capacity of the wall. Since typical precast construction practice in North America use prestressing for the precast insulated walls, it is unlikely that cracking capacity of the wall will govern the proposed connection. The proposed connections did exhibit negligible deflection at service loads, as mentioned earlier the corbel connections performs elasticity (un-cracked) up to the service loads due to the large cross section.

Proposed connections could be altered to provide larger capacities. The use of wider corbel cross sections and multiple GFRP or NU-Ties will increase the connections capacity. The embedment of the NU-ties should be taken into consideration in any different arrangement.

### **5.3. Future work**

There several areas that can be investigated to enhance the proposed connections performance as follow:

- Consideration of the horizontal load in the testing setup of the specimens will emulate the common loading in precast construction
- Sustained loading is the governing limit for the connections using GFRP. Therefore this loading should be confirmed against the code requirements adopted by this study.
- Evaluating the behavior of the proposed connections if used for prestressed walls, this behavior will emulate the majority of the precast construction.
- Various proposals for using FRP structural shapes can be included as continuation for this study.

# Appendix A

## A. Design calculation

Target load calculations:

Double-Tee length = 60 ft

Double-Tee cross section, SW = 81 psf  
Normal weight concrete 12' wide x 28" deep + 2" topping

Floor live load, LL= 55 psf, 25% of total live load is considered to be sustained load

Floor super imposed dead load, SIDL = 15 psf

$$\text{Dead load Reaction per corbel} = \frac{1}{2 \times 2} [60 \times 12 \times (81 + 15)] = 17.28 \text{ kip}$$

$$\text{Live load Reaction per corbel} = \frac{1}{2 \times 2} [60 \times 12 \times (55)] = 9.9 \text{ kip}$$

Strength Combinations:

$$1.4 D = 1.4 \times 18.18 = 25.45 \text{ kip} \quad \text{ASCE 7 (2005)}$$

$$1.4 D + 1.6 L = 1.4 \times 18.18 + 1.6 \times 9.9 = 41.29 \text{ kip, governs} \quad \text{ASCE 7 (2005)}$$

Service load combinations:

$$D+L = 17.28 + 9.9 = 27.18 \text{ kip}$$

Sustained load combinations:

$$D + 0.25 \times L = 17.28 + 0.25 \times 9.9 = 19.76 \text{ kip}$$

Theoretical load to cause cracking:

$$V_{\text{crack}} = \frac{M_{\text{crack}}}{a_v}$$

$$a_v = 5.0 \text{ in.}$$

$$M_{\text{crack}} = \frac{f_r \times I_g}{y_t}$$

$$I_g = \frac{b \times h^3}{12} = \frac{10 \times 14^3}{12} = 2286.67 \text{ in}^3$$

$$f_r = 7.5 \sqrt{f'_c} = 7.5 \sqrt{8000} = 670.82 \text{ psi}$$

ACI 318 (2011) Eq. 9-10

$$M_{\text{crack}} = \frac{670.82 \times 2286.67}{14/2} = 219134.5 \text{ lb. in} = 219.13 \text{ kip. in}$$

$$V_{\text{crack}} = \frac{219.13}{5.0} = 43.83 \text{ kip}$$

Cracked moment of inertia: PCA Notes (2008), Equation 9.5.2.2

$$I_{\text{cr}} = \frac{b \times (kd)^3}{3} + nA_s(d - kd)^2$$

$$kd = \frac{nA_s}{b} \left( \sqrt{\frac{2bd}{nA_s} + 1} - 1 \right)$$

$$A_s = 2 \times 0.11 \times 2 = 0.44 \text{ in}^2, (2) \text{ U shaped Bars}$$

$$d = 12 \text{ in.}, b = 10 \text{ in.}$$



$$n = \frac{E_s}{E_c}$$

$$E_c = 33 w_c^{1.5} \sqrt{f_c} = 33 \times 150^{1.5} \times \sqrt{8000} = 5422 \text{ ksi}$$

ACI 318 (2011), Equation 8.5.1

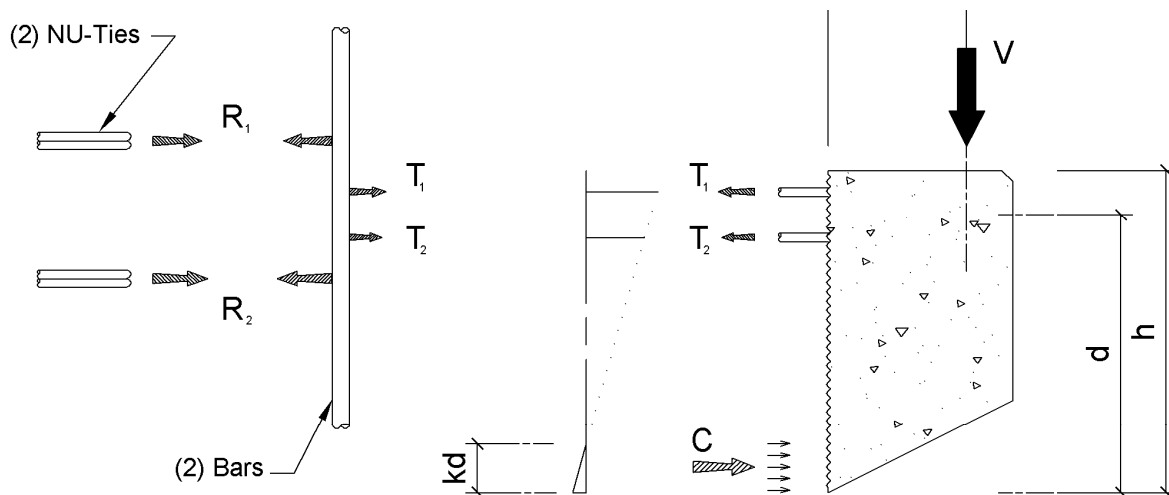
$$E_s = 29000 \text{ ksi}$$

ACI 318 (2011), Equation 8.5.2

$$n = \frac{29000}{5422} = 5.35$$

$$kd = \frac{5.35 \times 0.44}{10} \left( \sqrt{\frac{2 \times 10 \times 12}{5.35 \times 0.44} + 1} - 1 \right) = 2.153 \text{ in.}$$

$$I_{cr} = \frac{10 \times (2.153)^3}{3} + 5.35 \times 0.44 (12 - 2.153)^2 = 261.52 \text{ in}^3$$



- Calculated forces shared among the connection elements

Figure 5-1: Design forces for specimen A2

Stress at sustained load:

$$f_f = n \frac{M_{sus}}{I_{cr}} y$$

$$M_{\text{sus}} = P_{\text{sus}} \times a_v = 20 \times 5 = 100 \text{ kip. in}$$

$$f_{T1} = 5.35 \times \frac{100}{261.52} \times 11 = 22.50 \text{ ksi}, \quad T1 = f_{T1} A_{s1} = 22.50 \times (2 \times 0.11) = 4.95 \text{ kip}$$

$$f_{T2} = 5.35 \times \frac{100}{261.52} \times 9 = 18.42 \text{ ksi}, \quad T2 = f_{T2} A_{s2} = 18.41 \times (2 \times 0.11) = 4.05 \text{ kip}$$

$$f_c = 1 \times \frac{100}{261.52} \times 2.153 = 0.82 \text{ ksi}, \quad c = \frac{f_c b kd}{2} = \frac{0.82 \times 10 \times 2.153}{2} = 8.86 \text{ kip}$$

NU-Ties forces, Refer to Figure 5-1 and Figure 5-2.

$$R_1 = \frac{4.95 \times 3.81 + 4.05 \times 1.81}{6} = 4.37 \text{ kip}, \quad R_2 = (4.95 + 4.05) - 3.44 = 4.64 \text{ kip}$$

Distribution of forces in the NU-Ties is dependent on the location of the Steel Ties; therefore the detailing of the connection should consider locating the NU-ties as symmetric as possible to the steel ties.  $R_1$  and  $R_2$  are calculated for the complete corbel connection, these reactions are shared among 2 longitudinal bars which are supported by total of 4 NU-Ties.

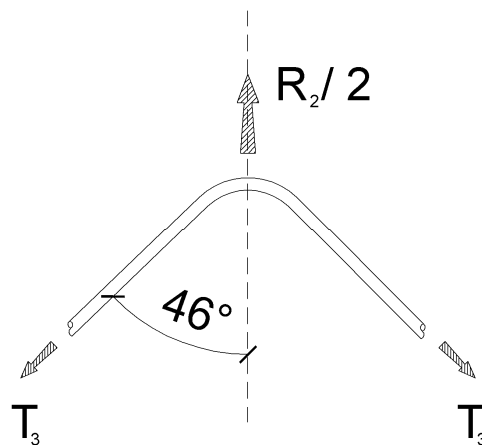


Figure 5-2: Forces in NU-Tie

$$\text{Force per NU-Tie leg } T_3, \quad T_3 = \frac{\left(\frac{R_2}{2}\right)}{2 \cos \alpha} = \frac{(4.64/2)}{2 \cos 46} = 1.67 \text{ kip}$$

Creep ruptures capacity of NU-ties:

$$f_{f,s} = 0.2 C_E f_{fu}^* = 0.2 \times 0.7 \times 110 = 15.4 \text{ ksi} \quad \text{ACI 440 (2006) Table 8.3}$$

$$T_{f,s} = f_{f,s} \times A_f = 15.4 \times 0.11 = 1.69 \text{ kip}$$

Flexural strength:

NU-Ties are stressed at an angle to the reaction, Equivalent to:

$A_{f,eqv.} = (2 \text{ Bars}) \times (2 \text{ Legs per NU-Tie}) \times A_f \times \cos \alpha$ , This approach ignores the bottom row of NU-Ties ( $R_2$ )

$$A_{f,eqv.} = 2 \times 2 \times 0.11 \times \cos 46 = 0.31 \text{ in}^2$$

$$\rho_f = \frac{A_{f,eqv.}}{bd} = \frac{0.31}{10 \times 15} = 0.00207$$

Where  $A_f$ : area of FRP reinforcement, in.2

$$\rho_{fb} = 0.85 \beta_1 \frac{f'_c}{f_{fu}} \frac{E_f \epsilon_{cu}}{E_f \epsilon_{cu} + f_{fu}} = 0.85 \times 0.65 \times \frac{8}{110} \times \frac{5422 \times 0.003}{5422 \times 0.003 + 110} = 0.0051$$

ACI 440 (2006), Equation 8-3

$$\text{Since } \rho_f < \rho_{fb} \rightarrow M_n = A_f f_{fu} \left( d - \frac{\beta_1 c_b}{2} \right), \quad \phi = 0.55$$

$$c_b = \left( \frac{\epsilon_{cu}}{\epsilon_{cu} + \epsilon_{fu}} \right) d = \left( \frac{0.003}{0.003 + 0.014} \right) 15 = 2.647 \text{ in.}$$

$$M_n = 0.31 \times 110 \times \left( 15 - \frac{0.65 \times 2.647}{2} \right) = 482.16 \text{ kip.in}$$

$$\phi M_n = 0.55 \times 482.16 = 265.19 \text{ kip.in}$$

$$\phi V_n = \frac{\phi M_n}{a_v} = \frac{265.19}{5} = 53 \text{ kip}$$

# Appendix B

## **B. Testing specimen details**

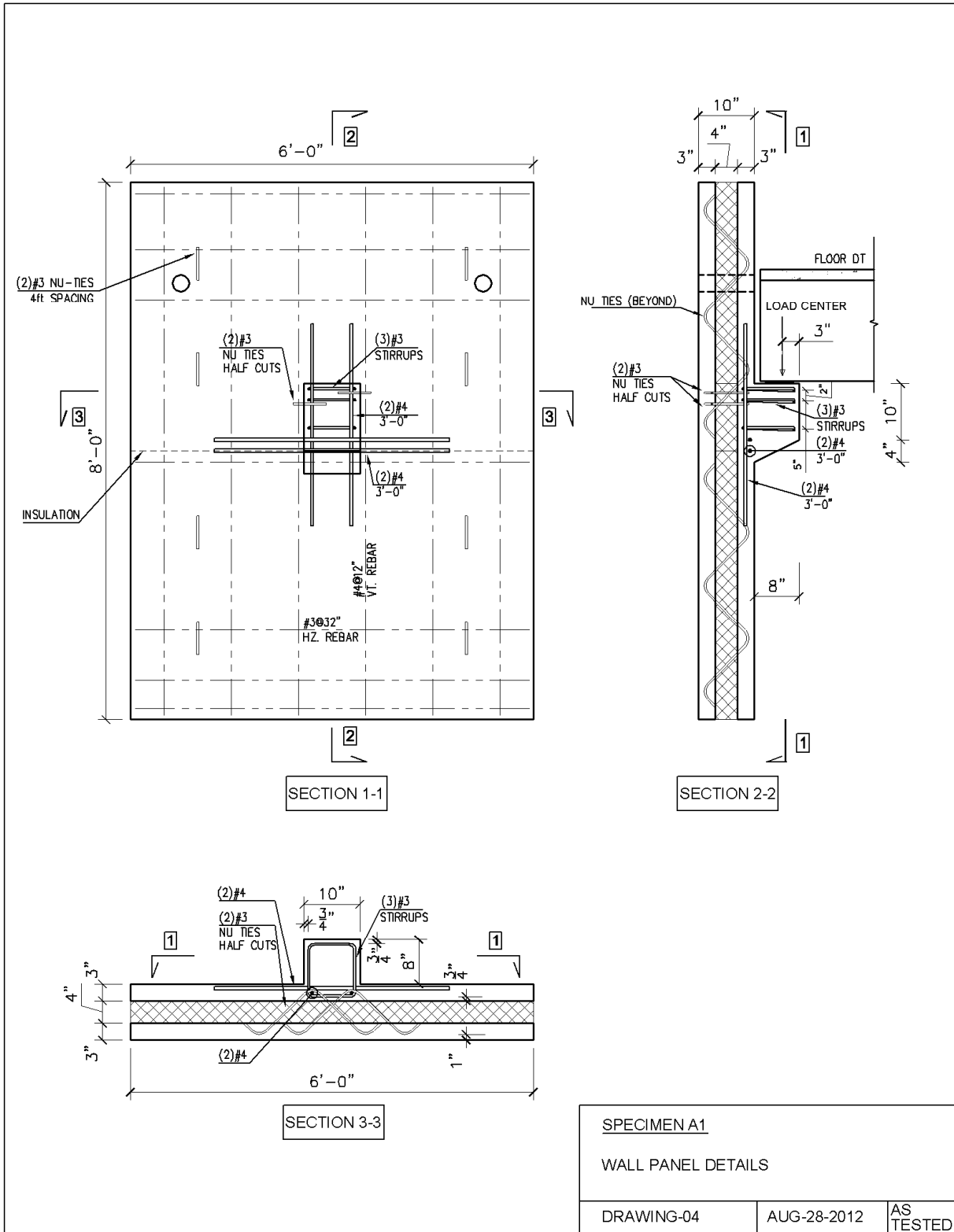


Figure 5-3: Specimen A1- Details sheet 1

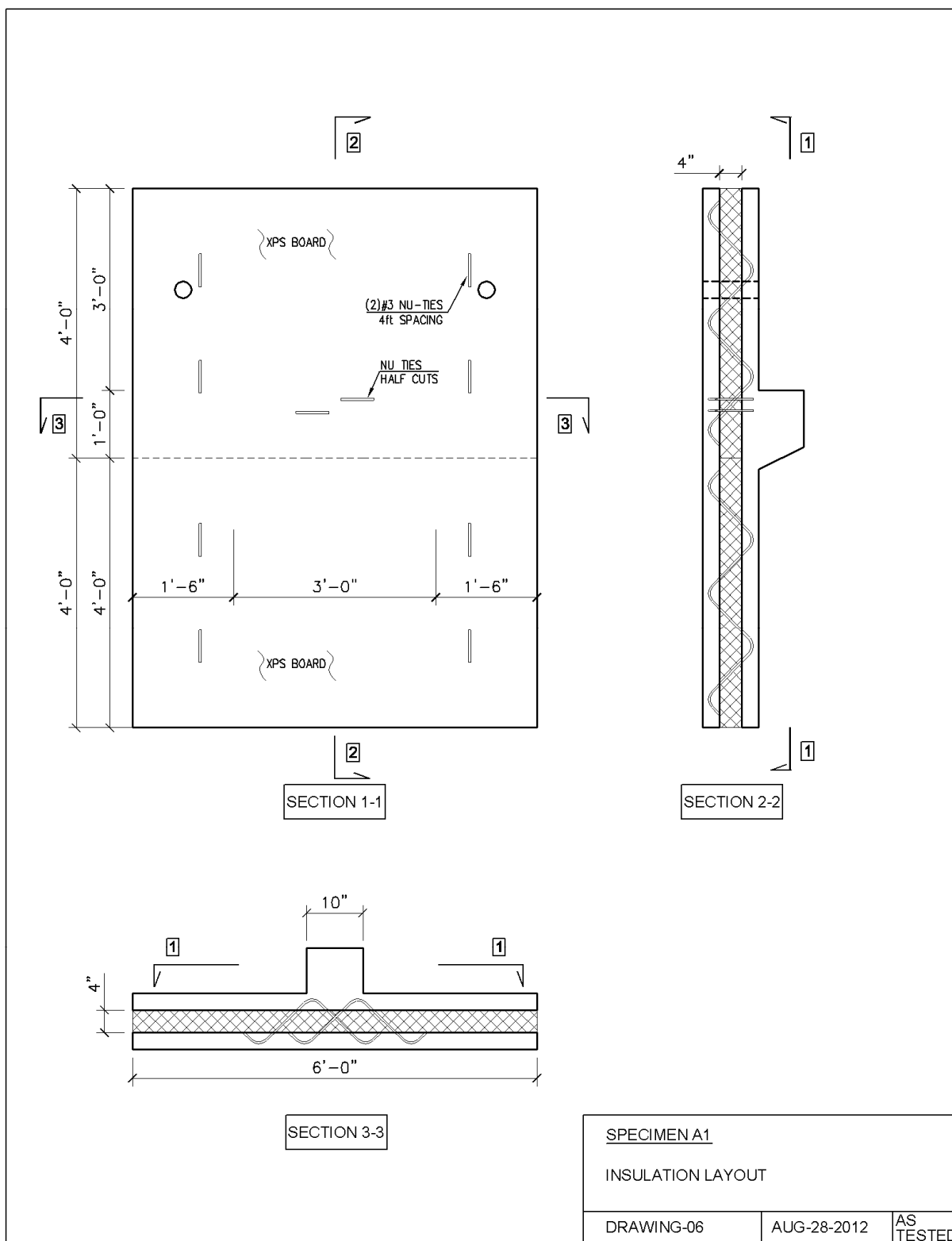


Figure 5-4: Specimen A1- Details sheet 2

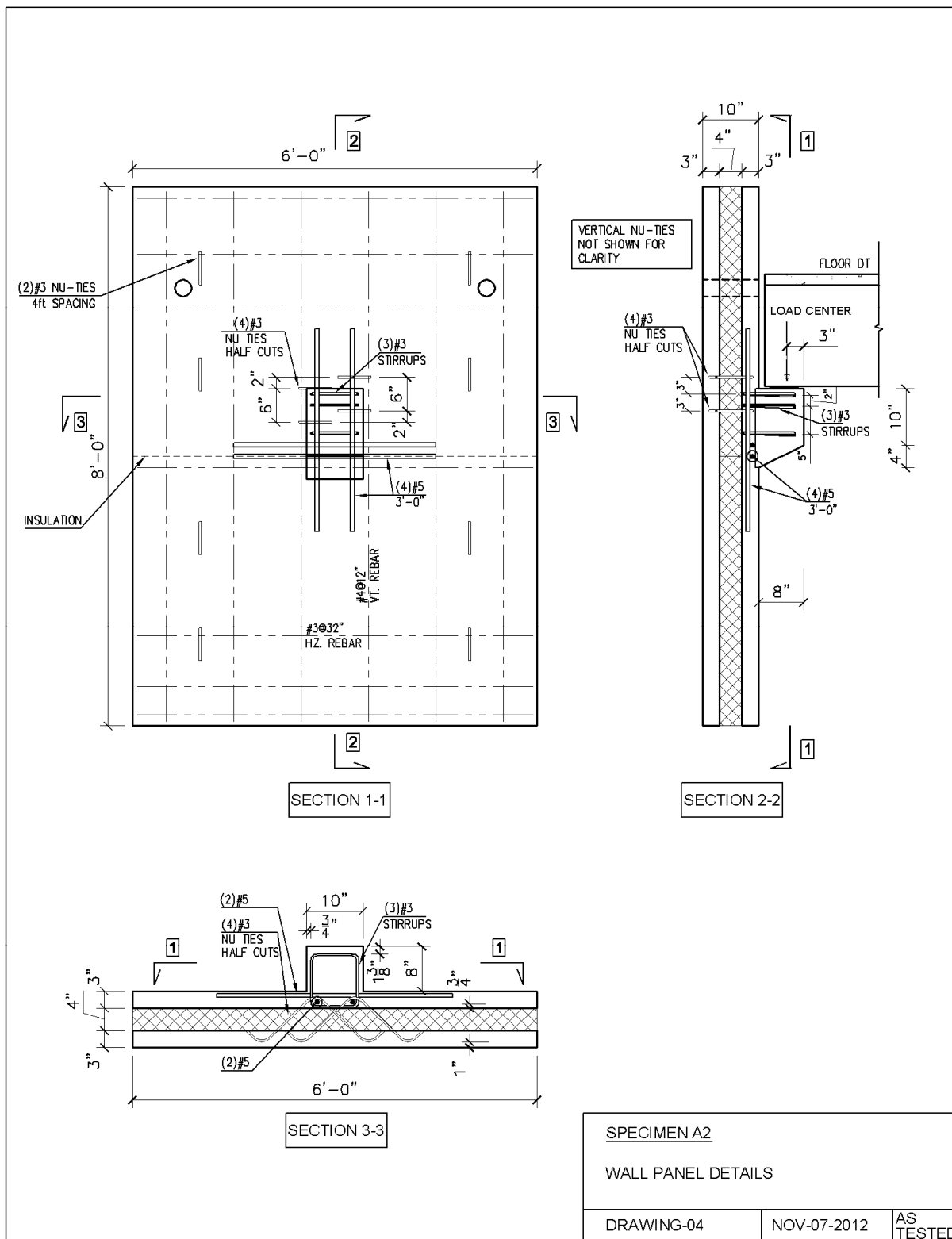


Figure 5-5: Specimen A2- Details sheet 1

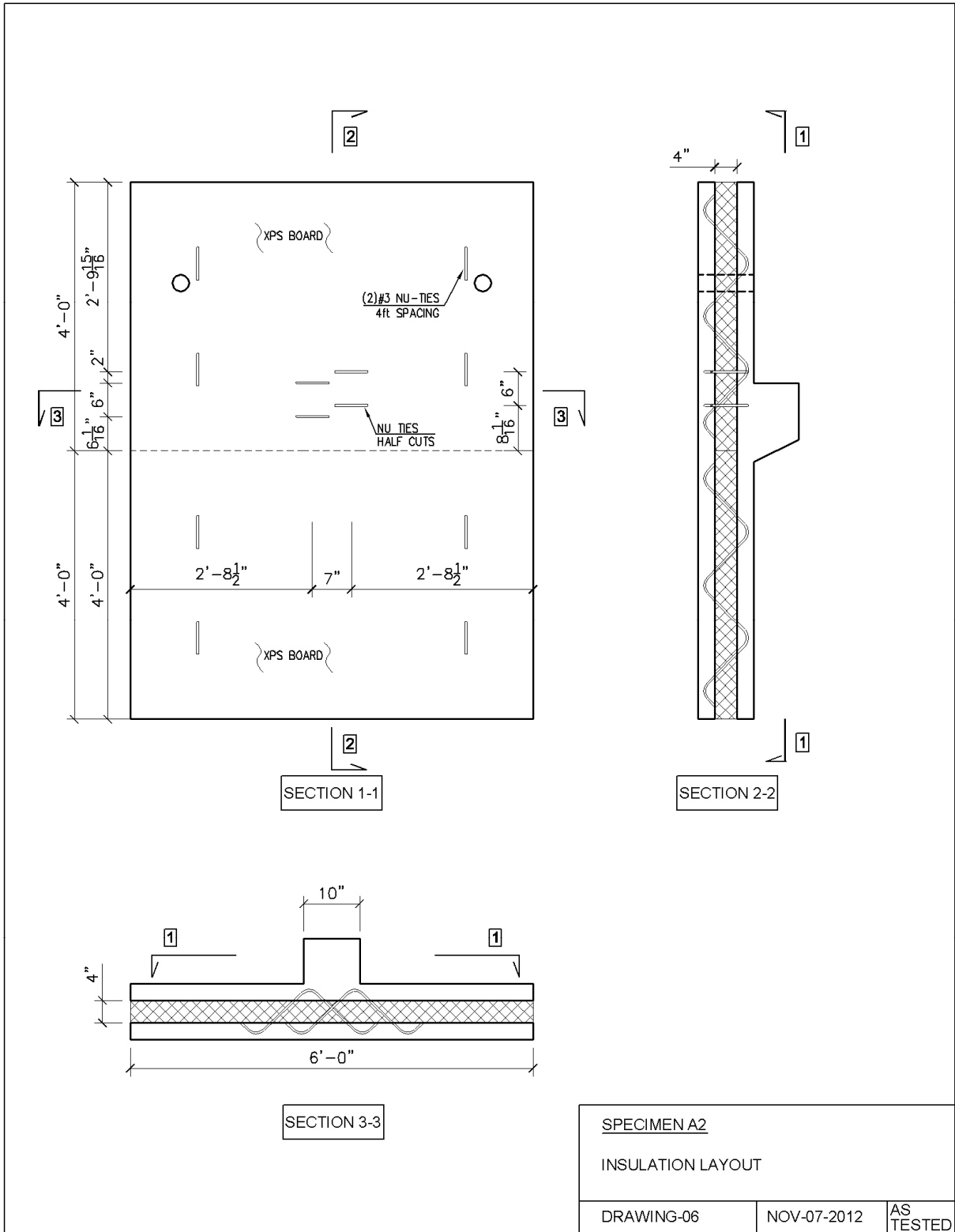


Figure 5-6: Specimen A2- Details sheet 2



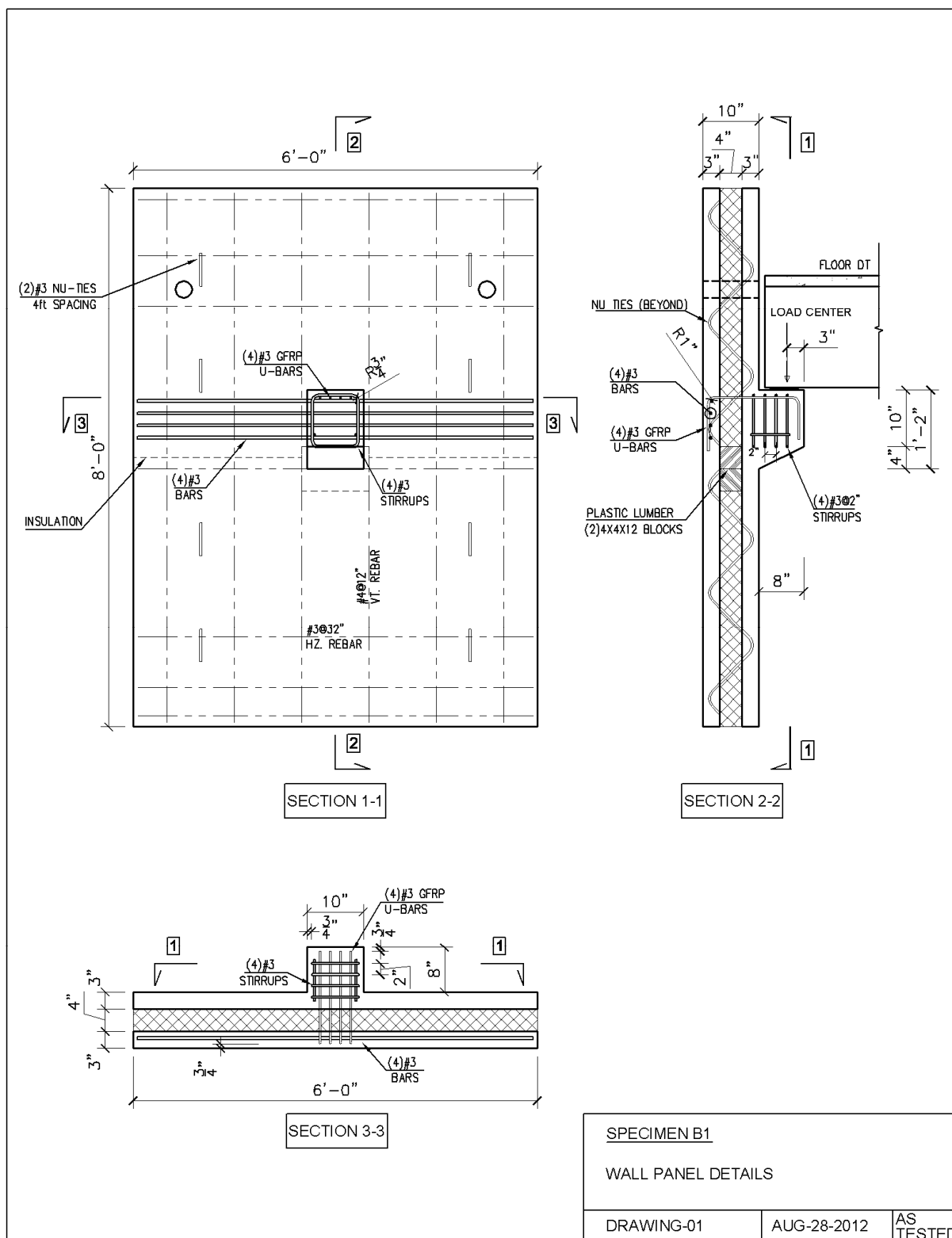


Figure 5-7: Specimen B1- Details sheet 1

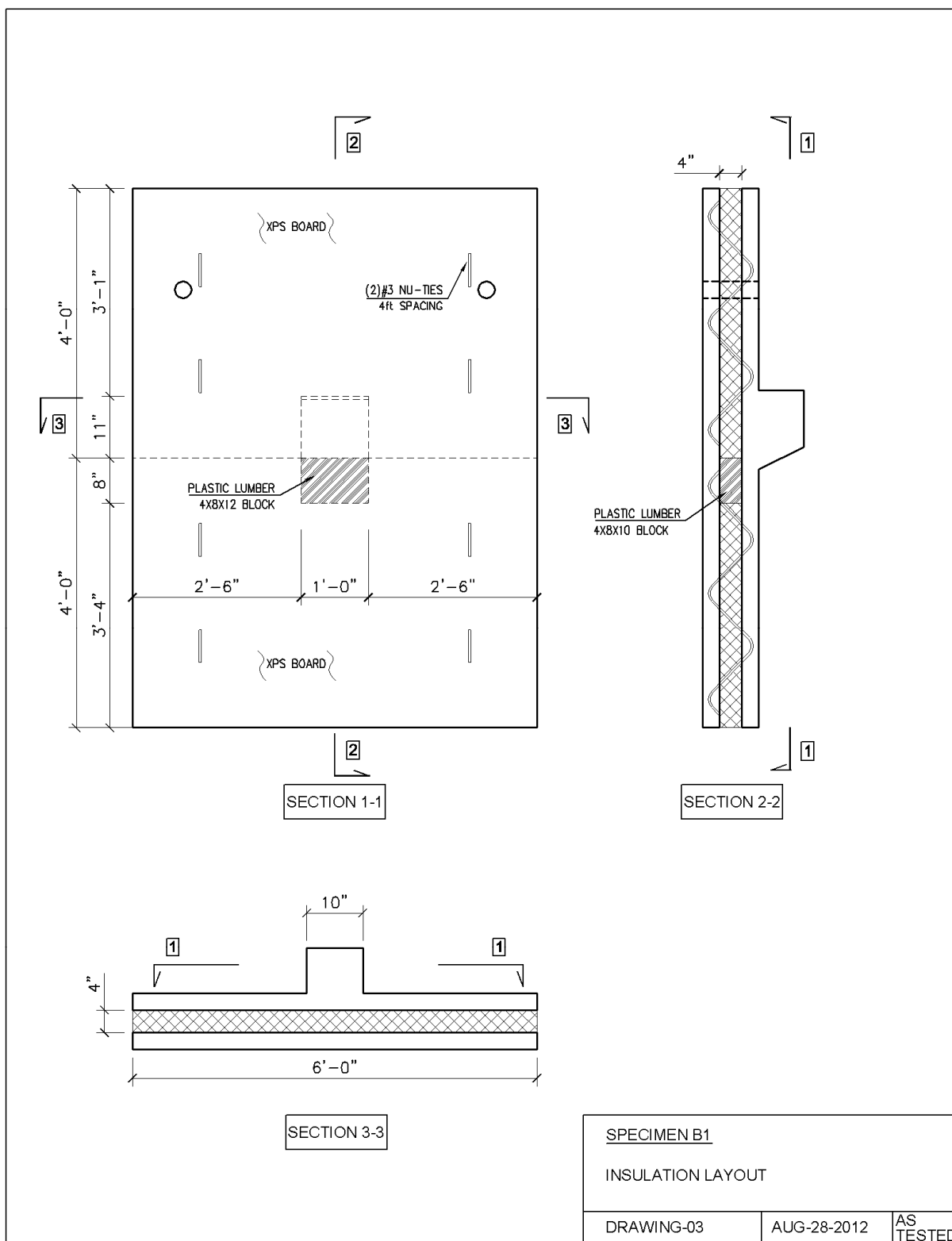


Figure 5-8: Specimen B1- Details sheet 2

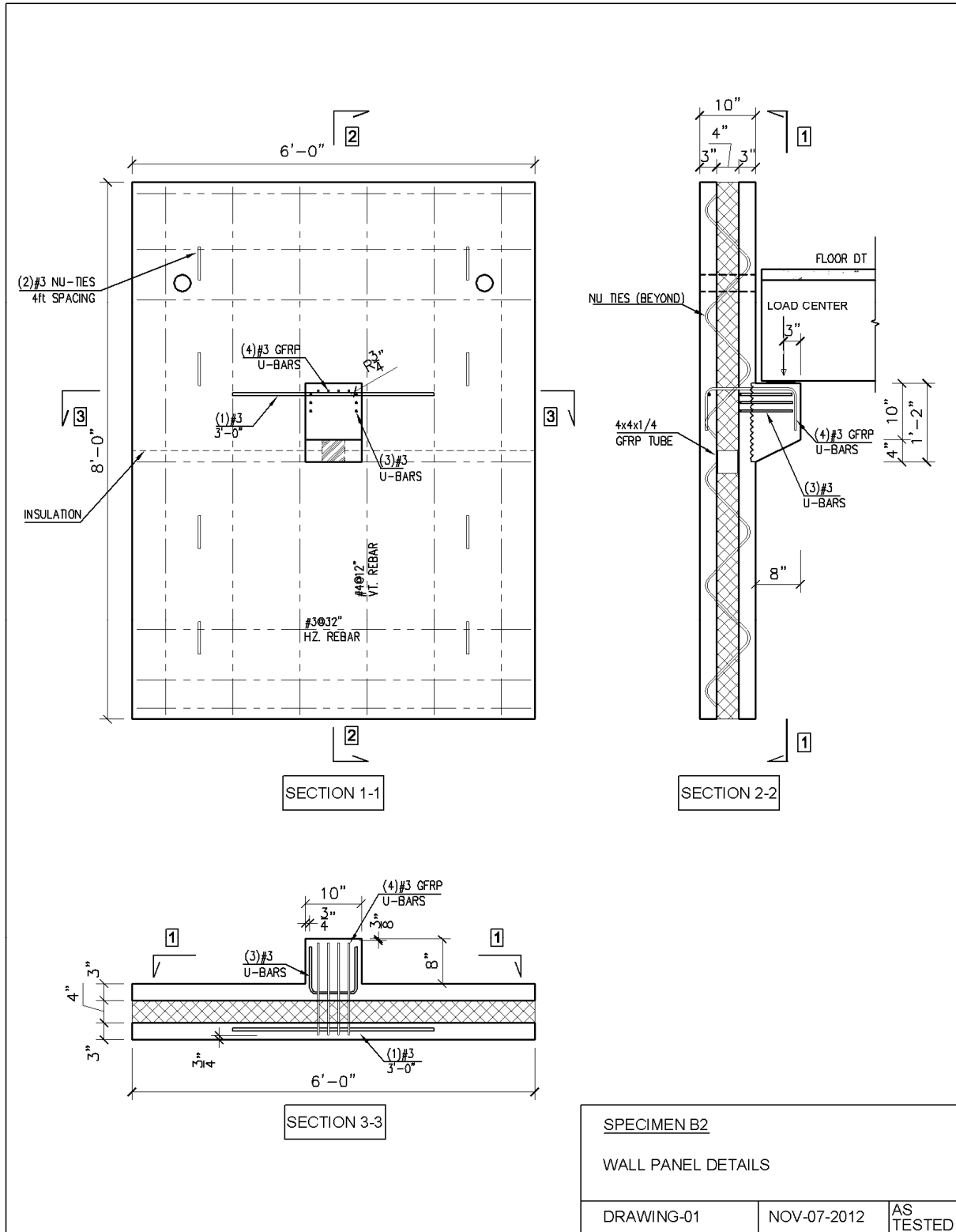


Figure 5-9: Specimen B2- Details sheet 1

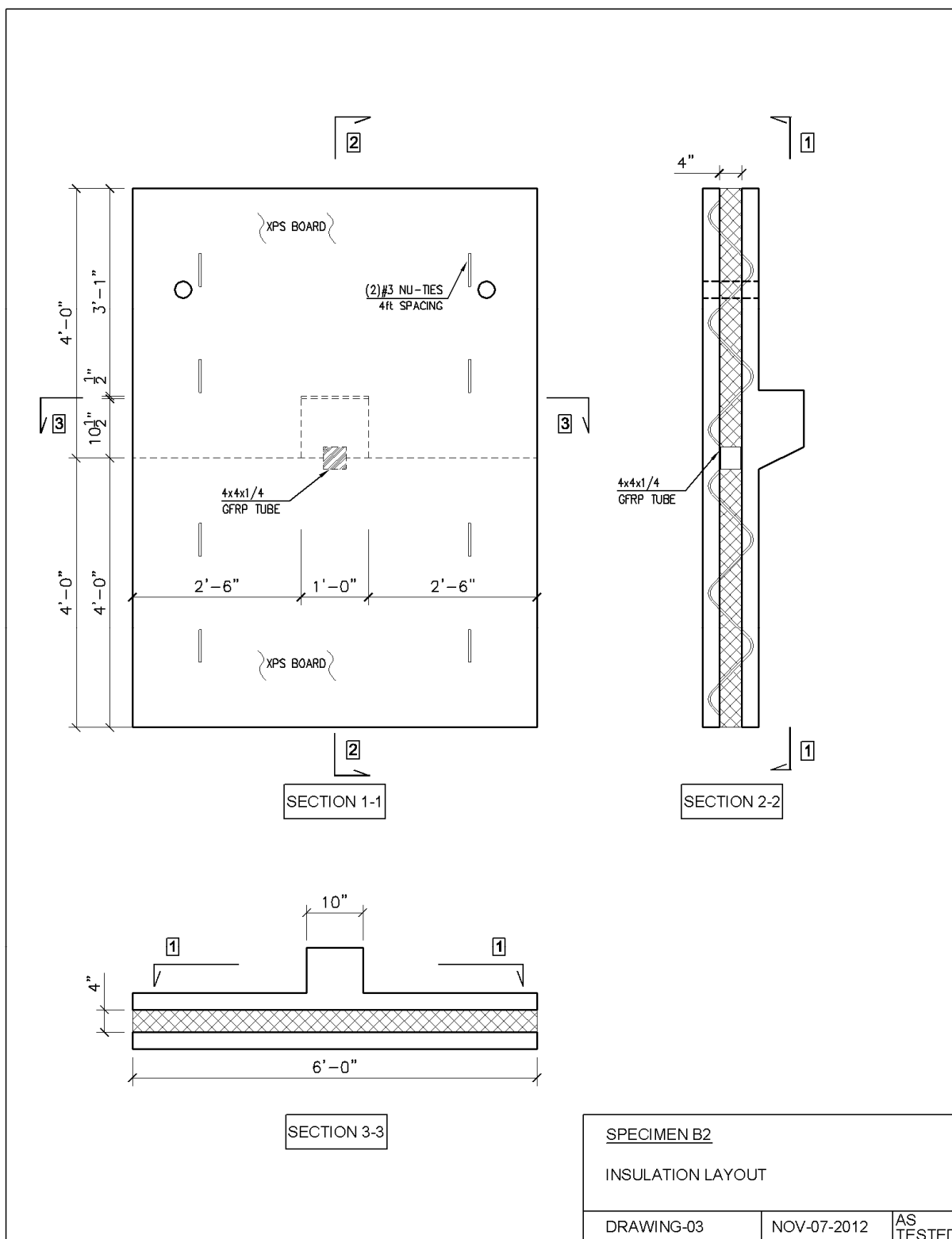


Figure 5-10: Specimen B2- Details sheet 2

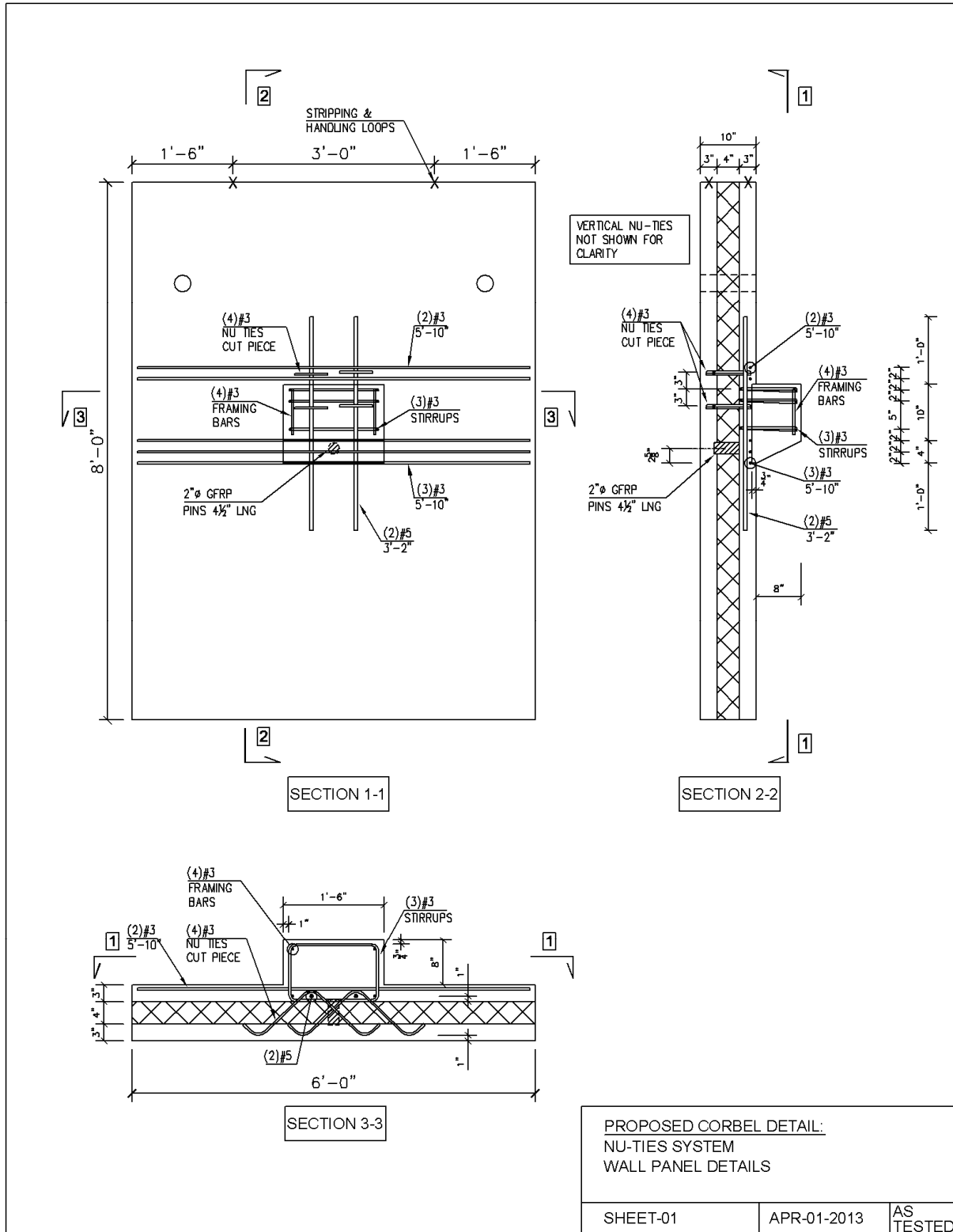


Figure 5-11: Specimen A3, A4 and A5- Details sheet 1, Unreinforced Wall

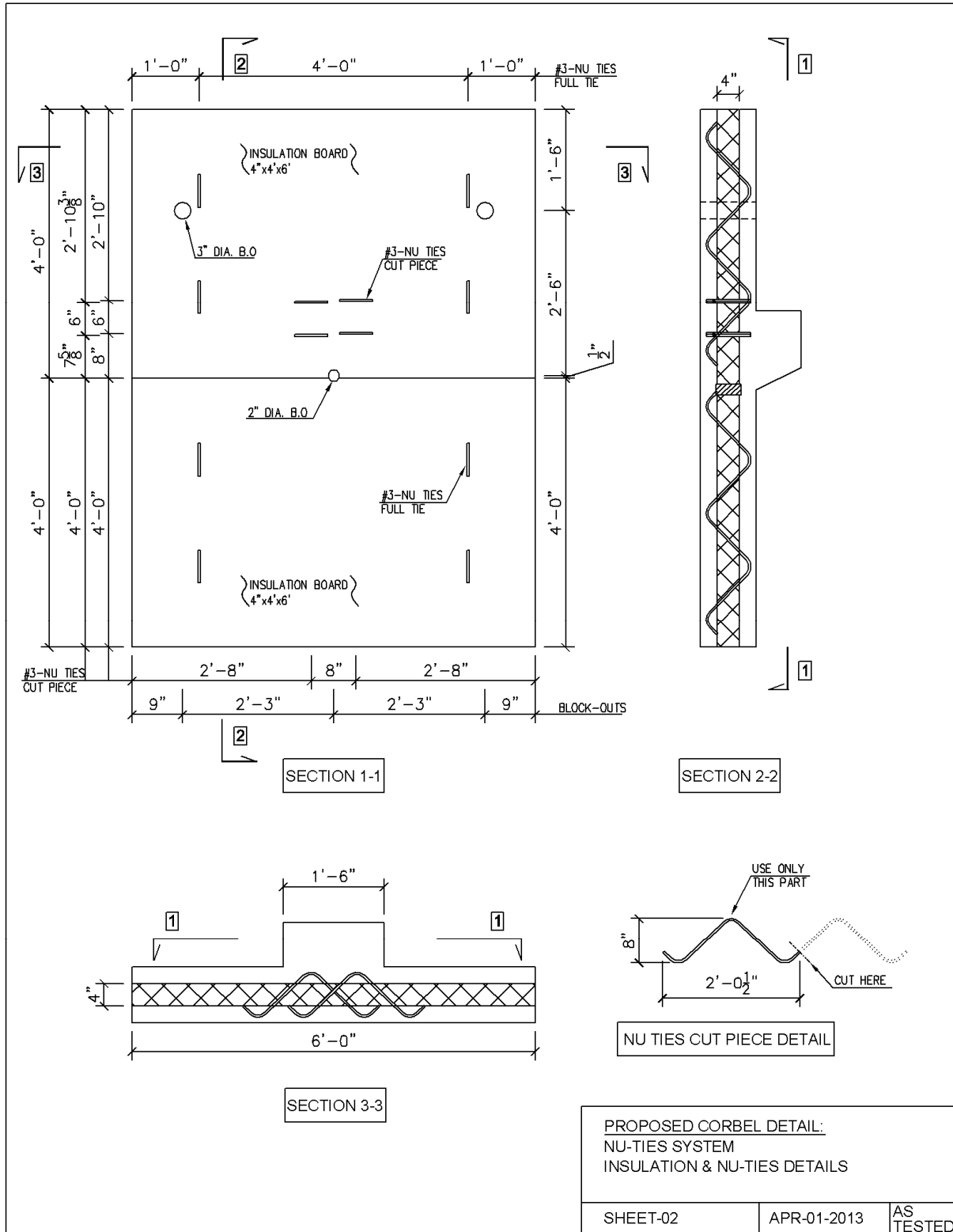


Figure 5-12: Specimen A3, A4 and A5- Details sheet 2

# Appendix C

## C. Notations and Definitions

$a, a_v$	:	Shear span for applied load, distance measured from face of interior wythe to center of concentrated load, in.
$A_f$	:	Area of reinforcement in corbel resisting factored moment, in <sup>2</sup>
$A_s$	:	Area of tension reinforcement, in <sup>2</sup>
$A_v$	:	Area of horizontal stirrups, in <sup>2</sup>
$b$	:	Width of corbel at wall-corbel interface, in.
$d$	:	Effective depth of the corbel, distance measured from centroid of tensions reinforcement to end of sloped face of corbel, in.
$D$	:	Dead load or related internal moments and forces
$c$	:	Distance from extreme compression fiber to neutral axis, in.
$c_b$	:	Distance from extreme compression fiber to neutral axis at balanced strain condition, in.
$C$	:	Resultant concrete compression force at wall face, kip
$C_E$	:	Environmental reduction factor for various fiber type and exposure conditions
$E_c$	:	Modulus of elasticity of concrete, psi
$E_f$	:	Design or guaranteed modulus of elasticity of FRP defined as mean modulus of sample of test specimens, psi
$E_s$	:	Modulus of elasticity of reinforcement, psi
$f_3$	:	Fraction of live load considered to be stained, varies based on the occupancy and use
$f'_c$	:	Specified compressive strength of concrete, psi
$f_f$	:	Stress in FRP reinforcement in tension, psi

$f_{f,s}$	:	Stress level induced in FRP by sustained loads, psi
$f_{fu}$	:	Design tensile strength of FRP, considering reductions for service environment, psi
$f_{fu}^*$	:	Guaranteed tensile strength of an FRP bar defined as the mean tensile strength of a sample of test specimens minus three times the standard deviation
$f_r$	:	Modulus of rupture of concrete, psi
$f_y$	:	Specified yield strength of reinforcement, psi
$f_{yv}$	:	Specified yield strength of transverse reinforcement, psi
$F_{nn}$	:	Nominal strength at face of a nodal zone, kip
$F_{ns}$	:	Nominal strength of a strut, kip
$F_{nt}$	:	Nominal strength of a tie, kip
$h$	:	Overall height of corbel at wall interface member, in.
$H$	:	Horizontal force applied to the corbel, kip
$I_g$	:	Gross moment of inertia, in <sup>4</sup>
$I_{cr}$	:	Moment of inertia of transformed cracked section, in <sup>4</sup>
$L$	:	Live loads, or related internal moments and forces
$M_{cr}$	:	Cracking moment, kip-in.
$M_n$	:	Nominal moment capacity, kip-in.
$M_{sus}$	:	Moment due to sustained load, kip-in.
$M_u$	:	Factored moment at section, kip-in.
$n$	:	Modular ratio
$N_u$	:	Tension force applied to the corbel, kip
$V$	:	Shear force applied to the corbel, kip
$V_{crack}$	:	Shear force corresponding to $M_{cr}$ , kip
$V_n$	:	nominal shear strength at section, kip
$V_u$	:	factored shear force at section, kip
$w_c$	:	Weight of unit volume of concrete, pcf



$y_s, y_t$	:	Distance measured from neutral axis to extreme fiber tension, in.
$\beta_l$	:	Factor relating depth of equivalent rectangular compressive stress block to neutral axis depth
$\beta_n$	:	Factor to account for the effect of the anchorage of ties on the effective compressive strength of a nodal zone
$\beta_s$	:	Factor to account for the effect of cracking and confining reinforcement on the effective compressive strength of the concrete in a strut
$\epsilon_{cu}$	:	Ultimate strain in concrete
$\epsilon_{fu}$	:	Design rupture strain of FRP reinforcement
$\lambda$	:	Modification factor reflecting the reduced mechanical properties of light-weight concrete all relative to normal weight concrete of the same compressive strength
$\mu$	:	Coefficient of friction, ACI 318 (2011)
$\mu_e$	:	Coefficient of friction, PCI Handbook (2010)
$\rho$	:	Ratio of $A_s$ to $bd$
$\rho_{fb}$	:	FRP reinforcement ratio producing balanced strain conditions
$\phi$	:	Strength reduction factor

AASHTO	-	American Association of State Highway and Transportation Officials
ASTM	-	ASTM International, formerly known as the American Society for Testing and Materials (ASTM)
GFRP	-	Glass fiber-reinforced polymer
NU-Tie	-	Proprietary product of Hughes brothers, Used as shear connector in insulated concrete wall panel system
XPS	-	Extruded polystyrene foam

## D. Bibliography

ACI 318. (2011). Building Code Requirements for Structural Concrete. Farmington Hills, MI.: American Concrete Institute.

ACI 440. (2006). Guide for the Design and Construction of Structural Concrete Reinforced with FRP Bars. Farmington Hills, MI.: American Concrete Institute.

ASCE 7. (2005). Minimum Design Loads for Buildings and Other Structures. Reston, Virginia: American Society of Civil Engineers.

Ehsani, M. R.; Saadatmanesh, H.; and Tao, S. (1995). Bond of Hooked Glass Fiber Reinforced Plastic (GFRP) Reinforcing Bars to Concrete. *ACI Materials Journal* , 92 (4), 391-400.

infraredimagingservices.com. (n.d.). infraredimagingservices.com. Retrieved from infraredimagingservices.com/home: <http://www.infraredimagingservices.com/home>

Kriz, L. B. and Raths, C. H. (1965). Connections in Precast Concrete Structure-Strength of Corbels. *Journal of the Prestressed Concrete Institute* , 10 (1), 16-61.

Mattock, A. H., Chen, K. C., and Soongswang, K. (1976). The Behavior of Reinforced Concrete Corbels. *Journal of the Prestressed Concrete Institute* , 21 (2), 52-77.

Niederhoff, H. (1961). Investigation of behavior and strength of short cantilevers. Technische Hochschule Karlsruhe.

PCA Notes. (2008). Notes on ACI 318-08 Building Code Requirements for Structural Concrete with Design Applications. Skokie, Illinois: Portland Cement Association.

PCI Handbook. (2010). PCI Design Handbook. Chicago, IL: Precast/Prestressed Concrete Institute.

PSWP PCI Report. (2011). State of the Art of Precast/Prestressed Concrete Sandwich Wall Panels. Chicago, IL: Precast/Prestressed Concrete Institute.

Rausch, E. (1931). Shear in Reinforced concrete Structures. Der Bauingenieur , 12 (32/33), 578-581.

Schlaich , J., Shafer, K., and Jennewein, M. (1987). Toward a Consistent Design of Structural Concrete. Journal of the Prestressed Concrete Institute , 32 (3), 74-150.

solarcrete.com. (n.d.). solarcrete.com. Retrieved from <http://www.solarcrete.com>

Wight, J. and Macgregor, G. (2009). Reinforced Concrete Mechanics and Design (Fifth ed.). Upper Saddle River, New Jersey: Pearson Education.